MSc thesis in Building Technology

Cloud-based room-centric daylight simulation application for environment design:

a case study using the BIM model of TU Delft architecture faculty

Yangyu Liu

June 2024

A thesis submitted to the Delft University of Technology in fulfillment of the requirements for the degree of Master of Science in Building Technology

The work in this thesis was carried out in the:

Building Technology Track
Delft University of Technology

Supervisors: Dr. Azarakhsh Rafiee
Dr. Eleonora Brembilla
External Examiner: Dr. Manuela Triggianese

Acknowledgement

I would like to express my sincere gratitude to everyone who supported me throughout the journey of completing my Master's Thesis.

First and foremost, I extend my deepest appreciation to my mentors, Dr. Azarakhsh Rafiee and Dr. Eleonora Brembilla. Your invaluable guidance and unwavering patience were crucial to the development of my thesis. Your encouragement and expertise helped me navigate the complexities and details of this challenging project. Throughout the process, their regular meetings were essential in keeping me on track and focused, and the advice and feedback helped me refine my approach and move forward with confidence. The detailed insights they provided on specific aspects of my research greatly enhanced the quality of my work.

I would also like to extend special thanks to Abdullah Alattas, who built and provided the BK BIM model for my case study. The model was perfectly suited to initiate my research and showcase the final results. Without your contribution, this thesis could not have continued.

A heartfelt thank you to my family, boyfriend, and friends for their unwavering support and encouragement throughout the challenging times. Your support has been a constant source of strength and motivation.

Finally, I am grateful to all my professors and classmates for their willingness to share their expertise and experiences. This journey of my master study in TU Delft has been wonderful, and I am thankful to have had the opportunity to learn from so many talented individuals.

Thank you all for your invaluable contributions and support. This thesis would not have been possible without your help and guidance.

Abstract

Balancing the requirements of urban planning with the need for rapid and efficient iterative design, while accurately assessing its detailed impact on existing surrounding buildings at a per-room level, presents a significant challenge in architecture and design, the conversion and integration between multiple platforms introduce additional complexity, establishing high standards for designers to achieve. Integrating Building Information Modeling (BIM), Geographic Information Systems (GIS), and per-room daylight simulation into a unified workflow offers a promising solution. This thesis develops a web application that leverages Grasshopper (GH) scripts for backend processes, Rhino Compute as the intermediary API, and MapboxGL as the GIS-based front-end platform, enabling seamless user interaction with BIM data for customized daylight simulations.

Since the advent of digital tools, architects have sought ways to enhance and streamline the design process. The integration of these technologies bridges the gap between urban planning and indoor daylight simulation, facilitating real-time interaction and data manipulation. Grasshopper scripts are developed to compute Aperture-Based Daylight Modeling (ABDM) metrics, Sunlight Beam Index (SBI), and sky lumen, providing a foundation for evaluating their relationships with traditional Climate-Based Daylight Modeling (CBDM) metrics like Daylight Autonomy (DA), Spatial Daylight Autonomy (sDA), and Useful Daylight Illuminance (UDI).

This research explores the potential of combining these advanced tools to create an interactive web application that allows users to manipulate building typology, location, scale, façade materials, and levels of detail (LOD) for surrounding city models. The study demonstrates a robust linear relationship between SBI and the daylight metrics DA, sDA, and UDI, with room geometry playing a crucial role. Sky lumens, however, show limited effectiveness as a CBDM alternative.

The thesis concludes that MapboxGL is a promising platform for integrating BIM models into room-based daylight simulations, offering an intuitive user interface for urban planners and designers. Rhino Compute technology ensures smooth data transfer and interaction, significantly enhancing the workflow. The study results show that SBI has a linear relationship with traditional CBDM metrics. However, multiple moderating variables affect this relationship, and it does not apply to north-facing rooms. Thus, SBI is not a current substitute for traditional CBDM metrics. Overall, this thesis provides a comprehensive framework for integrating BIM, GIS, and daylight simulation into a cohesive system, paving the way for more efficient urban planning and design practices.

Keywords: GIS, BIM, WebGL, Daylight, Simulation, 3D model, Interactive Application, Workflow, BIM Visualization, Urban Planning, Aperture-based daylight modelling, BIM & GIS, BIM – GIS integration

Nomenclature

ABDM	Aperture-based daylight modelling
AM	Airmass
ASI	Aperture Skylight Index
BIM	Building Information Modeling
BPSTs	Building Performnance Simulation Tools
CAD	Computer-Aided Design
CBDM	Climate-based daylight modelling
DA	Daylight Autonomy
EN	European Standards
EPW	EnergyPlus weather
GH	Grasshopper
GIS	Geographic Information Systems
HB	Honeybee
IES	Illuminating Engineering Society
LB	Ladybug
LEED	Leadership in Energy and Environmental Design
LOD	Level of Detail
OA	Obstruction Angle
R^2	Coefficients of determination
sDA	Spatial Daylight Autonomy
SBI	Sunlight beam index
SBI-AM	Sunlight beam index - Airmass
UDI	Useful Daylight Illuminance
Ai	Illuminated Area
γ_s	Sun Altitude
S_{tot}	Total Sunlight Beam Index
θ_z	Zenith Angle
I_{am}	Clear Sky Direct Beam Solar Radiation
θ	Angle of Incidence

Contents

1 / Introduction

1.1 CONTEXT

Daylight standard

European standard EN 17037 for daylight in buildings was approved in 2018 and became applicable to all participating countries in 2019. (Mardaljevic & Brembilla, 2022). In the Netherlands, according to Koster's research (2023), NEN 2057, Dutch Building Code 2012, is planned to be replaced in 2024 by the EN 17037 for a more accurate assessment methodology. However, its implementation of, as per NEN-EN 17037, is officially scheduled for January 1, 2026, pending a decision by the ministry in 2025. But this research will be based on EN 17037 and other Green certificates. This research prioritizes EN 17037 and other Green certificates over the original Dutch code, considering its imminent execution in the near future and clear standard. In Koster's research (2023) about daylight simulation in Dutch urban context, it is mentioned that in Dutch context for Green certificates, BREEAM-NL and WELL certificates are mostly preferred over the LEED (Leadership in Energy and Environmental Design) v4.1 certificate, which is based on Northern American standards. But in Shoshev's research (2023) about per room daylight simulation in Italy, LEED v4.1, and is also considered Illuminating Engineering Society (IES). In Schouws's research (2022) about EN 17037, LEED, and BREEAM, the difference between them is discussed. Both BREEAM and LEED include specific metrics to comprehensively quantify daylight performance. Given the consistency in building types used in these studies and the similarity in their results, this research will align with the metrics explored in Shoshev's work.

New houses' daylight impact

To address the increasing population and the resulting pressure on the housing market, many Dutch cities are planning significant expansions in housing. For instance, Amsterdam aims to build 7,500 new homes annually until 2035 (Wedia, 2024). The construction of new buildings impacts the visual comfort (daylight and views) of occupants in existing buildings. Visual comfort could be a trade-off between a lot of perspectives, and daylight simulation software is commonly used to consider and compare various visual comfort parameters, aiming to mitigate the negative impacts of new building at the planning phase (Rajus et al., 2022). In recent years, there has been less daylight research on the reflections in architectural elements and building exterior materials (Nasrollahi et al., 2016). However, this is a crucial factor in how new additions affect the daylighting of existing buildings.

Mardaljevic (2016) introduced Aperture-based daylight modelling (ABDM) standards, which offers the advantage of analyzing windows and assessing interior daylight levels without requiring knowledge of the house's interior layout. He highlighted the importance of this criterion in urban environments, noting its significant potential to make reasonable extrapolations of indoor daylight performance. This capability aids decision-making processes during the preliminary planning stages. This efficient standard also demonstrates potential for evaluating the impact of new housing developments on the daylighting of existing buildings.

Current usage of digital daylight simulation tools

According to a survey conducted by Fernandez-Antolin's group in Spain (2020-2022) with 170 people working in architecture field, complexity of use, large amount of data entry (Schlueter & Thesseling, 2009) and a poor interface are barriers to the usage of current simulation tools. And compatibility with computer-aided design (CAD) tools is the most important criteria for them. In real projects, they have to access to variety of daylight simulation tools, which can be extremely complicated (Shoshev, 2023). But 92% of them they have confidence in the future of simulation tools. Therefore, it is crucial to develop user-friendly simulation tools for designers and provide architects with clear instructions for optimal daylight analysis, especially in the context of rapid urban development and growing construction demands (Choi, 2016).

Radiance is embedded widely in variety of architectural related software (Figure 1), functioning as the most widely used daylight simulation engine (Radiance, n.d.). The significant variability among different software necessitates the use of specific tools for daylighting simulations, which complicates collaboration within design teams, hinders the sharing of results, impedes the integration of workflows, and increases the complexity of software learning.

Figure 1: Daylight simulation tools with Radiance embedded (Radiance, n.d.)

BIM – GIS integration

The integration of Building Information Modeling (BIM) and Geographic Information Systems (GIS) has been recognized as essential for improving the efficiency, safety, and performance of complex urban infrastructure projects (Song et al., 2017). However, a significant challenge to this integration is the inherently disparate data formats. When domain-specific data are not interoperable, they create data silos that restrict access to information and resources for other stakeholders (Boschken et al., 2013). These data silos impede productivity, efficiency, innovation, and service quality (de Waal et al., 2019).

Several available map libraries including Mapbox, Cesium, and kepler.gl require technical expertise to integrate map views into applications and to enhance their functionalities (Computational Modelling Group, 2023). BIM integration with asset management and GIS technologies faces the issue of creating "island solutions" (Celeste et al., 2022). Current technological trends tend to produce isolated data silos with limited interoperability, which are neither scalable nor extensible (Quek et al., 2023). BIM GIS integration is usually restricted to certain platform with little possibility of generalization (Celeste et al., 2022).

1.2 Problem Statement

In the field of urban planning, especially in the early stages of design and planning, the ability of users to interact with 3D city models through interfaces is critical for effective indoor daylighting simulations and for analyzing the impact of additional buildings on existing buildings. But the current workflows and existing tools face several challenges. One major issue is the difficulty in user interaction with 3D city models. Additionally, integrating BIM with daylight simulation tools and GIS platforms is complex. This complexity hampers the intelligent identification and segregation of components by room, which is crucial for accurate and automated daylight simulation. As a result, users cannot interact efficiently with per-room BIM segments, reducing BIM's overall utility in daylight analysis. Furthermore, there is uncertainty in applying ABDM standards for urban-scale daylight studies and correlating these with traditional Climate-based Daylight Modeling (CBDM) standards. Lastly, the impact of varying Levels of Detail (LODs) on computational efficiency poses another challenge.

Sub-problems:

1. Existing 3D city modeling tools lack user-friendly interfaces for seamless interaction and daylight simulation. The process of loading and integrating 3D city models into Rhino and associated applications for simulation purposes is complex and inefficient.
2. There is a lack of effective methods for integrating BIM models into GIS platforms for daylight simulation. Users cannot interact with BIM segments at a room level within the application, impeding detailed and accurate daylight analysis.
3. It is unclear whether ABDM standards are related to traditional CBDM standards, and there is a lack of implementation strategies for ABDM standards in urban-scale daylight applications to enable effective visualization and reduce times.
4. Higher LODs in 3D city models might increase computational time. Current workflows for managing LODs are not optimized for daylight simulation efficiency in urban environments of varying densities, and it is uncommon for daylighting software to offer users the option to select different LODs.

1.3 Research Questions

Main research question:

To what extent can a web application conduct per-room daylight analysis on BIM models to effectively demonstrate the influence of dynamic changes within an urban context?

To answer the main research question, four sub-questions must be answered first. The four sub questions are:

Sub-questions:

1. To what extent can users interact with 3D city models through the interface? How can they be loaded in Rhino and the application for simulation and interaction?

2. How can a BIM model be integrated into Rhino and GIS platform to intelligently identify and segregate components by room, thereby facilitating automatic integration with daylight simulation? How can users interact with per-room BIM segments within the application?

3. Are the ABDM standards (SBI and view-lumen) appropriate for urban-scale daylight studies aimed at reducing simulation time, as compared to traditional CBDM standards? If applicable, how can these simulations be implemented within the application to enable effective visualization?

4. What is the impact of varying LODs in 3D city models on computational accuracy and time, and how can the overall workflow be optimized for efficiency?

1.4 Design Objective

The design objective is to create an innovative cloud-based daylight simulation application within a WebGL-based 3D GIS platform that enables room-specific simulations based on a BIM model, allowing users to interact with and modify urban environment (such as adding new buildings, adjusting heights, and roof types). Users can visualize the impact of these changes on indoor daylight performance in user-friendly interface with dropdown menus, checkboxes, sliders, and be able to easily compare the results before and after the changes. This research will also improve its efficiency by improving the overall workflow and details.

This thesis will also quantitatively examine the relationship between the daylight metrics of ABDM standers and those of the traditional annual CBDM standard metrics to ascertain whether SBI and sky lumen could serve as alternative metrics to Daylight Autonomy (DA), Spatial Daylight Autonomy (sDA), and Useful Daylight Illuminance (UDI) metrics, with the objective of expediting the simulation of indoor daylight outcomes in urban settings. Additionally, the study will attempt to integrate the computational capabilities of suitable ABDM within the application.

The BK faculty BIM model and its surrounding environment is used in this thesis as a case study. However, the presented development workflow is widely applicable to various BIM models. This thesis will provide a generalized methodology, including suggestions for modifying the workflow based on different levels of BIM inputs, and specify the basic requirements for BIM inputs to ensure scalability. Ultimately, its goal is to function as a valuable tool and more important, a digital workflow, for visualizing daylight performance

based on changes in environment in the early design stage, providing insights and suggestions for designers, urban planners, architects, and building owners involved in environmental design.

1.5 Project scope

Daylight Metrics

Aspects	Metrics		Target value	Reference	Honeybee
Daylight	DF	Daylight factor	⩾2%	EN 17037	√
	DA	Daylight autonomy	> 50%	IESLM-83-12	√
	UDI	Useful daylight autonomy	<500lux - insufficient illumination 500 lux-2500 lux- acceptable >2500lux - bad	LEED v4.1	√
	cDA	Continious daylight autonomy	> 55%	IESLM-83-12	√
	sDA	Spatial daylight autonomy	$sDA_{300, 50\%}$ ⩾40% - sufficient $sDA_{300, 50\%}$ ⩾55% - preferable $sDA_{300, 50\%}$ ⩾75% - optimal	LEED v4.1	√
	ASE	Annual sunlight exposure	$ASE_{1000.250h}$ < 7% - neutral $ASE_{1000.250h}$ < 3% - clearly acceptable	LEED v4.1	√
Glare	GA	Glare autonomy	$GA_{40\%}$	EN 17037	√
	sGA	Spatial glare autonomy	$sGA_{40\%,5\%}$	EN 17037	√
	DGP	Daylight glare probability	<20% - not validate 20%-35% - imperceptible 35%-40% - perceptible 40%-45% - disturbing >45% - intolerable	EN 17037	√
View out	/	Width of view window/s	⩾ 14° (based on a 360° field of vision)	EN 17037	X
	/	Outside distance of the view	> 6m	EN 17037	X
	/	Landscape layer to be seen (sky, landscape and ground)	⩾70% of the utilised area	EN 17037	X
Openings	SBI	Sunlight beam index	/	ABDM	X
		SBI 'efficiency'	/	ABDM	X
	ASI	Aperture Skylight Index	/	ABDM	X

Table 1: Common daylight Metrics

Apart from the traditional standards CBDM, ABDM in 2019 is an upgrade of those methodologies. In EN 17037:2018, ‘Daylight should be a significant source of illumination for all spaces with daylight opening(s).’1 The word ‘opening’ appears 139 times in the standard (Mardaljevic & Brembilla, 2022). For this part the script will be coded by my own for simulation. These metrics are designed to measure the available daylight in urban settings, providing a clear quantification of how the outdoor environment impacts window daylighting capacity. This concept is relatively new, resulting in a limited number of studies and cases, and the scripts are not available in Honeybee (Table 1). Recognizing this research gap, this thesis aims to incorporate these new methodologies, considering their absence of a target value by focusing on absolute values and changes under varying conditions. Additionally, this research will explore their correlation with traditional annual daylight metrics like DA, sDA and UDI, bridging the gap between the ABDM method and conventional CBDM approaches.

Daylight Parameters

Figure 2 offers a clear static representation of the components of daylight entry, illustrating how daylight enters and is distributed within a space through direct entry (SC), external reflections (ERC), and internal reflections (IRC) to calculate the illuminance level of a room together (Hopkinson, 1966). Based on this, DA (and sDA, UDI similarly) requires consideration of these components dynamically over time and the percentage of occupied hours during which a space receives adequate daylight, accounting for varying sky conditions, sun positions, and reflections throughout the year.

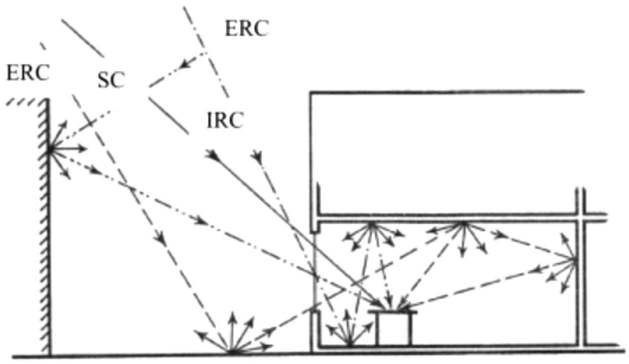

Figure 2: Different ways of daylight penetration into the building: Directly from the sky. Direct reflection from an external barrier. Reflection from the floor and ceiling. Reflection from the ground, ceiling and the walls. (Nasrollahi & Shokri, 2016)

Reflectivity of buildings and their urban context influence the energy consumption of buildings. (Chen et al.,). Also, reflections of surfaces externally and internally and urban canyons considerably contribute to the distribution of daylight in building interior. (Nasrollahi & Shokri et al.,) Light impacting the facades of surrounding buildings within an urban canyon context—often exerts a substantial influence on the overall daylight within a room. This heightened impact is attributable to the fact that vertical surfaces, such as building facades, are typically more expansive and proximal to windows compared to horizontal surfaces, and thus, they reflect light more directly into interior spaces, particularly within dense urban environments or "urban canyons." In densely populated areas with tall, reflective buildings, the facades may contribute more significantly to indoor daylight. While in less dense settings, reflections from the ground may be more influential, especially where ground surfaces are designed to enhance reflectivity, such as through the use of light-colored paving materials. Trees and vegetation also significantly affect indoor daylight performance in practical scenarios. However, due to the complexities associated with simulating paving systems and 3D vegetation within the timeframe of this thesis, this research does not account for the variation of ERC from exterior ground surfaces of different materials or plants. To simplify this, a generic material with 20% reflectivity is used as a standard. (Section 6.3).

Ideally, modifications could also be applied to the existing surrounding buildings, and in theory, this could be accomplished using 3D tiling technique. At the inception of this thesis, the integration of 3D BAG 3D tiling technique with Mapbox was still in a preliminary experimental phase (see Section 6.3 of this report). So, the focus here is solely on the addition of new buildings in this research. But this is a trajectory worth exploring as the technique becomes more accessible.

Initial BIM model

The fidelity and quality of BIM models are significantly influenced by the actual conditions of the buildings and the modeling practices employed by the modelers. Consequently, BIM models will exhibit considerable variability, necessitating adjustments of varying degrees to conform to this universal workflow proposed in this thesis. But modifications arising from informational deficits, particularly manual alterations, do not constitute the primary focus of this thesis or the workflow. These issues will not be extensively discussed but the requirements of data input at each stage and outline potential corrective measures that may be implemented will be covered in this thesis. Certain input values are held constant during the daylight simulation and are not examined in this study.

It is requested that the initial BIM model incorporates precise Type of each element, distinguishing between materials type for interior and exterior, as well as detailed room information. Ideally, the floors category should be segmented by room to facilitate detailed analysis. If the room plans are polygonal in shape, the Boundingbox method discussed in this thesis might prove inadequate; instead, the use of a Room Boundaries node would be necessary in the new workflow. Ideally it should also include large furniture information, and some interior material details, as interior daylighting simulations prioritize large surfaces as they play a crucial role in reflecting light. More information can be found in Section 6.2.

GIS platform as client

Utilizing the C# library for Rhino Compute and selecting Unity as the platform presents a potentially advantageous alternative workflow. However, given that the content related to this is primarily developed and disseminated by Jhorikawa (n.d.) and is partly utilized for commercial purposes, this approach is not explored as an alternative workflow in this study. Instead, this thesis concentrates on exploring possibilities of WebGL based GlS platform options, specifically Mapbox and Cesium. Given that Cesium Ion requires token each time a new geometry is uploaded, and considering the application's requirement for dynamic transfer of new simulation results, the implementation poses challenges. Furthermore, MapboxGL incorporates a plugin, Threebox, which integrates certain functions from Three.js to Mapbox GL. This plugin is updated and maintained more frequently compared to Cesium's Three.js plugin. This thesis selects Mapbox as the GIS platform (Section 2.5).

2 / Literature Review & Related Work

2.1 Indoor Per-room Daylight Analysis

2.1.1 Urban canyons' impact

For surrounding environment, façade materials of surrounding buildings are important factors affecting building's access to daylight. (Alenius et al, 2019). Using highly reflective materials for façades of new building in development can help compensate for interior daylight losses. (Formolli et al., 2022). Alenius's team (2019) also introduced Obstruction angle (OA), the angle between the horizontal plane and a line connecting the center point of a window and the tip point of surrounding buildings (Figure 3). This metric aims to help real estate developers meet daylight requirements during the urban planning stage.

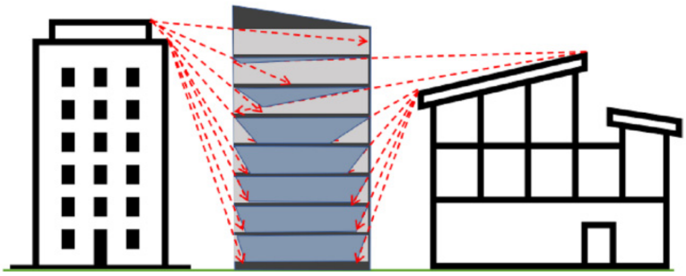

Figure 3: Obstructing angle between neighbouring buildings in an urban setting. The highlighted sections correspond to apartment areas that do not have direct access to skylight, (Pantazatou et al., 2023)

In practice, since the original building remains unchanged and only the urban context is considered, OA is typically influenced by two primary factors: the type and height of the roofs of surrounding buildings, taking into account building additions and roof replacements.

Based on several research projects (Figure 4, Figure 5), influential parameters on amount of radiation reaching building surfaces, visual comfort are as followings, listing according to their priority: geometry of Urban canyons, reflectivity of surfaces, external shading devices, roof shapes, street orientation and sky view factor (SVF). (Nasrollahi & Shokri., 2016). The more visual comfort and solar radiation reaching building facades, the higher the SVF. And study shows when height of building increases, the SVF decreases accordingly. (Nasrollahi & Shokri, 2016).

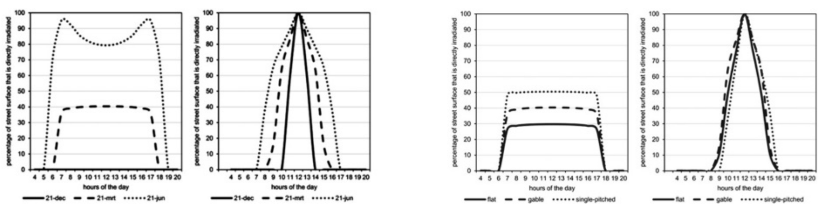

Figure 4： Influence of street direction (left two) and influence of roof shape (right two), both with east-west street(left) and north-south(right). (Van Esch et al., 2012)

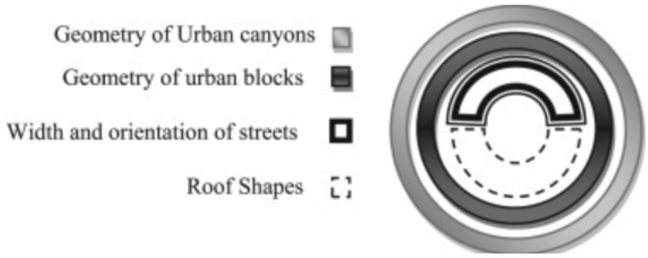

Figure 5: Hierarchy of the factors affecting the amount and quality of solar radiation

(Nasrollahi & Shokri, 2016)

2.1.2 CBDM & ABDM

DA, sDa & UDI

DA measures the percentage of occupied time that daylight provides the specified illuminance at a particular spot in a space, indicating daylight availability. In Equation 1 for DA calculation, t_i is occupied hour in a year, wf_i is a weighting factor that depends on the values of $E_{Daylight}$ and E_{Limit}, which are the horizontal illuminance at a specific point due to daylight alone and the illuminance limit value, respectively.

$$DA = \frac{\sum_i (wf_i \cdot t_i)}{\sum_i t_i} \in [0,1]$$

$$with\ wf_i = \begin{cases} 1, & if\ E_{Daylight} \geq E_{Limit} \\ 0, & if\ E_{Daylight} < E_{Limit} \end{cases} \quad (1)$$

sDA annually assesses if a space receives sufficient daylight on a work plane during normal business hours (Equation 2). The target, as set in this thesis, is 300 lux for at least 50% of the occupied time. Typically, sDA is calculated using a daylight simulation program that measures the daylight levels in the area for each hour of the year (Council, 2013).

$$sDA = \frac{\sum_i (wf_i \cdot DA)}{\sum_i p_i} \in [0,1]$$

$$with\ wf_i = \begin{cases} 1, & if\ DA \geq DA_{Limit} \\ 0, & if\ DA < DA_{Limit} \end{cases} \quad (2)$$

$$UDI = \frac{\sum_i (wf_i \cdot t_i)}{\sum_i t_i} \in [0,1]$$

The evaluation of UDI is based on hourly or shorter time-step illuminances over a year, it divides annual illuminance into three ranges: insufficient (<lower bin), excessive (>upper bin), and useful (between). Exceeding UDI values can cause issues like glare and overheating, while too little leads to insufficient illumination. Typically, 100 lux and 3000 lux are the thresholds (Nabil, A., & Mardaljevic, J., 2005), in this standard, daylight between 100 and 3000 lux is considered "useful" for lighting. This thesis uses the common standard thresholds of 100 and 3000 lux (Equation 3).

$$UDI_{Overlit} \quad with\, wf_i = \begin{cases} 1, & if\ E_{Daylight} \geq E_{Upper\ Limit} \\ 0, & if\ E_{Daylight} < E_{Upper\ Limit} \end{cases}$$

$$UDI_{Useful} \quad with\, wf_i = \begin{cases} 1, & if\ E_{Lower\ Limit} \leq E_{Daylight} \leq E_{Upper\ Limit} \\ 0, & if\ E_{Daylight} < E_{Lower\ Limit} \cup E_{Daylight} > E_{Upper\ Limit} \end{cases} \qquad (3)$$

$$UDI_{Underlit} \quad with\, wf_i = \begin{cases} 1, & if\ E_{Daylight} < E_{Lower\ Limit} \\ 0, & if\ E_{Daylight} \geq E_{Lower\ Limit} \end{cases}$$

SBI & sky-lumen

ABDM introduces a novel approach to daylight simulation, focusing on assessing how effectively apertures connect with sunlight and the external environment. addressing the deficiency in evaluation frameworks that simultaneously consider both the solar energy potential and the qualitative aspects of sunlight/daylight during the planning stages of building projects. (Mardaljevic & Brembilla, 2021). In theory, any 3D CAD/BIM tool capable of assessing on-site visibility between two points—one within the building model and the other representing the position of the sun on the sky dome—can compute Sunlight Beam Index (SBI) and ASI (Mardaljevic & Roy, 2016). Consequently, the computations of SBI and ASI can significantly reduce computation time compared to traditional sunlight analysis via ray tracing in the early stage of design, which could take tens of minutes or even hours to complete. SBI provides a quantifiable estimate of potential sunlight availability, while the view lumen is considered an indicator of sky connectivity, suggesting a measure of potential skylighting received through openings. However, the relationship between these indices and actual indoor daylight performance remains to be fully elucidated. Specifically, the correlation between ABDM and CBDM requires further investigation (Mardaljevic & Brembilla, 2021). SBI-AM and connectivity to the sky have notable potential to make reasonable extrapolations of indoor daylight performance, thereby assisting decision-making processes during the preliminary planning stages. (Mardaljevic, 2021)

SBI is a single figure can characterize the sunlight beam potential of a building or space (Mardaljevic et al., 2016) functioning as an indicator of sunlight potential of rooms, that can clearly present the influence of outdoor environment's impact. SBI has units of ㎡ hours, and it works for any given period of time. And it can be calculated by any 3D CAD/BIM tools as it is only based on a line-of-sight calculation, and the incorporation of inter-reflection modeling and/or the consideration of light transmission/scattering effects is unnecessary.

$$S_{\Delta t} = A_g \cos\theta\, \Delta t \qquad (4)$$

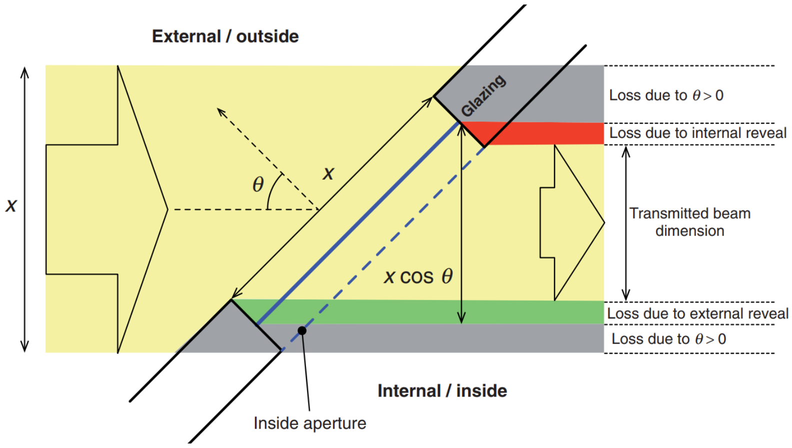

Figure 6: Definition of beam sunlight cross-sectional area entering a space (Mardaljevic & Roy, 2016)

In Equation 4, the SBI value $S_{\Delta t}$ for a duration of time can be calculated by the direct sunbeam enters a glazed aperture of area A_g with an angle of incidence θ for a time period Δt (Mardaljevic & Roy, 2016). With no obstructions, the illuminated area is equal to A_g (Figure 6).

ASI quantifies the degree of connectivity between an opening and the sky vault by assessing the illumination it receives from a uniformly bright sky dome, with the measurement averaged over the opening. In the apartment ABDM evaluation, the sky lumens lost because of the balcony, overhang and external obstruction can be calculated and visualized (Figure 7), and the actual lumen loss is always greater than that which seems apparent from the hemispherical image (Mardaljevic., 2020).

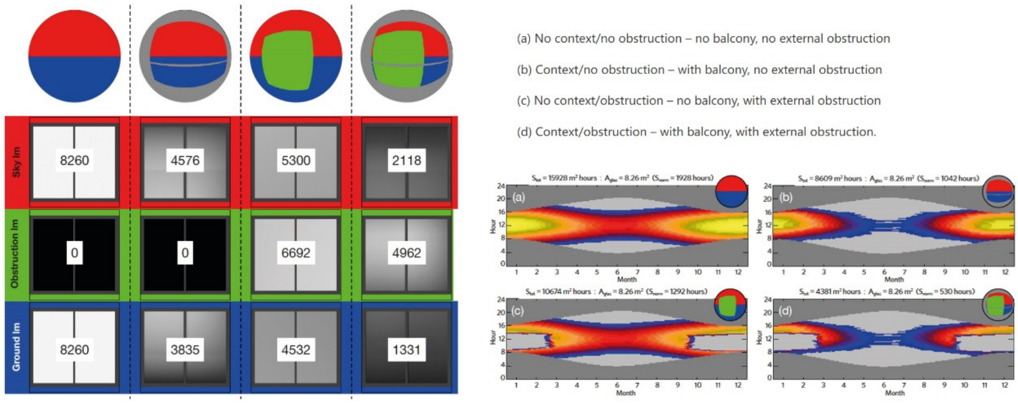

Figure 7: Lumens received at the glazing aperture of the apartment in four cases (left) and temporal maps showing annual SBI across the apertures (at 15-min timesteps) for all four cases (right) (Mardaljevic, 2020)

2.1.3 Existing Workflow for BIM Daylight Simulation

- Revit ↔* Dynamo (Ladybug, Honeybee, Energy Analysis for Dynamo);
- Revit →** Export as .DXF/.DWG → Import to Rhino ↔ Grasshopper (to analyze all components need to be specified);
- Revit ↔ Rhino Inside Revit (RIR) ↔ Grasshopper (Honeybee, Ladybug, Dragonfly, Bombyx, Pachiderm, OneClickLCA);
- Revit ↔ Revit Connector → Import to Speckle Stream → Open Speckle Web Account Copy the link → Import as link connected to Grasshopper "Receive" node from Speckle Connector → Define objects attributes → further analysis on Grasshopper (Honeybee, Ladybug, Dragonfly, Bombyx, Pachiderm, OneClickLCA).

Figure 8: four possible BIM daylight workflow (Shoshev, 2023)

In Shoshev's research (2023), daylight simulation software like Desktop Radiance, Rayfront, Ecotect, Open Studio, Macumber, Diva4Rhino, LadyBug tools (LB), Sefaria, Climate Studio are compared and considering with BIM model, and four promising, most used and accurate workflows of transmitting data from BIM for daylight simulation purpose are listed, and the one using Rhino Inside Revit is chosen and implemented in details steps, but the rest are not tested and explained (Figure 8).

Dynamo is a text-based programming language for Revit that operates efficiently in real-time for tasks such as data transfer and geometry construction (Alisherbek, 2021). Revit has featured an accessible API since the early 2000s, designed to accommodate multiple users, including those in structural and MEP disciplines. When writing scripts targeting Revit's API, the process can be viewed as making a series of database calls constrained by the API's rules. Most online examples pertain to model management in conjunction with Dynamo (Green, 2020; Miller, 2012). The Revit API facilitates easier manipulation of properties and components, simplifying and automating processes for family creation (Shah, 2021). However, running simulations using Dynamo workflow relies on the desktop version of Revit, which may not be as user-friendly as desired. Nonetheless, Dynamo can be utilized within Revit to manage BIM information.

Both the Speckle stream and DXF/DWG workflow face challenges regarding potential loss of elements or properties during translation in post-experiment phases. This research will adopt a workflow similar to that of Porsani, additionally exploring user interaction for controlling simulations with BIM models. This approach aims to replace the conventional method of initiating simulations locally on the Grasshopper (GH) canvas with a click, thereby providing a more comprehensive exploration of the topic.

2.2 3D City Models & Daylight Analysis

The most comprehensive standard for semantic 3D city models today is CityGML (City Geography Markup Language), developed by the Open Geospatial Consortium. (Pantazatou et al., 2023), Currently the most used version is CityGML 2.0 (Noardo et al., 2020), which defines five LODs (Figure 9).

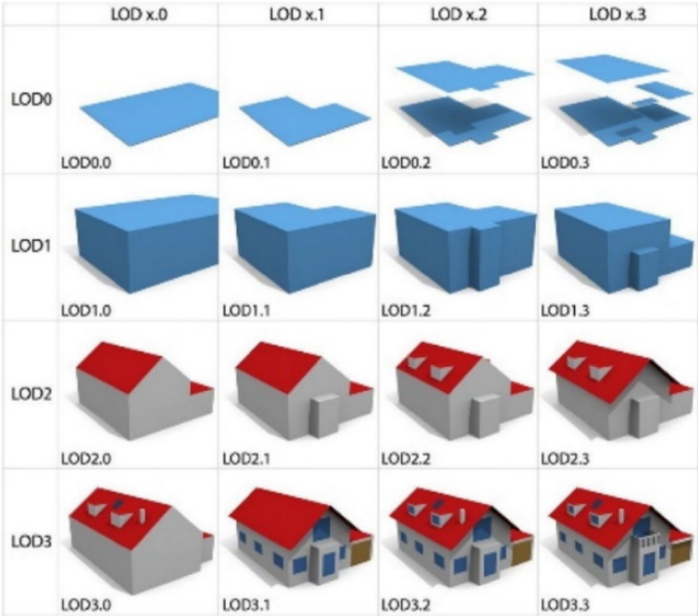

Figure 9: A refined version of LOD definitions in CityGML 2.0. LOD4 indoor representations are not included. (Biljecki et al., 2016)

In Pantazatou's team's research (2023), it is possible to use LOD1.3 3D city model for daylight analysis, since the most of the results show that both LOD2 and LOD1.3 yield similar OA-value results that don't differ more than 1° in most roof types. But in neighborhoods characterized by buildings with gabled roofs should preferably be handled utilizing 3D city models whose LOD allows for a more detailed representation of the roof geometry as the difference in OA degrees sometimes exceeds 10° (Figure 10). LOD 1.2, 1.3, and 2.2 are supported by the regional database of Delft in the Netherlands (3DBAG Viewer, n.d.). In this case study, LOD1.3 and LOD2.2 of model will be used and compared.

Figure 10: Examples of how lower LOD versions of the same building may generate higher OA than their corresponding LOD2 counterpart, when the roof type is gabled roof (Pantazatou et al., 2023)

2.3 Desktop Rhino vs. Rhino Compute

Rhino with its visual programming language GH are particularly popular choices for modern workflows working with parametric models. However, as many CAD tools, Rhino and GH has certain level of complexity to learn, even for the most dedicated 'students' within a professional architect team that use Rhino as the working tool, it still takes 4-6 weeks for GH beginner to using it independently on projects. (Tait, 2022). Sending GH script to designer's desktop and executing locally would require designer to understand GH and set correct input and output on the script canvas, this was once also a problem in KPF team. (Leon & Pachuca, 2022). As 3D modeling and design grow more intricate, more designers and engineers are opting for cloud-based solutions to simplify their workflows and enhance collaboration with colleagues, clients, and other stakeholders (ShapeDiver, 2024). Rhino Compute, different from Rhino Desktop, can do geometry calculations through a cloud based stateless REST API, and access 2400+ RhinoCommon API calls from outside Rhino, and provides libraries with standalone C#(.NET), Python and JavaScript. (McNeel, 2020). It is an opensource project that allows you to run Rhino.Inside on a local server or in the Mcneel Rhino Compute cloud, allow you to access Rhino and GH through a web API to run the program. (Ronald, 2021). Rhino Compute helps lowers the entry barrier by simplifying complex workflows for typical architectural designers while enhancing extensibility for computational designers. As a geometry solver back-end, it facilitates the development of user-friendly front-end applications accessible through a web browser, allowing architects to perform complex parametric workflows with minimal technical effort. (Leon & Pachuca, 2022). Table 2 shows the comparison between desktop rhino and rhino compute.

Difference perspectives \ Options	Rhino Desktop	Rhino Compute server
Deployment	Installed and run locally on a user's computer	Typically deployed on a server or cloud environment, allowing users to access Rhino functionality remotely.
Access	Requires installation on individual machines, and users interact with the software directly on their local devices.	Allows users to access Rhino functionality through APIs (Application Programming Interfaces) over the internet, enabling remote computation.
Performance	Performance is dependent on the user's local hardware.	Performance is influenced by the server or cloud environment's capabilities. It can provide scalability and the ability to handle more complex computations.
Collaboration	Collaboration is limited to sharing files, and users need to have Rhino installed locally.	Supports collaborative workflows, as users can interact with Rhino functionality without requiring the software to be installed on their machines.
Scalability	Limited to the capabilities of an individual machine.	Offers potential scalability for handling larger datasets and complex computations by leveraging server resources.
Use Cases	Ideal for individual or small team projects where users have local access to the software.	Suited for scenarios where computation needs to be performed on a larger scale, shared across multiple users, or integrated into web applications, without local Rhino installation
Intergration	Typically used as a standalone application	Can be integrated into web applications, custom software, or other systems through APIs, enabling a more flexible and extensible use of Rhino functionality.

Table 2: Rhino Desktop vs. Rhino Compute Server

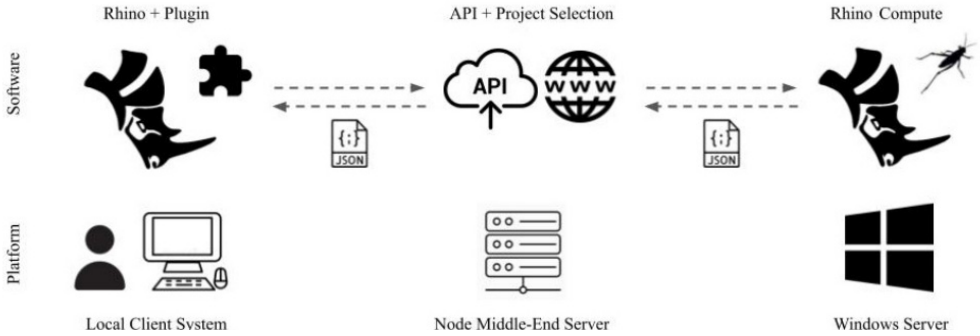

Figure 11: Rhino Compute technology (Azel, N., Pachuca, B., & Wilson, L., 2022)

Rhino Compute is used by some large architecture firms, with GH scripts managed and processed on a Rhino Compute Windows server, enabling teams to explore design alternatives without requiring GH expertise (KPF, 2020). Running complex simulations with GH plugins may require powerful hardware and user may experience long computation times for simulation, but it can save a lot of time if holding on a powerful server (Figure 11).

1. IAAC MaCAD track student projects (Ingrassia, M, 2021)
2. KPF Scout. (n.d.)
3. Web application workshop AEC Tech 2019 combine Rhino Compute, Three.js, vue.js, node.js, express.js, mongodb (Mm-Wang, 2019)
4. Arup InForm. (n.d.)
5. Daylight Compliance prediction web tool using Rhino.Compute (Pacheco Dieguez, A., & González, D, 2024)

Figure 12 demonstrates the results of daylight simulation of a simple room using Rhino Compute with webpage as client.

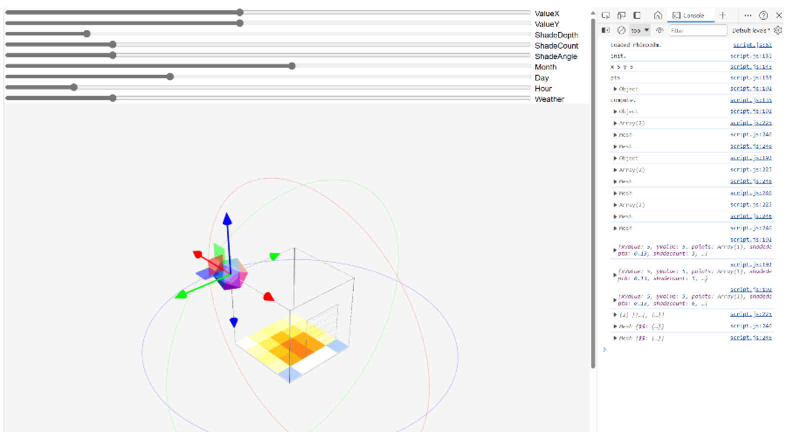

Figure 12: Daylight simulation trail using Rhino compute and hosting on a webpage

2.4 BIM AND SIMULATION IN MAPBOX GL

The visualization of BIM and GIS geometry data typically necessitates the integration of BIM data into GIS environments or vice versa, with the former approach being more common. Many of these conventional workflow process and visualize BIM a data on a GIS-based web platform, where user-friendly interfaces already exist. (Cambridge Computational Modelling Group, 2023). But not all possess the capabilities to process and manipulate BIM models (Shkundalov, D., & Vilutienė, T., 2020). Some study and examples posse capability to interact with BIM model, however, much of this interactivity is initially prominent, akin to a preview function that declines after the model is imported into the GIS platform, subsequently resulting in the loss of element-level interaction capabilities:

1. View Revit models inside Mapbox using Autodesk Forge (Wallabyway, 2019)
2. Place BIM model everywhere in Mapbox, reading IFC properties by clicking elements before placing. (Helenkwok, 2023)
3. A NYC park analysis tool using Rhino, Vue.js, Mapbox.gl, apex-charts, Three.js, and Tailwind CSS (Pachuca, n.d.)
4. The World Avatar: BIM-GIS Integration in CesiumJS (Cambridge Computational Modelling Group, 2023)
5. CDC BIM campus digital twin WebGL browser (CIMS lab, 2023)

The challenges of interacting with BIM data within MapboxGL are as follows:

1. The objects within the model lack coordinate system recalibration and inter-object relationships, classifying them as a collective rather than a complex entity. The individual objects face challenges of being positioned by geodesic coordinates. (Shkundalov, D., & Vilutienė, T., 2020)
2. WebGL doesn't directly support any BIM format, thus conversion to a format that retain attribute information with 3D objects for further processing and support interconnections among the objects within the BIM model is important. (Shkundalov, D., & Vilutienė, T., 2020) The semantic conversion faces challenges, many solutions from BIM to GIS, are one-directional (Celeste et al., 2022).
3. Conversion coordinates system between Web supportable Mercator projection and geodesic coordinates system. (Shkundalov, D., & Vilutienė, T., 2020)

2.5 TOOL SELECTION

The comparison of using Revit and Rhino is listed in Table 3. While Forge Design Automation for Revit enables task automation within the Revit platform, it is not ideally suited for hosting and displaying intricate simulation results such as 3D meshes directly. Its primary function centers on automation and computational design within Revit, with a focus on numerical data management rather than the direct hosting and visualization of complex simulation outcomes. Although visualization outputs are feasible, producing detailed meshes as explicit outputs from the API is not typically straightforward, ultimately necessitating the use of Forge Viewer as the sole hosting option, without the flexibility to employ third-party web viewers. Considering the workflow's complexity and the required detail level for visualization, Rhino Compute provides a more straightforward method for hosting and visualizing complex simulation results. Furthermore, Rhino offers enhanced user-friendly parameterization capabilities, aligning with the objectives of further design iterations. Although Revit may initially appear advantageous due to its direct linkage with BIM models at the outset of this research, Rhino ultimately proves to be the superior tool due to its broader compatibility.

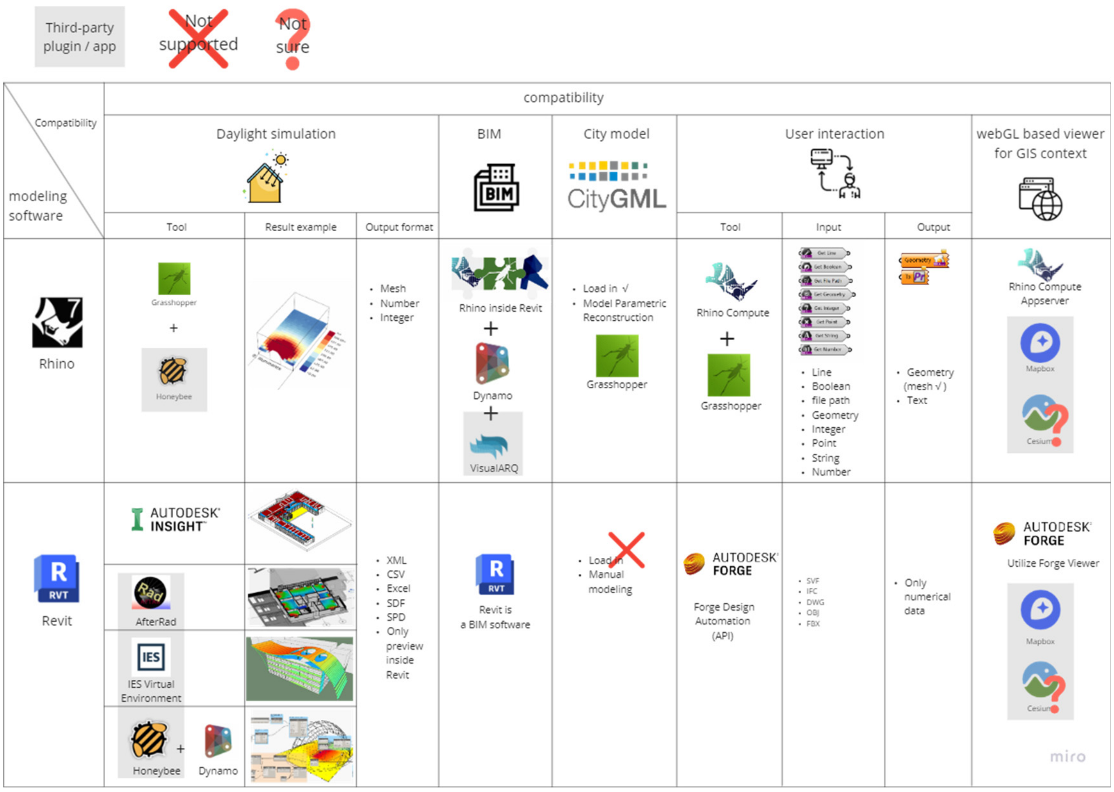

Table 3: Revit and Rhino workflow's compatibilities

The tools used in this thesis is listed in Table 4.

Dataset or Software	Source	Usage
3DBAG Delft	(3DBAG Viewer, n.d.)	Database containing detailed 3D model for Delft and BK building's neighborhood. Used as context geometry in HB daylight simulation.
Rhino 7.36	(Robert McNeel & Associates, n.d.)	Modeling software function as a visualization platform for setting up daylight simulation, built-in tool GH can parametrically adjust the geometry
Grasshopper	(Grasshopper, n.d.)	Visual programming language inside Rhino, used to give instruction to Rhino Compute to run daylight simulation
Ladybug/Honeybee 1.8.0	(Ladybug Tools | Home Page, n.d.)	Daylight simulation plugin for GH
Mapbox	(MapBox | Maps, Navigation, Search, and Data, n.d.)	WebGL based development 3D map platform for per-room daylight application
Threebox	(Jscastro, n.d.)	Three.js plugin for Mapbox GL JS, for loading and interacting with building geometries and simulation mesh result
Three.js	(Three.js – JavaScript 3D Library, n.d.)	JavaScript library using WebGL that enables the creation and display of 3D geometry in web browser
Revit 2024	(REVIT for Architecture & Building Design | AutoDesk, n.d.)	Modeling software to store and modify BIM information,
Dynamo	(Learn - Dynamo BIM)	Revit's API, used to tag room information and export BIM data
Rhino Compute	(Mcneel, n.d.)	Rhino's API, JavaScript library is used for web application
RhinoCityJSON	(Cityjson, n.d.)	Rhino/ GH plugin that enables direct use of the CityJSON format in Rhino and GH.
DiStem	(DiStem Bundle for Autodesk Revit - Productivity Revit Plugins by DiRoots)	To export Revit model to glTF file format
Conveyor v4	(Proving Ground)	Plugin for geometry and data management between Rhino and Revit
GitHub	(Github, n.d.)	Hosting of application
VS Code 2023	(Visual Studio)	Used to add functions and build dashboard on Mapbox

Table 4: Tools and data used in the thesis

3 / Methodology

3.1 Theoretical Framework

This thesis is centered around three primary themes: BIM, GIS, and daylight simulation (per-room), culminating in a web application that integrates these elements into a cohesive workflow. The workflow utilizes GH script as the back-end, Rhino Compute as the API connecting the front-end and back-end, and MapboxGL as the front-end and GIS platform for user interaction (Figure 13).

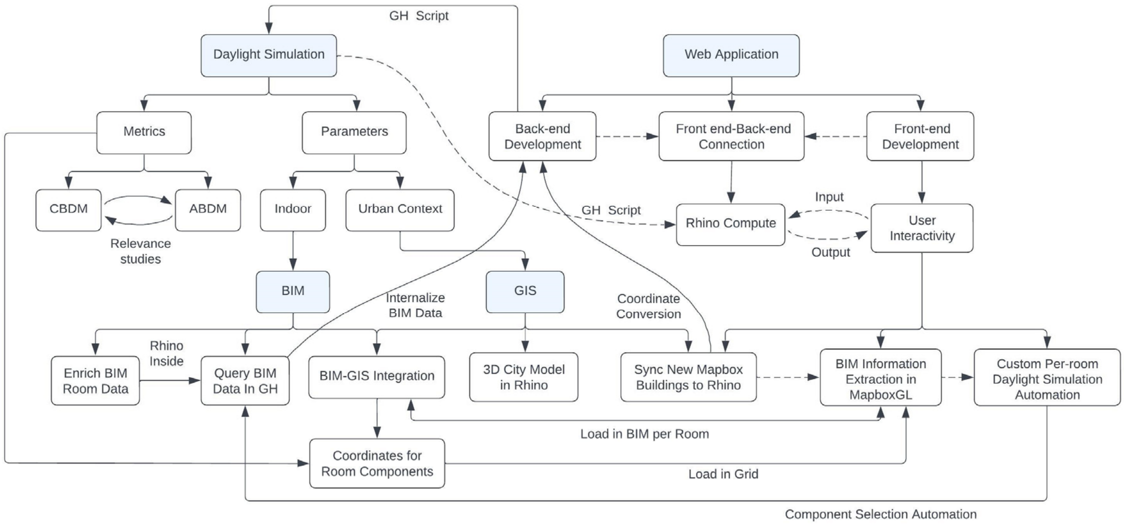

Figure 13: Project theoretical framework

The conceptual framework (Figure 14) depicts the transformation process of data and 3D information across multiple platforms. The result enables users to interact with the web application, utilizing BIM data extraction in MapboxGL and custom per-room daylight simulations, seamlessly integrating BIM into GIS for effective urban planning and design.

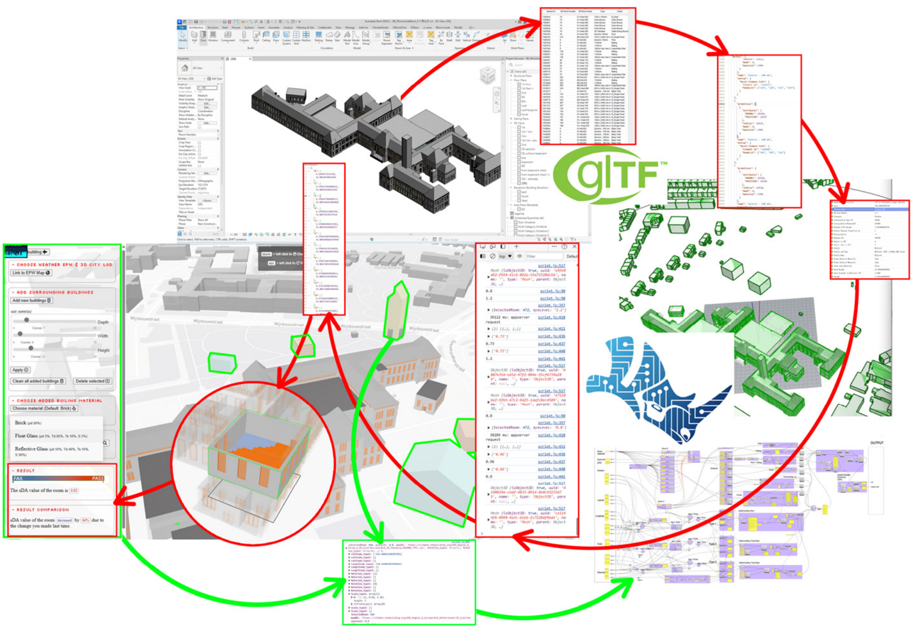

Figure 14: Project conceptual framework

3.2 Methodology Workflow

The methodology of this study is structured from four distinct perspectives: Daylight, BIM, GIS, and Application, which integrates the first three. This thesis is organized into several key sections: research framework, literature review, implementation section that includes settings and data preparation, and the final section that presents results, discussions, and conclusions (Table 5).

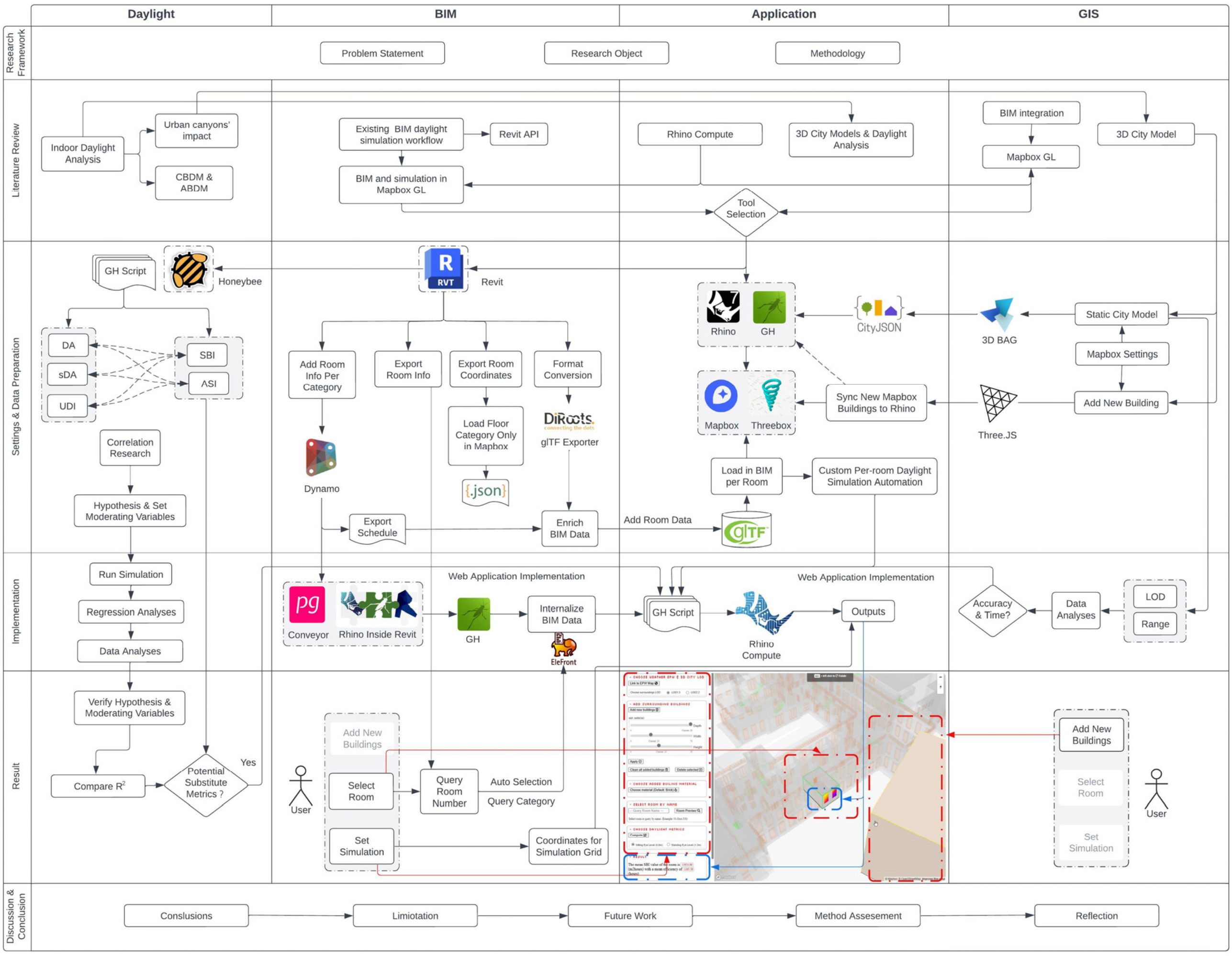

Table 5: Project workflow

SBI simulation

Mardaljevic (2021) highlighted certain factors such as space types, obstruction scenarios and climate conditions that needs further investigation to provide calibration data for comparative assessments between CBDM and ABDM. In practice, the configuration of a room and its windows is subject to a myriad of variables that impact "interior daylighting effect," consequently impacting the relationships among SBI , Sky lumen, and daylight metrics such as DA, SDA, and UDI. These variables encompass diverse factors including the quantity and dimensions of windows, their orientation, materials and angular disposition relative to the floor, their distribution within the room, window-to-wall ratios of the façade, height of window sills, the presence or absence of canopies and extended shades, the design of outdoor balconies, and the availability of internal shading mechanisms like curtains or blinds. Moreover, the intrinsic characteristics of the room itself, such as its dimensions and geometric layout, alongside external factors like geographic properties, surrounding environment, and local climatic conditions, contribute significantly to this complex interplay.

To compute total annual SBI, denoted as $Stot$, the cumulative sum of SBI throughout the entire year with a sun altitude γ_s greater than 0 was computed. This parameter, γ_s, can be acquired through the LB Sun Path component (Equation 5).

$$Stot = \sum_{\gamma_s > 0} (Ai\cos\theta\Delta t) \qquad (5)$$

Moreover, the individual St values spanning the entire year can be utilized to populate a two-dimensional matrix, T (Equation 6). For hourly data with a time step of 1 hour, T possesses dimensions of 24 * 365. The time step is set to 15-min interval as suggested by Mardaljevic & Roy (2016). The disparity between the actual solar position at each time step and the nearest precomputed point on the sky vault is less than 2.38. This discrepancy is approximately equivalent to a 9-minute interval, yet it does not entail unnecessary consumption of computational resources.

$$T = \begin{bmatrix} S_{1,1} & \cdots & S_{1,365} \\ \vdots & \ddots & \vdots \\ S_{24,1} & \cdots & S_{24,365} \end{bmatrix} \qquad (6)$$

In order to address the substantial impact of the low-angle sun on vertical apertures and its consequential effect on SBI value, a new airmass coefficient, is proposed by Mardaljevic & Brembilla (2021), which serves as an attenuation factor characterizing the optical density of the atmosphere from sea level to the zenith. Its introduction rectified the original formulation of SBI-Classic, enhancing its accuracy and comprehensiveness (Figure 15). thereby culminating in the revised model termed SBI-AM. AM is first employed by Kasten (1965) (Equation 7).

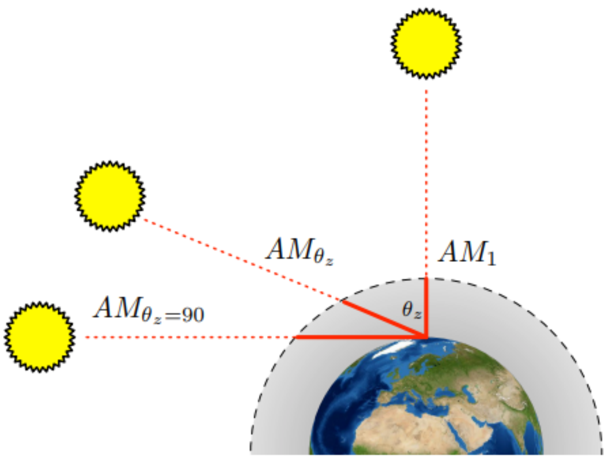

Figure 15: Airmass (AM) as a function of solar zenith angle θz (Mardaljevic & Brembilla, 2021)

$$AM = [cos_{\theta_z} + 0.15(93.885 - \theta_z)^{-1.253}]^{-1} \qquad (7)$$

The correlation between altitude angle, zenith angle and angle of incidence is shown in Figure 16. In the case study of this thesis, all apertures of BK building are perpendicular to the ground, Consequently, angle of incidence (the angle between the sunlight and the window normal), denoted as θ is numerically equivalent to γ_S.

$$\theta_z = 90° - \gamma_s \qquad (8)$$

$$\theta = \gamma_s \qquad (9)$$

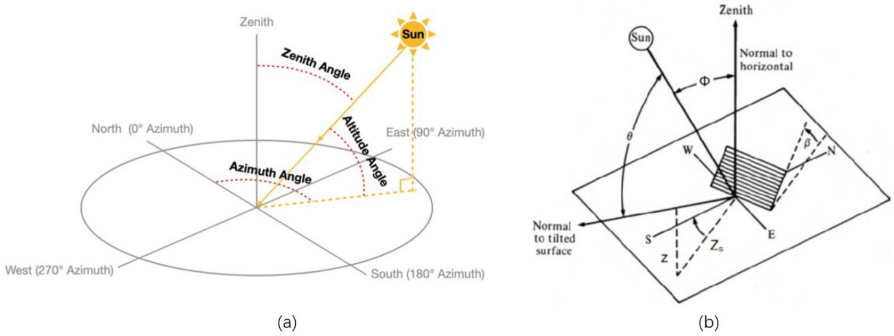

Figure 16: correlation between altitude angle, zenith angle and angle of incidence

The solar constant, representing the solar irradiance outside earth's atmosphere under air mass 0 conditions (Equation 10), is $I_0 = 1.353\, kW/m^2$ (Wikipedia, 2023). h is the elevation level above sea level in km (Meinel and Meinel, 1976). On Netherlands topographic map, the elevation level of Delft especially around the BK building is 0.004m (Netherlands Topographic Map, Elevation, Terrain, n.d.). This also functions as the elevation input for LB Construct Location component in GH, note that this input should be provided in meters.

$$I_{am} = I_0[(1 - 0.14h)0.7^{AM^{0.678}} + 0.14h) \qquad (10)$$

f_{am} (Equation 11) for a given solar angle is an inherent property of a particular location (Mardaljevic & Brembilla, 2021), Another metrics called SBI-efficiency can be calculated by deviding SBI by the area of the aperture (Equation 12).

$$f_{am} = \frac{I_{am}}{I_1} \qquad (11)$$

$$S_{tot_{eff}} = \frac{Stot}{S} \qquad (12)$$

Sky Lumen Simulation

In comparison to the angular view, the hemispherical fisheye view is of greater accuracy in depicting the illuminance received at the sensor point. (Mardaljevic, 2021). Existing photo processing methods predominantly entailed the transformation of fisheye images into conventional viewpoints, thus, the techniques for generating hemispherical fisheye view and conducting subsequent color analysis emerged as the starting point for resolving this challenge.

The approach adopted in this thesis is employing the imaging principle of hemispherical fisheye to construct circular geometric sensors units directly in Rhino. Inside these units, different segments corresponding to building projection, sky projection, ground projection, and shade projection are assigned specific colors. Subsequently, the area of each color-coded section was calculated and their respective proportions within the sensor unit is assessed. This approach is inspired by Inanici's research in 2009. The 3D geometry of the surrounding buildings is first projected onto a hemisphere that is perpendicular to the aperture plane (Figure 17).

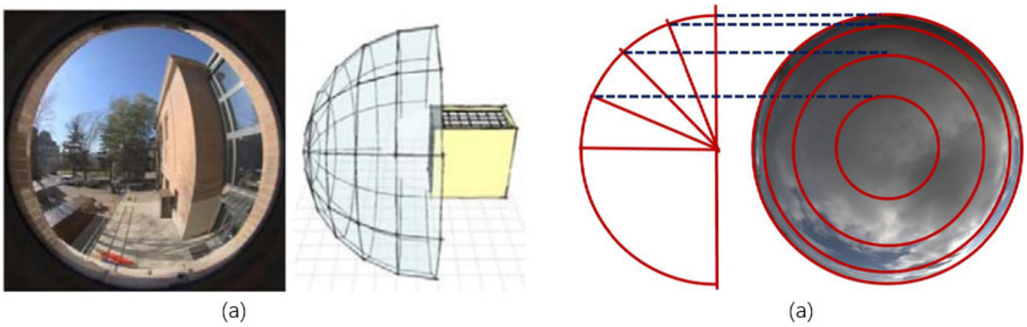

Figure 17: Vertical hemispherical fisheye image of the aperture (a); hemispherical projection of sky (b) (Inanici, 2009)

Subsequently, this projection onto the hemisphere is further transformed onto a circular sensor unit aligned parallel to the aperture. (Figure 18).

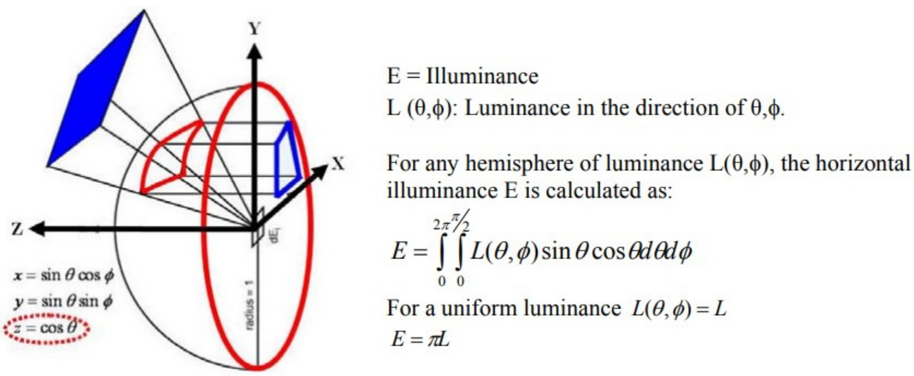

Figure 18: Calculation of illuminance from luminance values in hemispherical fisheye projection (Inanici, 2009)

As shown in Equation 13, the illuminance of three layers adds up to 2000lux (Mardaljevic, 2021).

$$2000 = E_{sky} + E_{sky} + E_{gnd} \qquad (13)$$

And according to Equation 14, the total lumens φ of an aperture with area of A can be determined by multiplying A by the mean illuminance $\overline{E}$ (Mardaljevic, 2021).

$$\varphi = \overline{E}A \qquad (14)$$

The "lost" lumens refer to those lumens that are obscured due to the shading effects of the reveal (Mardaljevic, 2021) can be calculated using Equation 15. φ_{sky}, which holds paramount importance in the study can be calculated in a similar approach..

$$\varphi_{lost} = 2000A - (\varphi_{sky} + \varphi_{obs} + \varphi_{gnd}) \qquad (15)$$

In the end, for any aperture of specific dimensions, the task is assessing the relative allocation of area occupied by different colored patches.

Daylight research

Simulations will be conducted in simplified room settings modeled under varying conditions to explore the correlation between SBI, sky lumens (ABDM), and CBDM daylight metrics DA, sDA, and UDI. Initially, GH scripts for SBI and sky lumens will be developed based on established physical principles and extant research. Subsequently, experimental rooms will be configured to facilitate the assessment of data correlations and potential influencing factors. Post-simulation, the data will undergo preliminary analysis. Should the correlation prove elusive or subject to numerous influencing variables, efforts will be made to elucidate the factors potentially affecting these correlations, with the aim of integrating these insights into the Mapbox application.

The hypothesis is: **There may exist a correlation between SBI, Sky Lumen (explanatory variable) with DA, sDA and UDI (independent variable), however, this correlation fluctuates depending on the influence of moderating variables.**

It can be readily pictured and comprehended that by dividing a central window on a façade and shifting each part towards the edges, the light distribution on a horizontal plane parallel to the floor inside the room changes. This adjustment likely improves illumination in the room's corners adjacent to the façade. However, the overall direct sunlight exposure and sky visibility through the two openings may remain relatively stable, especially when distant and small obstructions are present. This implies that the positioning of openings is a potential moderating variable affecting the correlation metrics.

It is important to note that validating the moderation variables involves comparing the fit of two subsets of data within the larger dataset. This is done by comparing the R^2 values between the two subsets and the regression line (Eqs. 16-19). An R^2 value can be negative, indicating a very poor fit. To calculate evaluate this, the mean of actual values $\bar{y}$ was calculated from actual values y_i and predicted values $\hat{y}_i$. With the number of data points n being 6 in this case, the total sum of squares SS_{tot} and the residual sum of squares SS_{res} were computed. The R^2 value was then determined.

$$\bar{y} = \frac{1}{n} \sum_{i=1}^{n} y_i \qquad (16)$$

$$SS_{\text{tot}} = \sum_{i=1}^{n} (y_i - \bar{y})^2 \qquad (17)$$

$$SS_{res} = \sum_{i=1}^{n} (y_i - \hat{y}_i)^2 \qquad (18)$$

$$R^2 = 1 - \frac{SS_{res}}{SS_{\text{tot}}} \qquad (19)$$

Get BIM 3D data to Rhino & Mapbox

There are four primary methods for transferring BIM models and information from Revit to Rhino (Table 6). The first involves using Speckle, an open-source 3D data platform widely recognized in the AEC industry (Speckle, 2024). One limitation of Speckle is that it transfers models as mesh surfaces, which complicates adjustments in GH during later stages, and it requires manual addition of attributes to maintain data index correspondence. Despite these challenges, Speckle holds considerable promise and warrants further exploration. The second method is by using VisualARQ, in preliminary trials, it was noted that some elements, such as walls, could not be converted. Due to the time constraints of this study, a comprehensive exploration of the plugin's extensive capabilities was not possible. Alternatively, Rhino Inside Revit allows direct BIM integration. Shoshev (2022) investigated per-room daylight simulations using this method. Nevertheless, the complexity and scope of the BIM model in this thesis, characterized by multiple room tags and a vast array of elements, make this approach less appropriate. A third-party plugin was necessary to effectively transfer attribute data, due to time constraints within this study, a more expedient commercial plugin was employed - Conveyor. Upon utilizing the surveyor, the value and key of all relevant Revit information can be accessed directly from the attribute column of the Rhino panel. This information can subsequently be retrieved using the eleFront plugin (eleFront, n.d.), as will be detailed in Section 4.3.

GLTF is identified as the best format for importing BIM models into Mapbox. In the study, the DiStem plugin is utilized, multiple comparable plugins are also available. The choice of plugin significantly affects the final file size and display materials. For instance, in this case study, the bin file generated using the e-verse plugin is 71,021kb, more than double the size of the bin file generated by DiStem, which is 32,536kb. A more extensive comparison of plugins is limited due to the commercial nature of most software, restricting the breadth of analysis possible within this study.

option / goal	Method	Tool	Result	Pros	Cons
Revit → Rhino		SPECKLE Way 1	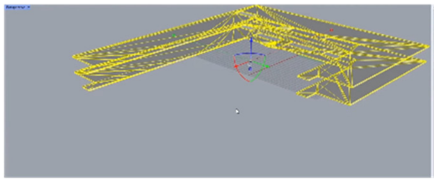	• Open source	• Mesh Difficult for component adjustment
	Rhino inside Revit	VisualARQ Way 2	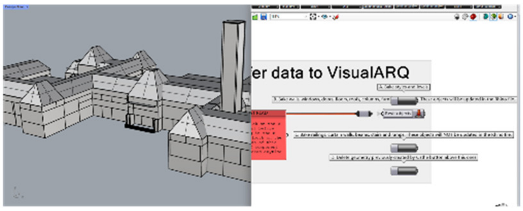	• Easy operation	• Commercial tool • Incomplete conversion
		pg Conveyor Way 3	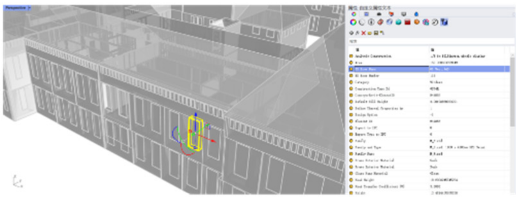	• Easy operation	• Commercial tool
		Way 4	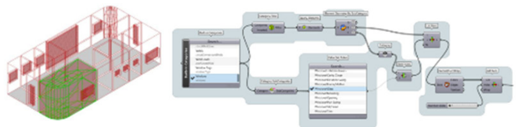	• Easy operation • Open source	• No Revit information

Table 6: Tool selection for Revit to Rhino conversion

BIM-GIS integration

For the BIM-GIS integration, the objective is to develop a web application using the BK BIM model as a case study, encompassing the entire workflow. Following the selection of tools based on literature review, the initial step involves setting up and preparing data for both BIM and Mapbox. Rhino serves as the intermediary platform connecting these two data formats during this stage. While Rhino is not necessary for the application to run, it plays a crucial role in the construction process. This process involves three key steps: extracting room information from BIM elements and preparing it for import into Rhino, importing the interactive BIM model into the Mapbox platform, and synchronizing user-added buildings in Mapbox with the back-end GH.

Integrating BIM to WebGL generally involves workflow in Figure 19 (Yan, Z et al., 2023), BIM data is first separated into geometric and non-geometric parts. Geometric data is processed as glTF to reduce the size of the 3D asset and the computational load required to unpack and use it at runtime. Non-geometric or attribute data is exported as JSON files, a lightweight data exchange format. Element IDs link these two data types. This workflow of first separating and then matching data enhances the flexibility of data integration.

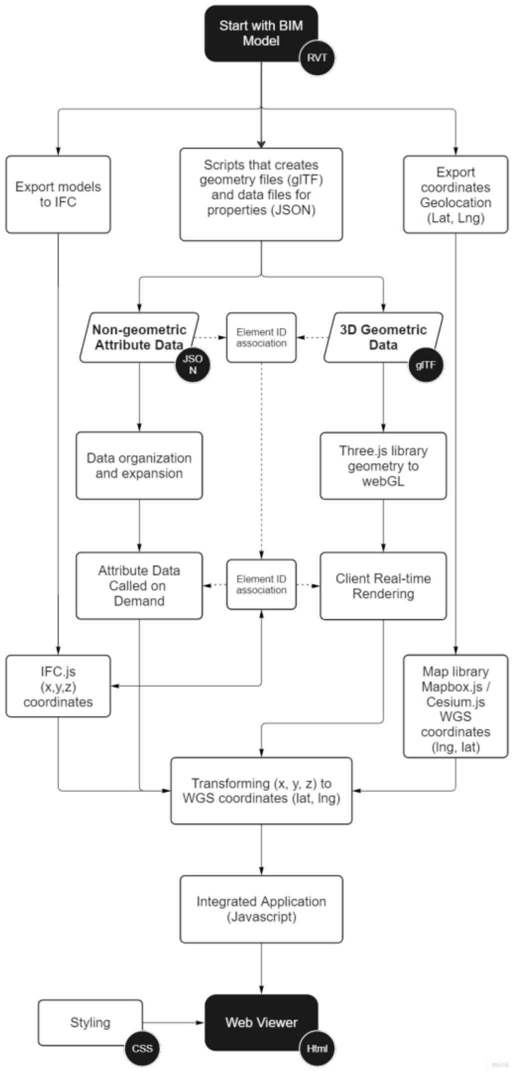

Figure 19: WebGL based interactive application workflow - BIM / GIS (Yan, Z et al., 2023.)

Synchronize added building coordinates in Mapbox & Rhino

Mapbox is proficient in interpreting the coordinates of all appended geometries, whereas Rhino operates with xyz coordinates rather than latitude, longitude, and altitude, underscoring the necessity of converting the coordinates from Mapbox to Rhino. Given the procedural sequence in which the BK BIM model is imported initially, followed by the user's addition of surrounding buildings for interaction, it is essential to ensure that the coordinates transmitted to Rhino as input exclude those of the previously added BK model. The amount of imported sub models of BK building is closely associated with the chosen method of import. This exclusion is crucial to maintain the integrity of the spatial data handling in the project.

The requisite coordinate transformation in this context entails converting Geodetic coordinates to ENU (East-North-Up) coordinates (Figure 20). This is due to the fact that within the Rhino, the model is pre-aligned with the correct north orientation, and the center of the imported BIM model is designated as the world's center.

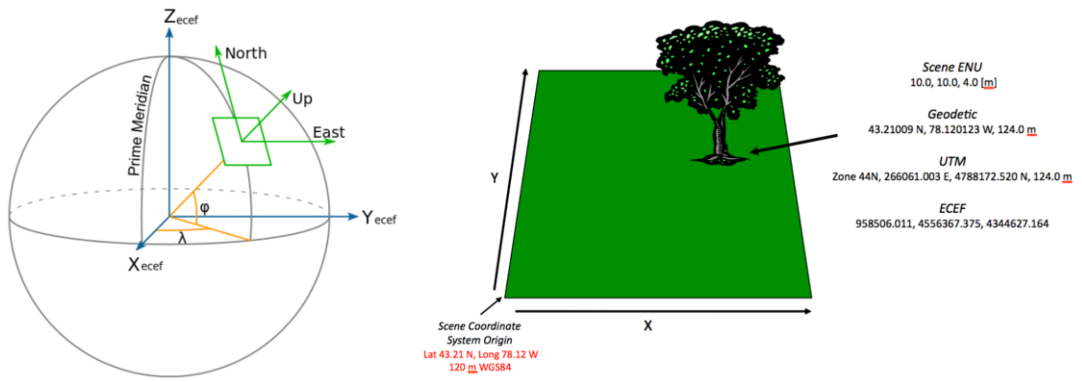

Figure 20: Relationships between Geodetic, ECEF and Scene ENU coordinate systems. (Wikipedia, 2010) (left) DIRSIG allows the user to use a host of coordinate systems to position objects (DIRSIG model, 2023) (right)

Tag elements' room information in Dynamo per category

Revit model exported in GLTF format includes an "Element ID" and "Family Name" for each mesh, which facilitates the subsequent enrichment of this data. It is necessary to identify each mesh by these identifiers before additional attributes can be appended. Choosing "Family Name" for identification is challenging because each name may correspond to multiple elements. Attempts to append suffixes to the Revit type have been made in Dynamo; however, due to the unique settings of system families such as floors and walls in Revit, this method proves infeasible. Consequently, "Element ID" has been selected for identifying individual elements. The initial step involves using Dynamo to label each element with a Revit "Element ID," which is then cataloged under the project parameter named "Element ID". The script is available in Appendix 4.

The principle is minimizing the number of project parameters created within Revit. Evidence from an experiment depicted in Figure 21 reveals that only a single data can be appended to each project parameter; creating lists is unfeasible because new data entries overwrite previous ones. Consequently, for elements that traverse multiple rooms (such as walls) or are shared by several rooms (such as doors), it is imperative to establish multiple room tags to adequately capture and store this information.

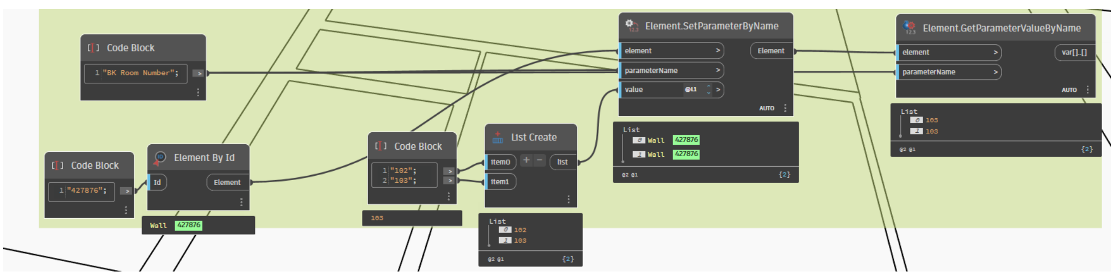

Figure 21: Every project parameter can hold one data in Revit

There is no standardized workflow for assigning room tags to elements across various categories. In a blog posted by Jeremy Tammik (2021), potential solutions proposed by Mastjaso and Matt were discussed. The applicability and outcomes of these solutions are contingent upon the initial BIM model. However, the overarching strategy involves implementing category-specific actions—such as creating dot matrices, offsets, etc.—to intersect with a room's bounding box or its boundary. These actions differ based on the type of element, such as floors, windows, doors, and walls.

In this thesis, the methodology primarily relies on whether the bounding box contains a center point or intersects with another bounding box, with the specific script detailed in Appendix 2, 3, 5. For the floor category, the center point is shifted upward for better accuracy. For doors, Clockwork package facilitates direct retrieval of information “from” and “to” rooms (Figure 22).

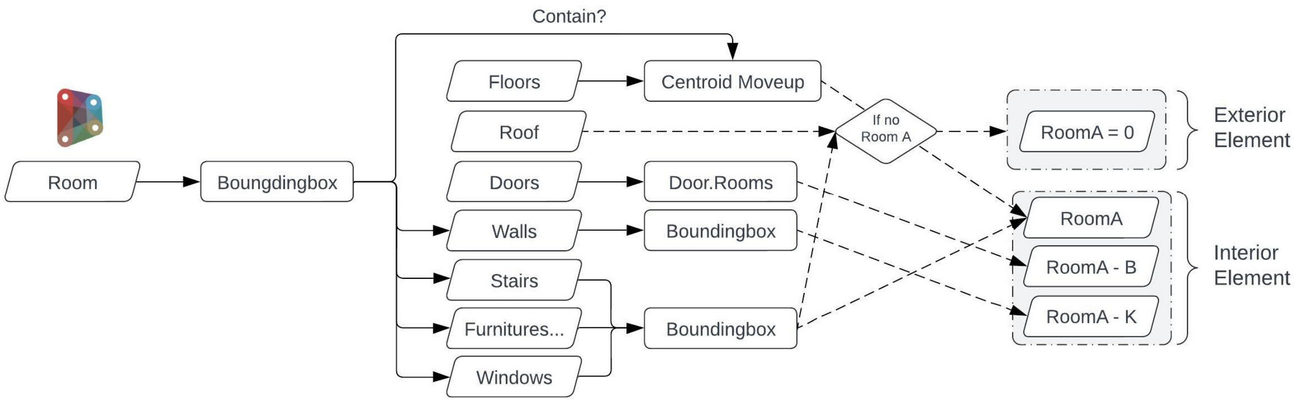

Figure 22: Framework for tagging room for different categories in Dynamo

Rhino Compute for Per room simulation automation

During the implementation phase, it is essential to filter elements and automate the process for each room, which includes converting the BIM model into GH. Another key focus is managing the inputs and outputs of Rhino Compute, ensuring that the simulation results are accurately displayed at the correct coordinates on the front-end.

Each time a user selects a room in the front-end, the room number, based on the CSV data from Section 4.1.3, is recorded and sent to Rhino Compute as input. The room number and category name are then queried in GH on the back-end to differentiate between the various rooms for the sunlight simulation. To accurately simulate sunlight, the geometry of the room must be processed to distinguish between different components and apply appropriate materials. For instance, since ceilings are not a predefined category in BIM, they can be created by copying and panning the floor (Figure 23).

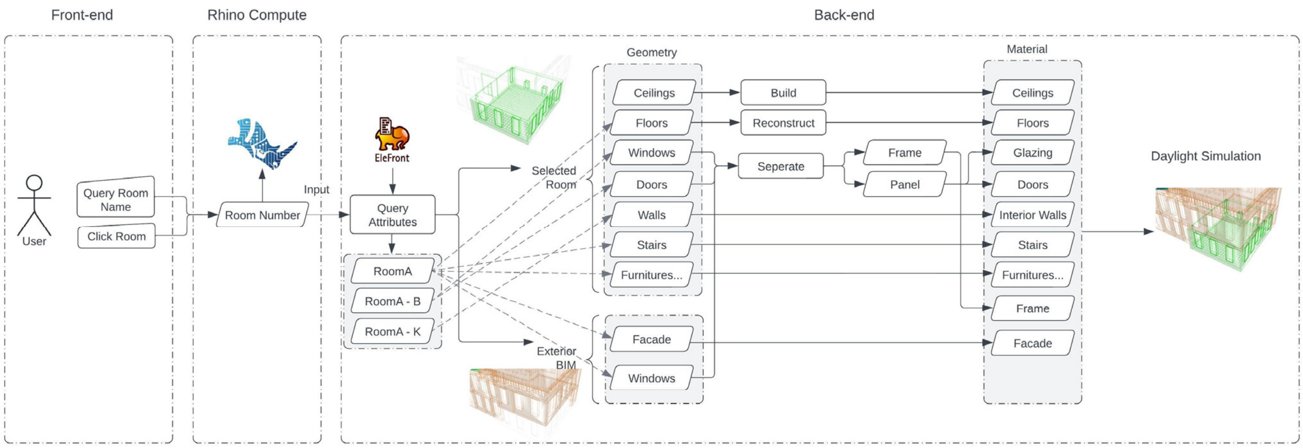

Figure 23: Workflow for BIM element selection automation in daylight simulation

At a broader level, the workflow for running a per-room daylight simulation involves the front-end, back-end, data processing, and Rhino Compute in between (Figure 24). When a user inputs data, it is transferred to Rhino Compute as integers, numbers, and strings. Based on the user's selection of LOD and metrics, Rhino Compute selects the corresponding GH script file (Appendix 12 is an example for DA simulation) for the server to execute (a copy of the GH file). The server performs the sunlight simulation according to the GH script instructions. Additionally, if the user adds extra buildings in Mapbox, the coordinates, materials, rotation angles, and other details are transmitted as lists to prevent null values when certain building types are

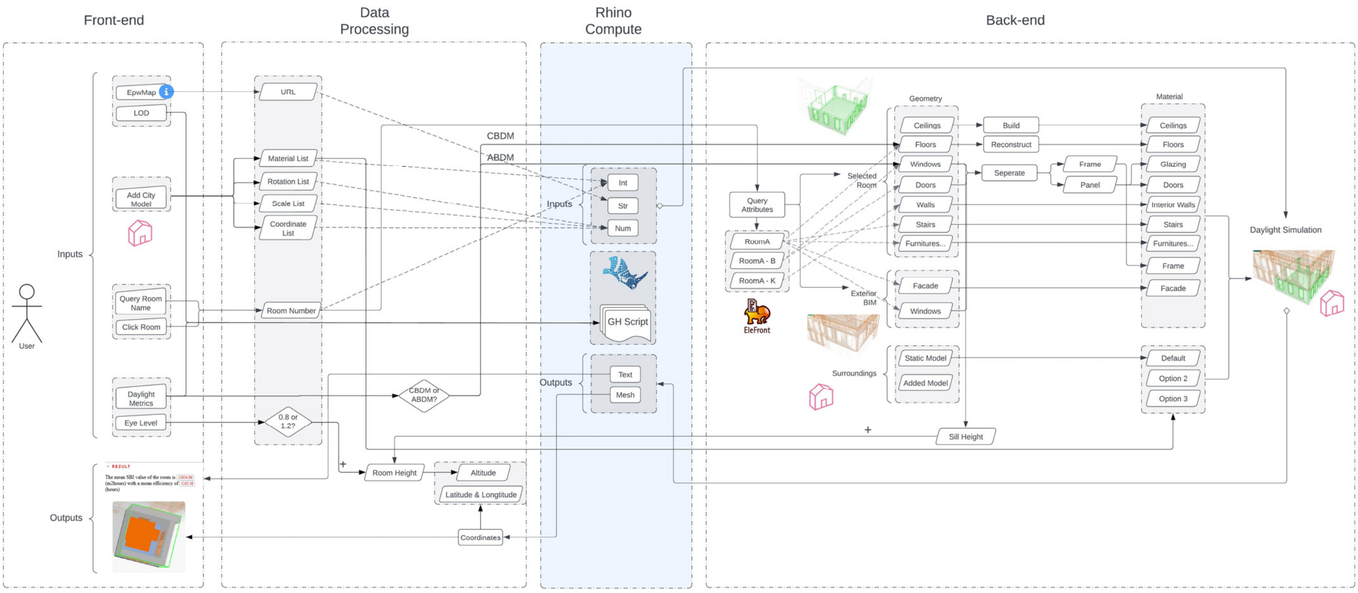

Figure 24: Rhino Compute workflow for BIM element selection automation in daylight simulation

absent, as discussed in Section 4.3.3.

Get Simulation Mesh Center of Selected Room

Another consideration in the data derived from the Revit model concerns the coordinate axes for each room for visualization of simulation result, which are indirectly obtained due to Revit's lack of a default latitude and longitude coordinate system. Two potential solutions are proposed to address this issue. The first involves integrating latitude and longitude information directly into Revit, assigning these coordinates as project parameters for each room for export in the same way as room tag information. The second solution requires separately importing the floors into Mapbox to ascertain latitude and longitude, followed by exporting in JSON format from Mapbox. The first approach carries a risk of discrepancies and uncontrollable deviations between the latitude and longitude assigned in Revit and those imported into Mapbox. In contrast, the second approach offers strategic benefits for future scalability. It allows for the workflow used in importing floors to be adapted for importing other elements into Mapbox at a later stage. This thesis employs the second approach based on its practical application and adaptability.

BIM models are frequently imported in Mapbox with an initial scale factor and a predefined degree of rotation, the process of rotating a point around a specific point on a 2D plane. When rotating a point situated at coordinates (x, y) around the origin, the coordinates of the newly positioned point will be (x', y'). θ represents the angle of rotation (Equation 20).

$$\begin{pmatrix} x' \\ y' \end{pmatrix} = \begin{pmatrix} cos\theta & -\ sin\theta \\ sin\theta & cos\theta \end{pmatrix} \begin{pmatrix} x \\ y \end{pmatrix} \qquad (20)$$

In Threejs, the children’s position is influenced by multiple layers of parents’ position (Figure 25).

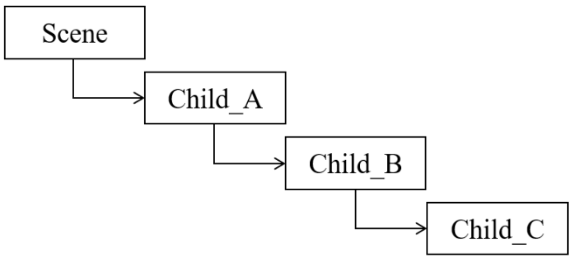

Figure 25: Children’s position and parents’ position

Workflow optimization

Comparing the effects of various LODs and static 3D data ranges is necessary to optimize the GH script and workflow. In the final phase, the main focuses are building the front-end platform, enhancing user functionality and interactivity, ensuring the correct input and output for Rhino Compute, and processing and storing detailed data to improve overall functionality.

The benchmark comparison evaluates the time and accuracy of daylight simulations using LOD 1.3 and LOD 2.2, with the assumption that LOD 2.2 provides more accurate results, which due to its inclusion of more detailed roof information, resulting in more precise OA values for per-room daylight simulations (Equation

21).

$$Percentage\ Difference = \frac{|Value_{LOD\ 1.3} - Value_{LOD\ 2.2}|}{Value_{LOD\ 2.2}} \times 100\% \qquad (21)$$

To optimize the workflow, the influence of the spatial extent of surrounding buildings on the accuracy and computational duration of daylight simulations are also evaluated. The geometric center of the BK model was used as the origin for range radius expansions, encompassing 200m, 250m, 300m, and 350m (There are different radius ranges for different BIM initial model sizes).

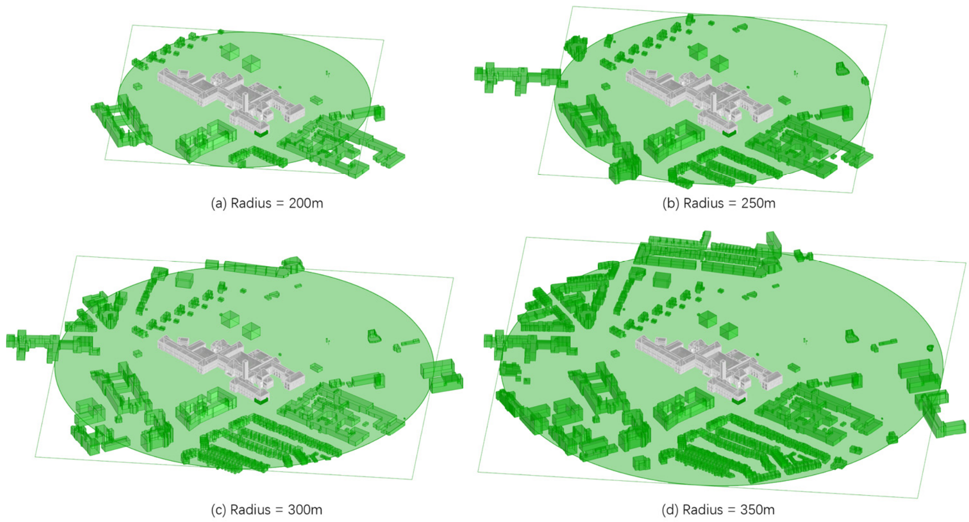

Figure 26: 4 radii for static 3D city model for case study

The benchmark for simulation accuracy regarding radius is based on the 350m range radius. This range is considered the most accurate as it encompasses the most extensive model information, ensuring a comprehensive analysis of surrounding buildings' impact on daylight simulation. Therefore, all other radius options (200m, 250m, and 300m) are evaluated against the 350m radius to determine their effectiveness and efficiency. For different radius, the dimensions of the planar geometry representing the ground varies, as shown in Figure 26. The ground material was configured using the HB Shade component and the HB Translucent Modifier. To simulate typical ground reflectance, the "diff_ref" value was set to 0.2, and the "diff_trans" value was set to 0. This represents ground materials like soil, grass, and concrete, which do not transmit light but instead reflect and absorb it

4 / Implementation

4.1 Settings & Data Preparation

4.1.1 Settings

Mapbox Settings

There are a few settings that need to be made to the Mapbox before the actual implementation (Figure 27).

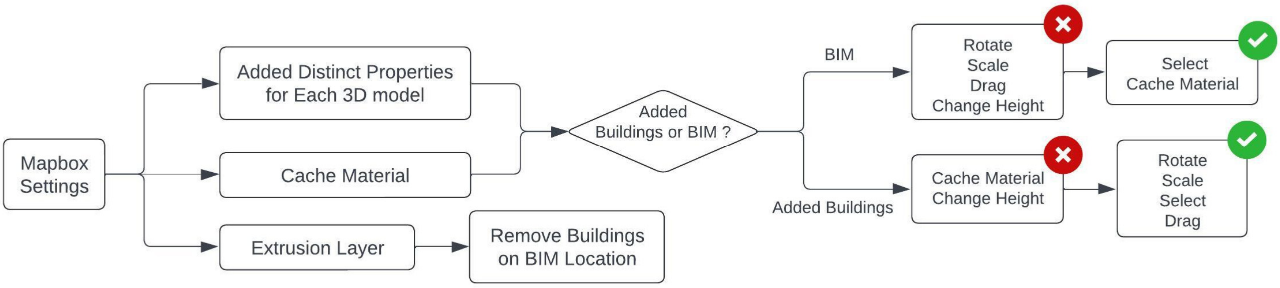

Figure 27: Settings in Mapbox

In the original Threebox library, the functionality over user interaction was limited to displaying Boolean values in the console bar to indicate whether an imported object had been selected. For enhancements, a more nuanced control mechanism was necessary, particularly for the manipulation of newly integrated 3D elements. The desired functionality for the newly added surrounding building geometry model included enabling selection, rotation, and translational movements without altering the object's altitude, while the BIM models imported subsequently were to be selectable without the capabilities for rotation, translation, or altitude modification.

Prior to the proposed modifications, the source code allowed only uniform properties of selectability, rotation, and movement across all objects rendered on the canvas. The specific requirement entailed the introduction of distinct properties for each loaded geometry within the application. These properties would govern the individual object's selectability, rotation, movement, and altitude change. Furthermore, it was imperative to develop a mechanism to store and display these properties within the console bar for continuous accessibility and monitoring. This enhancement would facilitate a more granular control over the interaction with different 3D models within the Mapbox environment. This enhancement was done by modifying the source code of Three.js as shown in Appendix 1.

Upon completion of the modifications, interacting with any geometry imported into Mapbox will allow for the retrieval of Boolean information, indicating whether the object is selectable, rotatable, draggable, and capable of altitude adjustment (Table 15).

To set up a 3D building layer within Mapbox, the default 3D buildings located in the vicinity of the BIM model on the 'add-3d-buildings' layer should be selectively filtered out by their IDs. This process requires manual adjustments. The integration of Threebox with Mapbox facilitates the activation of tooltips. These tooltips display on fill-extrusion layers and 3D models, allowing for the identification of existing building IDs at the BIM model's specified location. Subsequently, these buildings can be filtered using their IDs. In this case study of BK building, the relevant IDs are 44383237, 44383236, 253723359, 1081796637, 975016695, 975016694, 975016698, 975016697, 975016696, 1081796635, 1081796636, 253724106, and 44383240.

Threebox automatically caches materials, implying that any additional new buildings of the same type will retain the identical material. This function significantly enhances the efficiency of loading BIM model with static materials subsequently, but for newly added surrounding buildings, the cache must be manually deactivated to ensure material updates are applied.

GH Settings for per room daylight simulation

In less dense or low-rise areas where buildings do not over shadow each other significantly, the amount of light entering through windows primarily depends on direct sunlight and sky diffused light. The interior design elements have significant impact on indoor light levels. Thus, the selection of interior materials requires precise accuracy. This research will only focus on large surfaces and material options will also be set accordingly based on an additional requirement outlined in EN 12464-1.

The material database employed is sourced from the Spectral Materials Database: Home (n.d.). Selections were made based on the actual conditions within the BK interior. However, given the diverse color range of the flooring and walls, the materials were simplified for this analysis to a grey carpet and a white plaster wall. Since materials with roughness greater than 0.2 are not realistic in real life (Translucent Modifier | HB-Radiance Primer, n.d.), the roughness of some materials in the library has been slightly adjusted. The material selection can be found in Appendix 11.

Considering the current detail level of the BK BIM model and the need to balance accuracy with computing time, the input detail level for HB Radiance Parameter is set to 1, "medium". The recipe type is set to 2, "rfluxmtx | annual," to accommodate the annual daylight metric. The thresholds for metrics are listed in Table 7.

	DA	sDA	UDI
Settings	$E_{Threshold} = 300lux$ The minimum required illuminance level	$T_{Target} = 50\%$ 300 lux for at least 50% of the occupied time	$E_{Lower\ Limit} = 100lux$ $E_{Upper\ Limit}$ = 3000lux

Table 7: Settings of threshold for different daylight metrics in GH

Experiment and GH Settings for ABDM & CBDM correlation studies

Several potential moderating variables were investigated within the context of daylight simulation. Two basic room prototypes were modeled in Rhino: a small room (3m x 3.5m x 3m) and a larger room (5m x 4m x 3m). Two window sill heights (0.9m and 1.3m) were considered, with all windows sized at 2m x 1m. Windows were oriented either portrait or landscape, uniformly offset from the façade's center. Scenarios with (a) and without (b) extended shading were compared, as shown in Figure s, and denoted by letters A (North) to H, and I (North) to P. The angles shift counterclockwise with increasing alphabetical order (Figure 28). In (a), cells 4 and 5 are empty due to the inherent uncertainty regarding the number of windows and the presence or absence of a shading system, which could introduce additional moderating variables. Consequently, these scenarios are excluded from the experiment. Experimental room groups were named with a combination of letters and numbers (e.g., M4).

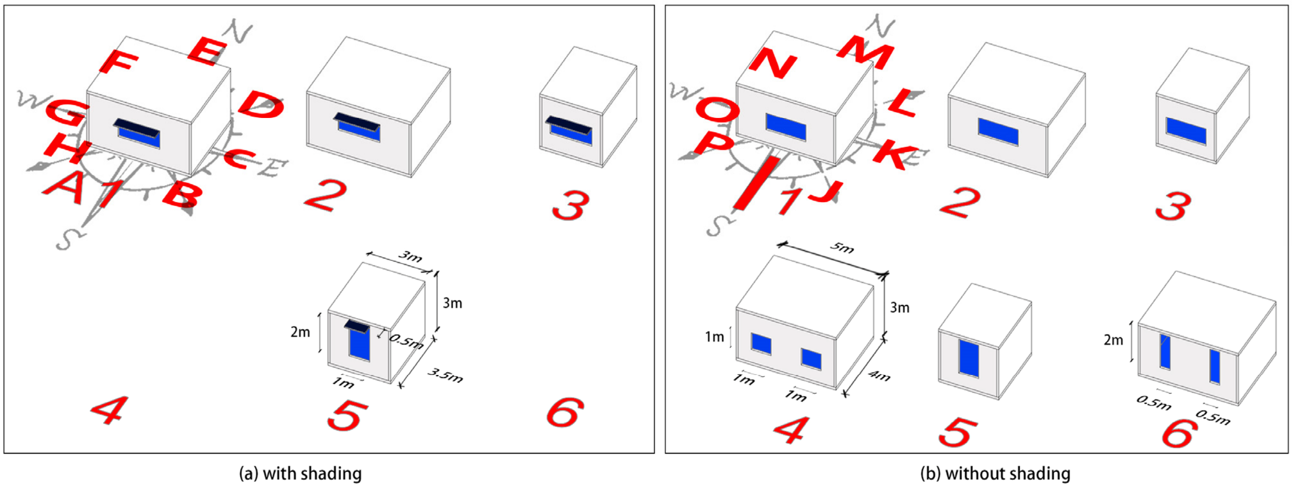

Figure 28: Settings of basic room modeled in Rhino (a) with shading, (b) without shading

The surrounding buildings were grouped into six clusters, varying from 1 to 4 stories in height. The distance from these buildings to the experimental room's center ranged between 31 to 42 meters, mirroring the building density and D/H ratio around the BK faculty building in Delft. The material composition inside the HB model was standardized, with the room's four façades set at 100mm thickness, and the ceiling and floor at 150mm. The glazing was 10mm thick (Figure 29).

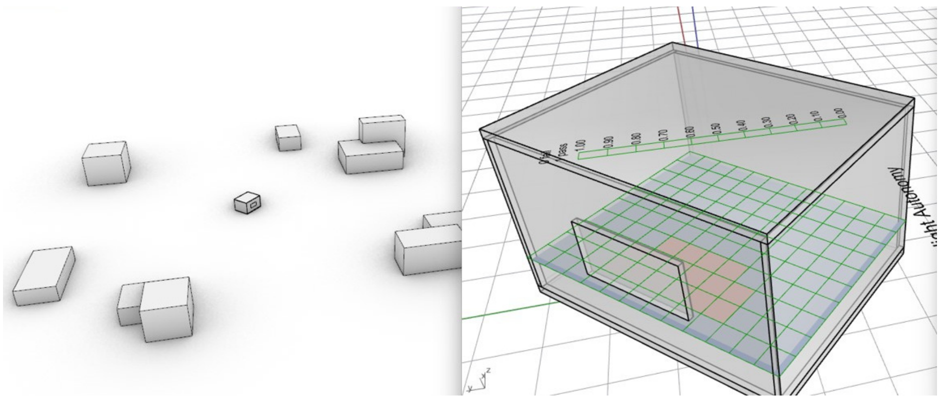

Figure 29: The settings of surrounding buildings and room daylight simulation

Compare:

The comparison scenarios and moderating variables settings in the experiment can be found in Table 8The simulation results were analyzed (Table 8) through fitting and regression line analysis, followed by a comparison of their R Square values. Conclusions were drawn based on the validity of assumptions regarding these moderating variables. Preliminary evaluations were made on how these variables impact correlation coefficients. The GH script for the simulation and the complete simulation results datasheet are available in the Appendix 10.

Table 8: Experimental comparison scenarios and moderating variable configurations

Rhino Compute Settings

The Rhino compute timeout threshold in App server Config.cs file need to be reset. In this case study, the value is set to 1000s in line 31(Figure 30).

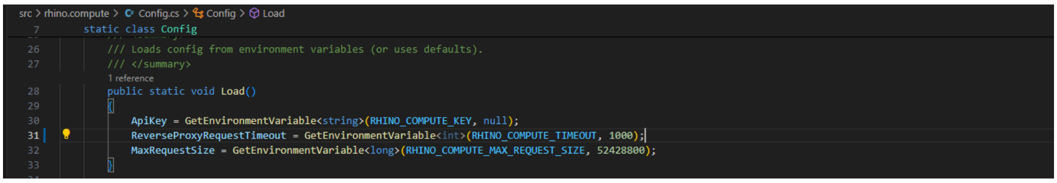

Figure 30: Reset Rhino compute timeout threshold

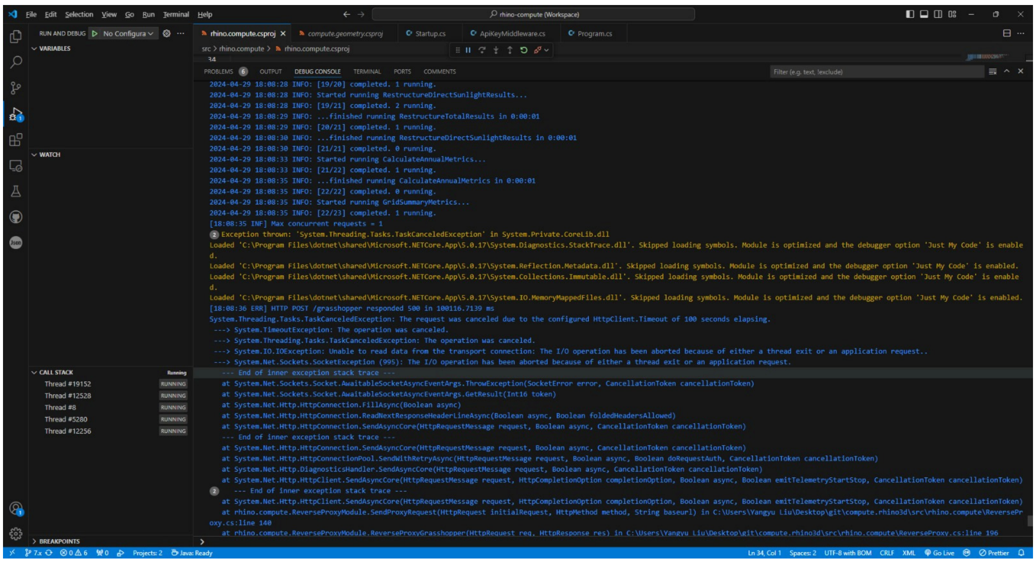

In the instance where the initial timeout setting is configured at 100 seconds, the web page will display an error as depicted in Figure 31. However, the webpage does not provide detailed content regarding the error. On the application server side, it is explicitly noted that the request was cancelled "due to the configured HttpClient.Timeout of 100 seconds elapsing."

4.1.2 Load 3D BAG in Rhino

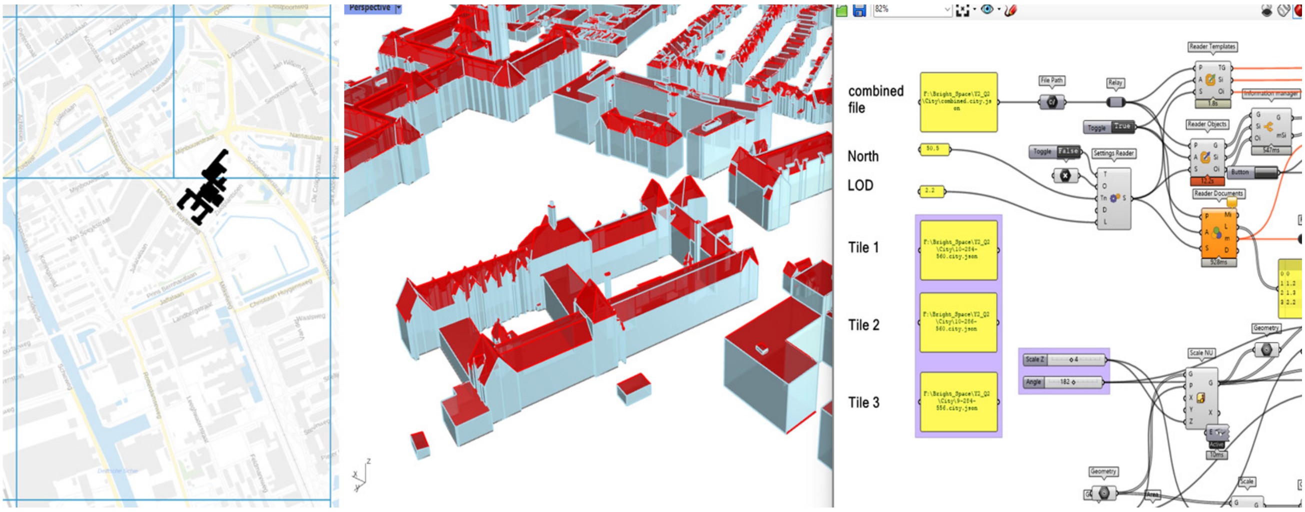

Figure 32: Load in 3D BAG combined tiles using RhinoCityJSON

Initially, the 3D tile location in the 3D BAG Viewer (3DBAG Viewer, n.d.) must be identifies where the relevant imported BIM model is positioned for daylight simulation surrounding settings. In this case study, BK building is situated at the confluence of tiles 10-284-560, 10-286-560, and 9-284-556, which encompass the modeling of the environment required for daylighting simulations. These three JSON files are merged into a single JSON file used as the input file (Figure 32) by using RhinoCityJSON plugin in GH (Cityjson, n.d.). Additionally, it is essential to ensure the north direction is set to align with the rotation angle of the BK BIM model imported into Mapbox later. The LOD in this thesis is specified as either 2.2 or 1.3, given as an input.

4.1.3 BIM Data Preparation

Tag elements' room information in Dynamo per category

This section starts with Create project parameters in Revit, set up as follows (Figure). The implementation follows the workflow in Section 3.2, tagging by category.

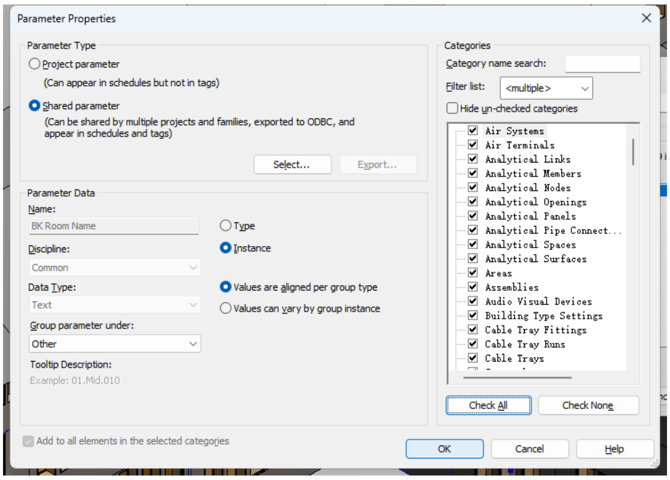

Figure 33: Create project parameters in Revit

Walls involve the creation of project parameters ranging from RoomA to RoomK, with the most intricate wall shared by 11 rooms (Figure 33). This aligns with actual construction practices, where walls are not segmented by room but cast as a single unit. While this does not compromise the accuracy of interior daylight simulations,

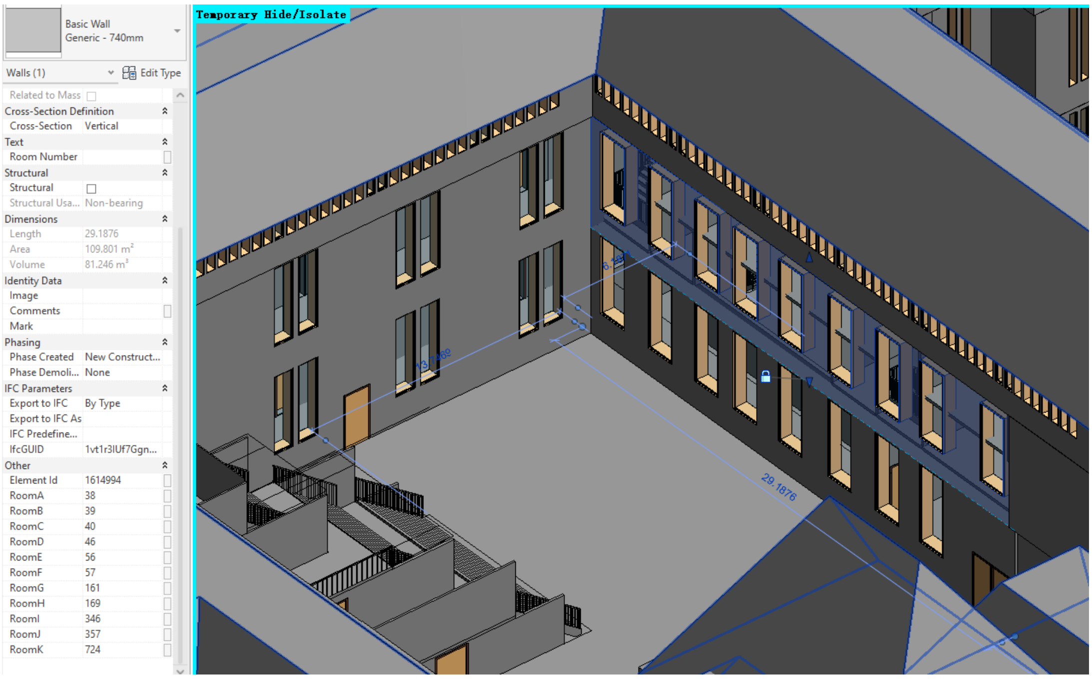

Figure 33: A wall in orange hall with 11 room tags in Revit

it does add complexity to the simulation process and affects visualization within web applications.

It should be noted that some elements, such as parts of the stairs, and the roof, do not belong to any room because they are positioned externally. Since all the RoomA tags were previously initialized to zero, all elements are tagged with room labels and thus further imported into Mapbox. Additionally, this workflow omits dealing with ceilings. Even in rooms with sloped roofs where the ceiling remains flat indoor, considering ceilings from a user interactivity perspective can obscure other room elements when selected. For the purposes of daylight simulation, the ceiling can effectively be regarded as a z-axis duplicate of the floor geometry, this means that the corresponding ceiling can be easily created while retrieving the floor of the room, rendering it unnecessary to include in the tagging process. This will be further discussed in Section 4.3.1 and follow Figure 23.

Get Room Info CSV

In this phase, it is necessary to generate two CSV files to export information about elements and rooms. This is achieved by navigating to Revit's "View" menu, selecting "Schedules," and creating a Multi-Category Schedule for the current phase. One of the schedules should capture room number, name, and level information. The room information csv data structure is shown in Table 9.

Room Number	Room Name	Room Level
341	BG.Oost.560	BG
497	BG+ west 610	BG+
12	01.Oost.010	1st floor
213	01+.West.866	1st floor +
215	02.Mid.010	2nd

Table 9: Room information csv data structure

In the BIM model used for this case study, measuring the height of each floor is straightforward. This measurement is crucial for acquiring the altitude data needed to display the simulation grid results on the front-end. In this case study, the original model included a basement level; however, since the basement lacked windows, studying daylighting for it was not relevant. Consequently, the basement portion was removed from the model, resulting in non-sequential numbering of the selectable rooms. The room level and height correlation in this case study is shown in Table 10.

Room Level	BG	BG +	1st floor	1st floor +	2nd
Height on floor surface (Unit: m)	0.15	2.85	5.85	9.05	11.75

Table 10: Room Level and height in case study

The other should document comprehensive details including all elements, element IDs, and information spanning from RoomA to RoomK like shown in Table 11. (Full csv of wall category can be found in Appendix 14).

Element ID	Room A	Room B	Room C	Room D	Room E	Room F	Room G	Room H	Room I	Room J	Room K	Category
730775	50	47										Doors
1478881	368											Doors
370171	25											Floors
1495879	143											Railings
1446262	44											Stairs
381882	400	435	436	450								Walls
1614994	38	39	40	46	56	57	161	169	346	357	724	Walls
1400406	251											Windows

Table 11: BIM element room information csv data structure

Get Simulation Mesh Center of Selected Room

Initially, an approach was employed where all BIM models were imported per room directly. The relative positioning was determined based on the hierarchical parent-child relationships, as illustrated in Figure 25. The coordinates for the room's bounding box were acquired using the unprojectFromWorld method. However, this method encountered issues with walls shared by multiple rooms, which resulted in deformation of the bounding boxes, which led to inaccuracies in the positions of the simulation results imported subsequently (Figure 34 (a)). Later considerations involved importing each room floor individually, utilizing the coordinates of the entire BIM model's parent element. But this resulted in a uniform displacement across all room coordinates, attributable to the alteration of the geometric center of the entire model when importing the complete BIM model versus only the floor category (Figure 34 b). The methodology and its implications shown in Table 15, with the final implementation outlined in Algorithm 1 (Figure 34 (c)).

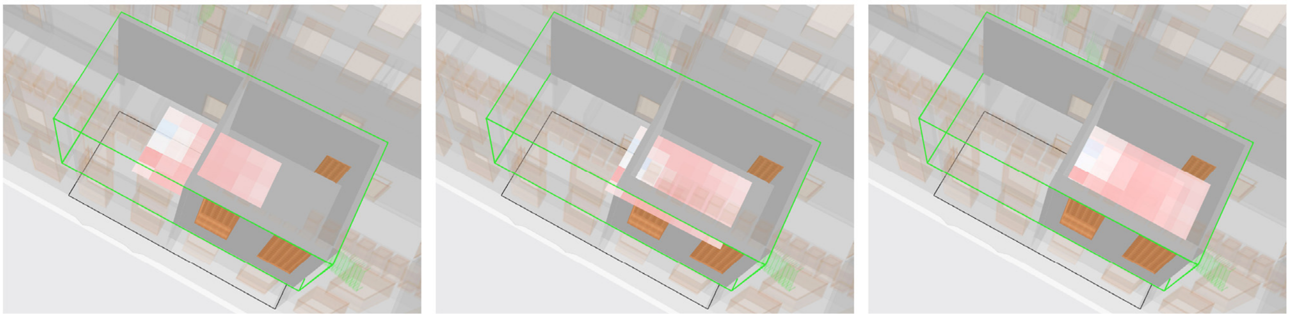

(a) (b) (c)

Figure 34: Coordinates of room in three methods

Algorithm 1: Get Simulation Center Coordinates JSON File of Each Room

Input: Floor GLTF, roomList of valid rooms, loadCoordinates, Initial Scale Factor (0.0415552), Initial Rotate Degrees (50.5)
Output: floorCoordinates.JSON

floorCoordinates ← { }
radRotate ← Initial Rotate Degrees * Pi / 180
procedure addElement (i, {roomNumbers})
  load Floor GLTF **on** \`custom-BKElement_layer\`
    at loadCoordinates **with** rotation: { x: 90, y: 0, z: 0 }
  old (x, y) ← Floor GLTF (position.x , position.y)
  new (x,y) ← (old_x * cos (radRotate) - old_y * sin (radRotate), old_x * sin (radRotate) + old_y * cos (radRotate))
  floorCoordinates (x, y) ← unprojectFromWorld (old_x + new_x * Initial Scale Factor, old_y + new_y * Initial Scale Factor)
  {floorCoordinates}[i] ← roomCoordinates (x, y)

procedure mapRoomNumber ({roomNumbers})
  load Floor GLTF
  for i **in** *Amount of* GLTF *meshes* **do**
    if mesh[i]["RoomList"] exist **and** mesh[i]["name"] = "Generic 150mm" **then**
      for *every RoomTag* **in** roomList **do**
        add i to {roomNumbers}[RoomTag]
    return {roomNumbers}

load GLTF **on** \`custom-BKElement_layer\`
  at loadCoordinates **with** rotation: { x: 90, y: 0, z: 0 }
  roomNumbers ← { }

```
    mapRoomNumber ({roomNumbers})
    for i in range (length of roomList) do
        addElement (roomList[i], {roomNumbers})
re-render the scene

procedure download
    JSON.stringify {floorCoordinates}
    createFile(JSON)
    generateURL(JSON File)
    download floorCoordinates.JSON by clicking the botton
    cleanup URL
```

Initially, when importing only the floor component, it is feasible to configure a download button on the webpage that facilitates the acquisition of the floor's coordinate data, in this case study a temporary “download” button is created on the dashboard on the left. This data file can be accessed and utilized during the comprehensive importation of all BIM elements (Section 4.1.4 per Element vs. per Room Method).This process is depicted in the console bar displayed on the right side of the picture. The evaluation of positional accuracy can be conducted by selecting a random room at and retrieving its central latitude and longitude from the Mapbox console bar. This geographic data can then be entered into Google Maps to ascertain the precise location of the point. floorCoordinatesJSON can be found at Appendix 13.

4.1.4 Load BIM Model & New Building Model On Mapbox

Enrich components' GLTF database with extra BIM information

JSON format is used to export the mesh components of the GLTF file, which encompass Section 4.1.3 containing the BIM data that require modification. Subsequently, incorporate the room tag list into the multi-category schedule CSV file, as also developed in Section 4.1.3. The final step involves reintegrating the revised JSON file into the preceding GLTF file. After revising, for instance, the “extras” key of element ID 528608 will be:

```
"extras": {
    "Revit Element Info": {
     "Element Id": "528608",
     "RoomList": ["503", "505", "518"]

}
```

These three processes can be efficiently executed using Python scripts, with Algorithm 2 specifically detailing the step involved in modifying the JSON file.

Algorithm 2: Enrich JSON File with Room Information Exported from Revit

```
Input: RoomTagMax (RoomK), originalJSON, BIM Information CSV
Output: newJSON

open originalJSON
open CSV skip the title line
for every row in CSV do:
    for every line in originalJSON do
```

```
        if line.ElementID = row.ElementID do
            listJSON ← [ ]
            for i in range (RoomTagMax) do
                if row.RoomTag = empty do
                    continue
                if row.RoomTag >= 0 do
                    add row.RoomTag to listJSON
            line.RoomList ← listJson
            break
open newJSON
JSONdump
```

per Element vs. per Room Method

The integration of BIM model into Mapbox requires a careful balance between interactivity, duration of import, and the precision of selection per room. This balance necessitates a strategic approach to segmenting the model and determining the appropriate geometry unit for user interaction. Furthermore, it necessitates tackling the complexities that arise with overlapping elements, such as shared walls. which is an inevitable complication in this context.

	Load in as a whole	Load in per BIM element	Load in per room way 1	Load in per room way 2	Load in per room way 2 (duplicate of multiple tag elements)
Element	1	7520	477	477	477
Time	10s	10+ min	1min	35s	48s
Interaction	-	++	+	+	+
Accuracy	-	++	+	+	++

Table 12: Comparison of different load in methods

Existing research predominantly focuses on importing the BIM model in its entirety, a method that is highly efficient in terms of time but offers limited interactivity. Importing each BIM element as an individual unit faces challenges of substantial number of units. Typically, a moderate-sized building could contain hundreds of elements, in this case study, can extend the import process to over ten minutes, significantly slowing down the webpage. To enhance efficiency, the model was initially imported by room, with each element possessing multiple room tags imported only once (attributed to the first room serial number that appears). which negatively impacted daylighting simulations, is no longer employed. A refined approach is importing these elements multiple times, assigning each import to a different room. Another strategy to expedite the process involved categorizing each element by room prior to importation (Algorithm 3). This method allows for iterating through a pre-organized list of rooms, which results in a time savings of 10-20 seconds compared to sequentially reading and immediately importing each element (Table 12).

Algorithm 3: Load GLTF BIM 3D Model Per Room on Mapbox

Input: GLTF, roomList of valid rooms, loadCoordinates
Output: GLTF 3D BIM geometry on Mapbox

filter default 3D buildings at BIM Model's location ***on*** 'add-3d-buildings' *layer by ID*
procedure addElement (i, {roomNumbers})

```
    load GLTF on `custom-BKElement_layer`
    if i < length of roomList then
    |   show spinner
    |   for j in range (length of {roomNumbers}[i]) do
    |   |   GLTF.{roomNumbers}[i][j].materialFormat ← THREE.RGBAFormat
    |   roomSimuResult[i] ← initial dummy value
    if i = 0 then
    |   mesh unselectable
    GLTF get BoundingBox

procedure mapRoomNumber ({roomNumbers})
    load GLTF
    for i in Amount of GLTF meshes do
    |   if mesh[i]["RoomList"] exist then
    |   |   for every RoomTag in roomList do
    |   |   |   add i to {roomNumbers}[RoomTag]
    |   return {roomNumbers}

load GLTF on `custom-BKElement_layer`
|   at loadCoordinates with rotation: { x: 90, y: 0, z: 0 }
|   roomNumbers ← { }
|   mapRoomNumber ({roomNumbers})
|   for i in range (length of roomList) do
|   |   addElement (roomList[i], {roomNumbers})
re-render the scene
```

It should be noted that at the time of import, each room is assigned a provisional simulation value. This facilitates the comparison of results, as detailed in Section 4.5.3 and Section 5.3.

Load 3 basic typologies on Mapbox FBX vs. glTF

Three foundational building typologies were initially modeled using Rhino: a flat roof, a single slope roof, and a double slope roof. Each model was constructed based on the dimensions of a 25m x 25m x 25m cube (Figure 35). A dropdown menu was implemented for user interaction on Mapbox web application, enabling users to select a specific added building type. Upon user's selection from the dropdown menu, the models are consistently positioned at a predefined location on the map each time. In this case study, the coordinates for this fixed point are set to [4.371029663172603, 52.007102014389176], located on the eastern side of the garden in front of the north gate of the BK building.

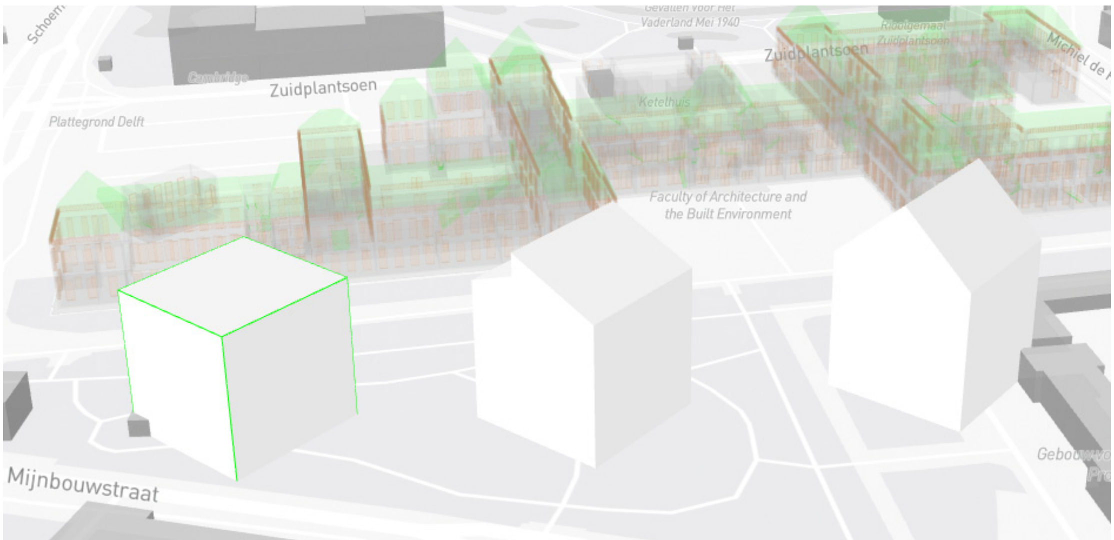

Figure 35: 3 typologies of added buildings

Threebox supports external 3D models files in OBJ, glTF, FBX and DAE formats (Jscastro, n.d.). In the conversion process, a Rhino model transformed into GLTF format typically exhibits a smaller file size compared to the FBX format, while also retaining the capability to preserve materials and alter colors for user interaction (Table 13). Therefore, the GLTF format has been selected in the thesis for importing new 3D building models into Mapbox. It is important to note that for GLTF format, the default rotation parameters should be set as { x: 90, y: 0, z: 0 }. Furthermore, the framework allows users to integrate their customized geometries into the map. It is crucial, however, to ascertain that the models defined in GH script are in alignment with these custom models to preserve a uniform workflow. This thesis provides a foundational workflow that could potentially be expanded to support such customization.

	Type 1	Type 2	Type3	Material
FBX	27kb	28kb	28kb	×
glTF	4kb	4kb	6kb	✓

Table 13: Comparison of FBX and GLTF file sizes and material retention

4.2 Potential to Utilize ABDM Standard Metrics

4.2.1 Implement GH script of SBI & View Lumen

SBI

Computing SBI doesn't require lighting simulation per se; instead, it relies solely on line-of-sight calculations. (Mardaljevic & Roy, 2016). The accuracy depends mainly on the simulation time-step, the solar discretization scheme (both are interrelated) and window aperture sensor grid density (Mardaljevic & Roy, 2016). The overall workflow in GH is shown in Figure 36.

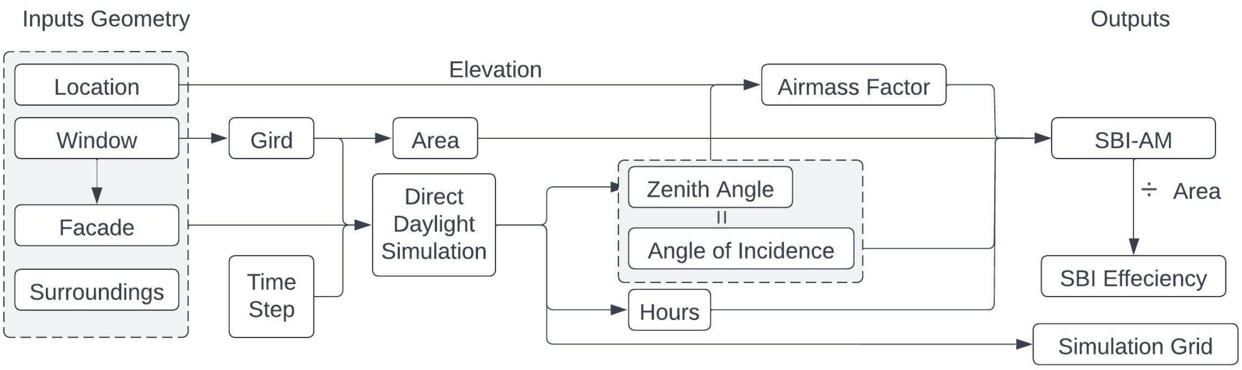

Figure 36: Workflow for implementing SBI in GH

As illustrated in Figure 37, an very simple space in Delft featuring a single window is used for the experiment: height width depth is 3m 5m 4m, with a 2m*1m glazed aperture positioned centrally in one wall at the height of 1.2m . with another sheltered building with a height of 12m (4 floors) positioned 4m in front of the space, affecting the direct sunlight hours. The grid size input of GH component LB Direct Sun Hours is configured at 0.2m (40 grids) to accommodate the experimental arrangement. Notably, Mardaljevic and Roy (2016) employed the Radiance toolkit to produce sensor grids for apertures and provided ‘stencil method’ of creating sensor grids for arbitrary shapes and non-horizontal planes through two rotational transformations. But in the context of this particular case study which mainly utilizing GH as back-end tool in workflow, considering that all windows are oriented perpendicular to the ground, direct utilization of the LB component was opted for.

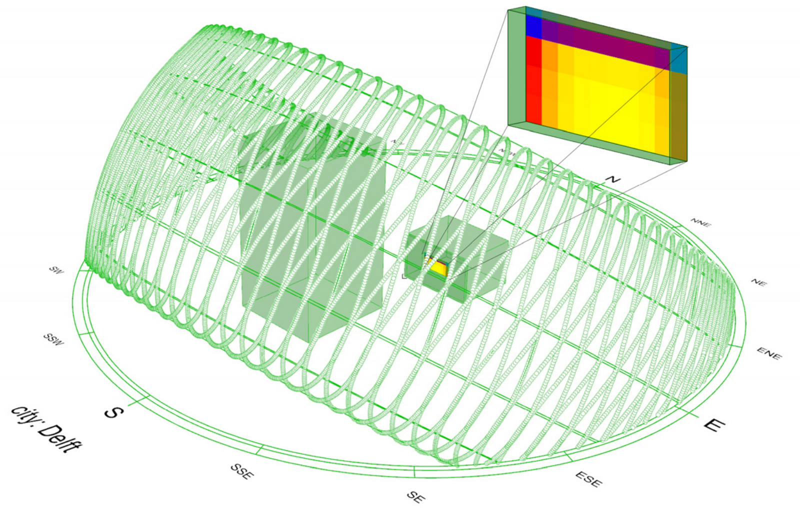

Figure 37: SBI of an example room in Delft

The TM array has dimensions 96 * 365. The GH script is implemented as shown in Figure …, 35040 time periods were created initially and 50.91% (17839) of the time has $\gamma_s > 0$ according to LB simulation result.

To compare among different individual windows, SBI efficiency, also called the normalized annual total SBI, can be calculated by SBI value divided by the sum area of the glazed aperture with unit of kW (Mardaljevic & Roy, 2016). The GH script used the Mass Addition component to aggregate the annual SBI values for the given aperture and subsequently divides this sum by the aperture's area to determine its SBI efficiency value. The entire GH script of computing SBI-AM and SBI efficiency can be found in Appendix 7.

In the context of application features, the aperture properties may serve as proxies for the daylighting attributes of the selected room. This chapter will explore the correlation between SBI and CBDM metrics, with the potential to establish them as viable indicators of indoor daylighting performance during the planning phase.

View Lumen

ASI metric measures how well an aperture connects to the sky dome by determining the average light it receives from a uniform luminance sky dome. In their study, Mardaljevic and Roy (2017) introduce the concept of "view lumen" to measure this connectivity to ground, foreground, and sky layers, using luminous flux as a proxy for quantification. The workflow is shown in Figure 38.

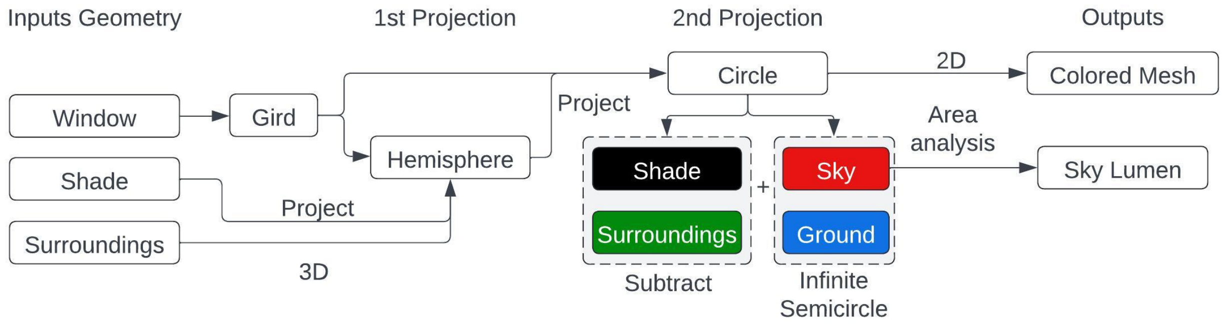

Figure 38: Workflow for implementing Sky lumen in GH

Very similar to SBI experiment, a simple room measuring 5m * 4m * 3m was built in GH, featuring a singular 2m * 1m aperture. Positioned before the aperture were 3 buildings as obstructions, serving to elucidate principles governing projection phenomena. The grid_size input of HB Sensor Grid from Apertures component is configured to 0.3m.

One may envision a hypothetical scenario wherein a vertical hemisphere is conceptually positioned in front of each of the 18 sensor units as delineated in Figure 39. The size of these hemispheres is immaterial, provided they do not overlap with the internal or external geometries. A straightforward method is creating spheres centered at each of the 18 sensors, subsequently trim them with aperture planes to yield hemispheres. It is imperative to scale them appropriately to prevent any intersection between the surface of the hemispheres, the shading geometry (not excessively small) and surrounding geometries (not excessively large). This adjustment process may require manual intervention. Note that the geometric seam inherent in spheres created in Rhino software exhibits a C-shaped seam, and in instances where the plane of this seam deviates from the plane of the window (e.g., when the window orientation is not South-North), it disrupts the outcomes of subsequent

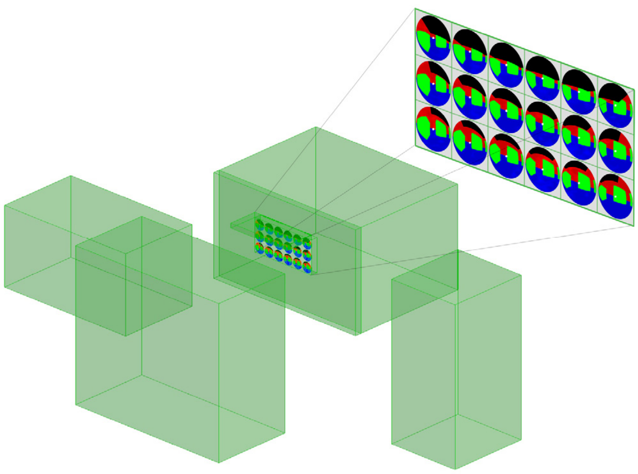

Figure 39: View lumen for an example room in Delft

cuts and projections. Thus, it's important to rotate the spheres to match the orientation of the aperture for consistency.

The two projections of the surrounding buildings and shading is similar, as shown in Figure 40. During the initial projection, the Deconstruct Brep component is utilized to extract all edges. Following this, the Extrude Point component is employed to establish connections between the center point of each sensor unit and these edges to form polyhedrons. The difference lies in the shading along the inner surface of the hemisphere, contrasting with the positioning of surrounding elements on the exterior, which involves intersecting the initial intersection of the shaded geometry with a scale factor corresponding to the previously constructed hemisphere dimensions. This intersection creates the result of the first projection by using Brep | Brep component. In the second projection, the project component is invoked to project the shape of the hemisphere onto the plane aligned with the sensor unit's position. The complete projection line is discernible by using the internal edges of the Brep Edges, as illustrated in Figure 40(b). Ultimately, all sensor grids are resized to their original diameter of 0.3 meters at their center points.

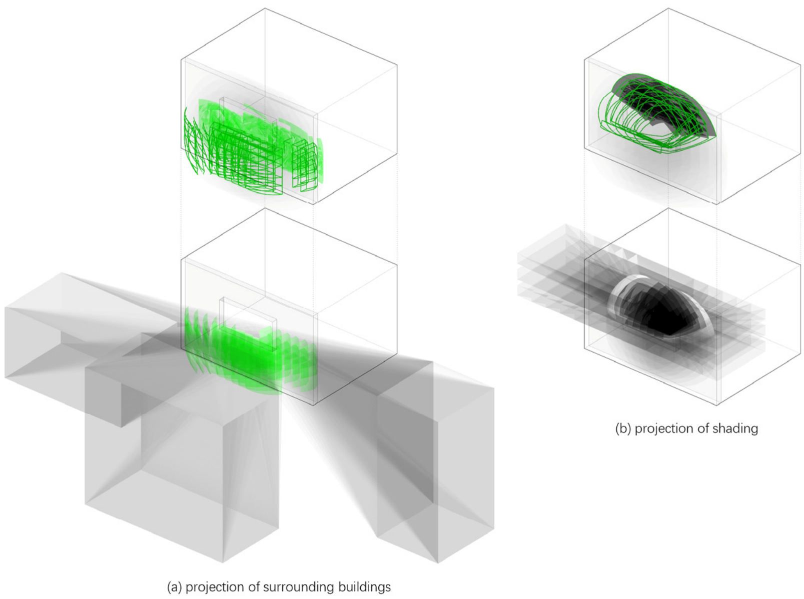

Figure 40: Two projections of surrounding buildings(a) and shading(b)

The original way was using Radiance lighting simulation system (Ward Larson et al., 1998), the sky and ground are at infinity. In Rhino, the infinite ground and sky planes can be represented directly in the second projection by simply bisecting the circular sensor from the center height. Note that these planes are frequently obscured by shading (black) and the surrounding buildings (green) layers, and attention must be devoted to both the stacking sequence and the arrangement of Region Difference operations (Figure 42). The principle is that objects situated further away from the aperture should occupy the lowermost positions within the projection layers and allow more overlaid layers. This approach aims to calculate the percentage of the overall sensor unit area occupied by the colored block by employing Region Difference component on the layers, executed in a sequential manner from the topmost to the bottommost layer thus duplication of area measurement should be avoided.

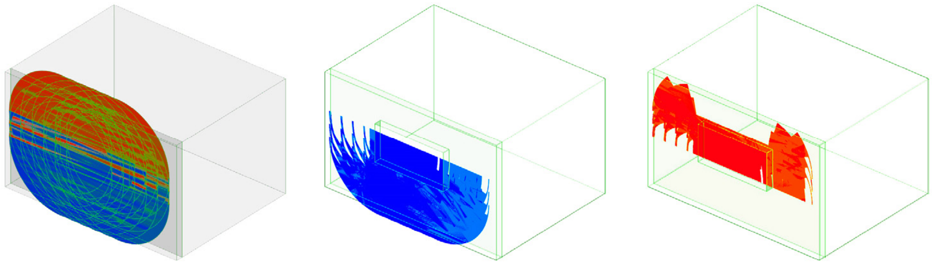

Figure 42: Create infinite sky and ground layers on sensor unit directly in GH

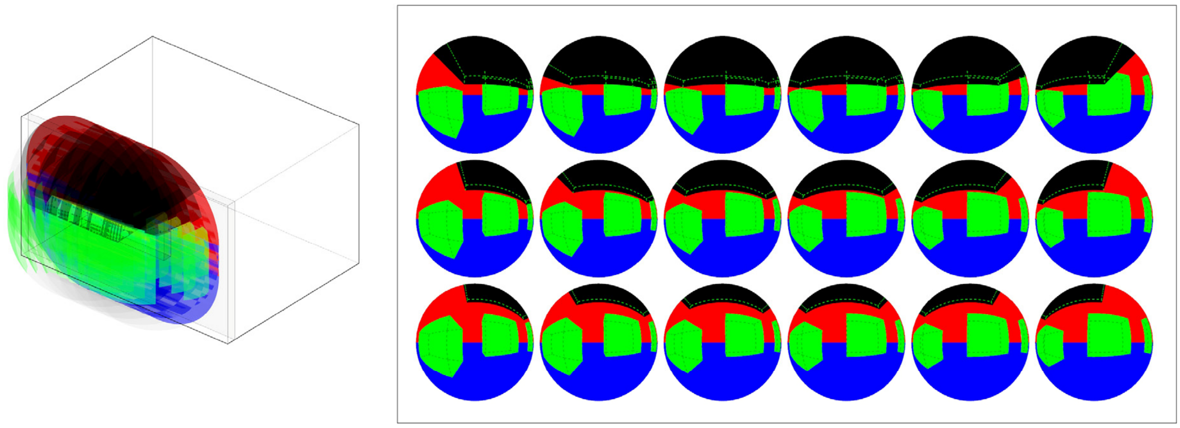

(a) 1st Projection

(b) 2nd Projection

Figure 41: Visualization for two projections

The other method of creating hemispherical view involves utilizing the HB View component in GH, which is primarily designed for glare analysis. A value of 1 is given as input for view_type for Hemispherical fisheye. Note that radiance_par for HB Point-In-Time View-Based should be configured to "-ab 0 -aa 0 -ad 0 -ar 0" to deactivate certain aspects of ambient lighting computations. This may lead to quicker renderings but with potentially reduced accuracy, as it disables various components such as ambient bounces, considering only direct sunlight, omitting ambient accuracy calculation and divisions, as well as neglecting ambient cache for indirect lighting. Given the primary emphasis on color block and outline within this implementation rather than intricate color differentials, such outcomes align with the intended objectives. HB Certain Illuminance component is used to create an evenly illuminated sky (Figure 43).

5

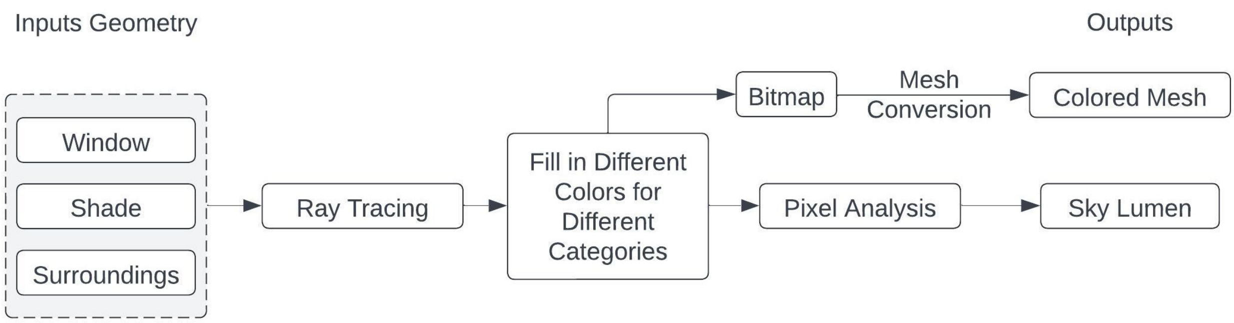

Figure 43: Workflow for implementing Sky lumen in GH (Ray tracing method)

Subsequent to this, there arises the necessity to contemplate methodologies for discerning and applying distinctive colors to buildings, ground and shade, alongside the undertaking of pixel analysis on fisheye photographs aimed at delineating the proportion of red, blue, green, and black (or varying shades of gray). Due to the length of the thesis and time constraints, this avenue of research is regrettably precluded from further exploration. Furthermore, although rendering time was greatly reduced by omitting some of the complex ray tracing, each simulation still demands approximately 20 seconds, thereby diminishing the discernible advantage of employing View Lumen as an ABDM metrics through arithmetic operations. However, this special approach holds potential for future research.

The complete GH script for view lumen can be found in Appendix 8, It is advised to carefully consider the data structure throughout the script's development process.

4.2.2 Simulation & Regression Analysis

The average simulation durations were 50 seconds per session for small rooms and 1.1 minutes per session for larger rooms. The following section details the regression analysis and conclusions:

DA and SBI-AM

Figure illustrates the relationship between the independent variable DA (x-axis) and the dependent variable SBI-AM (y-axis). Each line represents a distinct room scenario, denoted by different colors and point styles labeled 1 to 6. The regression lines, each with their equations and R^2 values, suggest varying degrees of positive correlation between DA and SBI-AM across different scenarios. This preliminarily confirms the previous hypothesis. The slopes of the regression lines range from 87.86 to 117.27, with R^2 values above 0.95, demonstrating a strong linear relationship in each dataset. Alterations in the variables do not significantly influence the gradient of the DA and SBI-AM relationship (Figure 44).

Comparing scenario 1(low sill height) to 2(high sill height), the rate of increase in SBI-AM with respect to DA is slightly steeper in scenario 1 compared to scenario 2, but scenario 2 starts from a higher initial value.1 has a slightly better fit to the regression model.

Comparing scenario 1(big room) to 3(small room), SBI-AM has a faster increase in scenario 3 but starts at a lower value, and 3 marginally lower R^2 value.

Comparing scenario 1(one aperture) to 4(two apertures), scenario 4 has a lower slope value suggesting a milder increase in SBI-AM with DA, but begins lower. 4 has a better fit than 1.

Comparing scenario 4(square aperture) to 6(rectangular aperture), SBI-AM in scenario 6 has a slightly slower rate with respect to DA, and has a much higher starting value, scenario 6 has the best fit in this chart.

In summary, the analysis reveals a robust linear relationship between DA and SBI-AM. The variables previously discussed all serve as moderators within the DA and SBI-AM relationship, indicating that variations in these factors can alter the linear association to some extent. The most prominent influencing factor is the geometry of the room; notably, in smaller spaces, the horizontal and vertical dimensions of windows significantly impact the relationship. Conversely, in larger environments, alterations such as modifications to the window sill height or the shape of the space predominantly affect the intercept rather than significantly altering the slope of the relationship. Thus, while the basic linear relationship remains strong across different conditions, the specific parameters of this relationship can vary depending on room size and configuration.

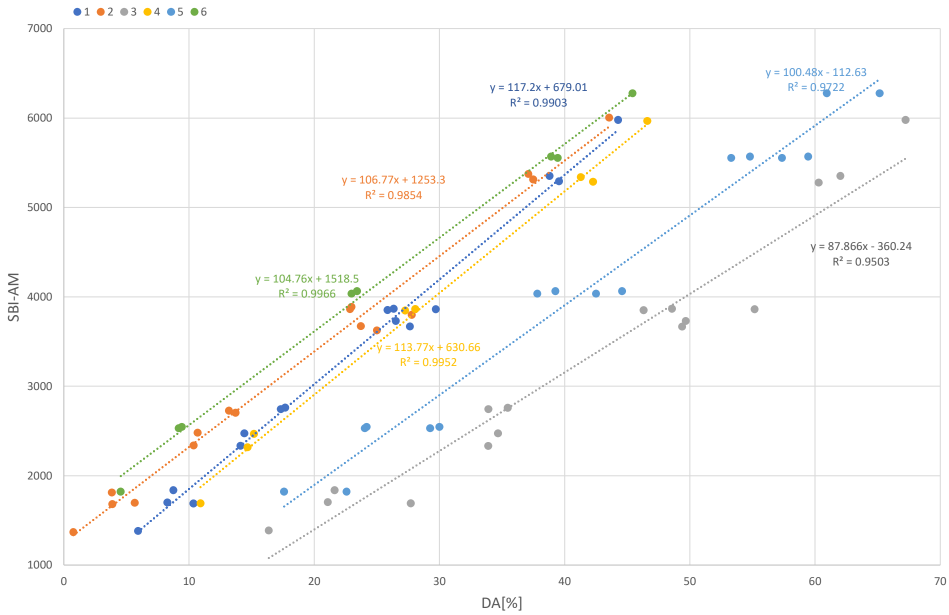

Figure 44: Linear regression plot of Relationship between DA and SBI-AM

A segregated analysis of data from four specific room scenarios (Rooms 1, 2, 3, and 5) based on orientation—southward (due south, southwest, southeast) and northward (due north, northwest, northeast)—as delineated in Figure, was conducted to determine which direction has a better fit.

As shows in Figure 45, across all scenarios, the South-facing direction generally shows a stronger correlation between DA and SBI-AM than the North-facing direction. This directional difference is most pronounced in scenarios with weaker overall correlations (Scenarios 3 and 5). When using DA to predict SBI-AM value, it is crucial to account for direction, and the South-facing direction tends to prove more reliable predictive power.

The variance of the combined dataset is typically lower than the variance of individual subsets, and the combined regression line can better capture the overall trend due to the increased number of data points and the reduction in the influence of outliers or extreme values.

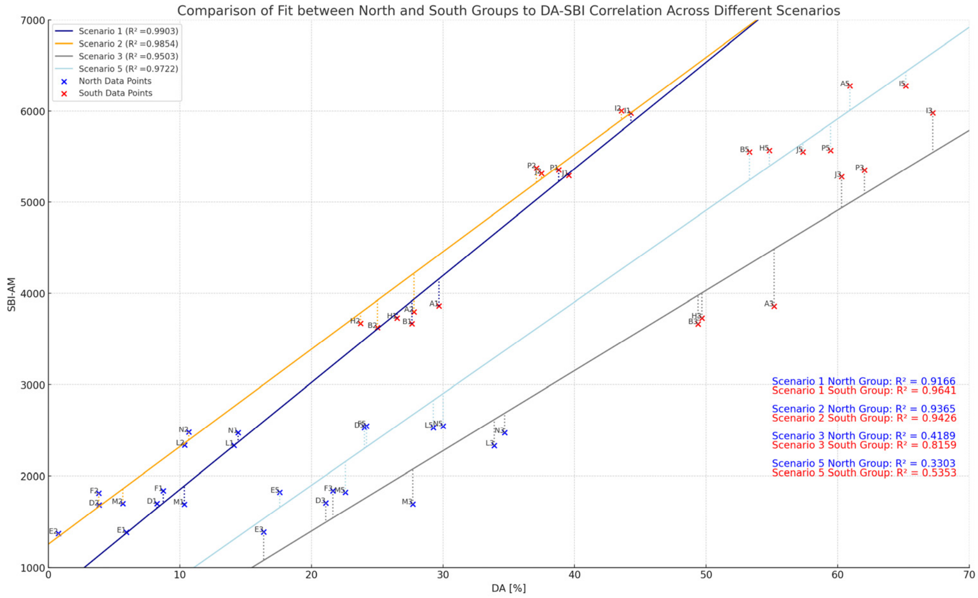

Figure 45: Comparison of linear regression plot of relationship between DA and SBI-AM in North facing direction and South facing direction

sDA and SBI-AM

A comparable analytical approach is employed to examine the relationship between sDA and SBI-AM, where generally, the linear correlation between these metrics is marginally lower than that observed between DA and SBI-AM. It is noteworthy that in scenario 6, an exceptionally low R^2 value of 0.0851 is recorded, suggesting that the relationship may be weak in certain real-world situations. Regarding variations in slope, Scenario 2 and 4 exhibit similar gradients, while Datasets 3 and 5, which represent the portrait and landscape orientations of apertures, respectively, also demonstrate comparable slopes. The similarity in slopes between Datasets 2 and 4 is coincidental, as there are alterations in two variables between these datasets. Consequently, it can be provisionally concluded that the portrait and landscape orientations of apertures exert minimal impact on the slope of the relationships between sDA and SBI-AM (Figure 46).

Comparing scenario 1(low sill height) to 2(high sill height), scenario 1 has a significantly steeper slope than 2, and higher R^2 value. But 2 start with much higher value.

Comparing scenario 1(big room) to 3(small room), scenario 1's slope is dramatically steeper than 3, but they both have high R^2 value.

Comparing scenario 1(one aperture) to 4(two apertures), scenario 1 has a steeper slope than 4, and has higher R^2 value, but starts with a lower intercept.

Comparing scenario 4(square aperture) to 6 (rectangular aperture), the relationship is very weak in scenario 6. Atypical orientations of portal windows may disrupt the correlation between sDA and SBI-AM in actual settings.

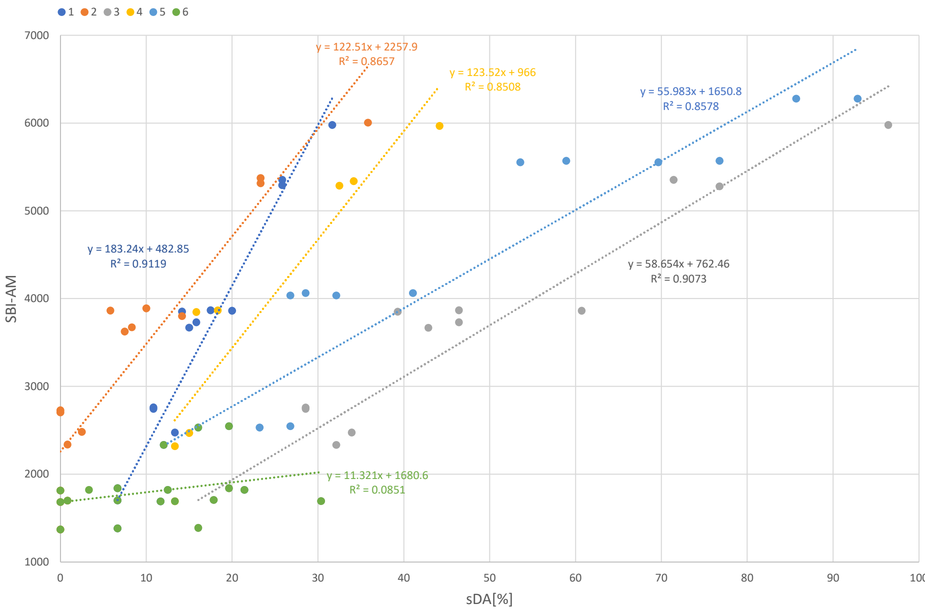

Figure 46: Linear regression plot of Relationship between sDA and SBI-AM

In a similar way, when comparing cases with south-facing and north-facing orientations individually (Figure 47), In most scenarios, the South group consistently shows better correlation, and the significant difference in R^2 values between two direction groups suggests that the orientation plays a crucial role in the relationship between sDA and SBI-AM.

The negative R^2 values observed for the North group in Scenarios 1, 2, and 5 suggest that the linear model is inadequate for these scenarios. This underscores the necessity for alternative modeling approaches or the inclusion of additional factors for North-facing directions.

More research and investigation are needed to understand the poor correlation for the North group in several scenarios. This includes examining environmental factors, data collection methods, and non-linear models.

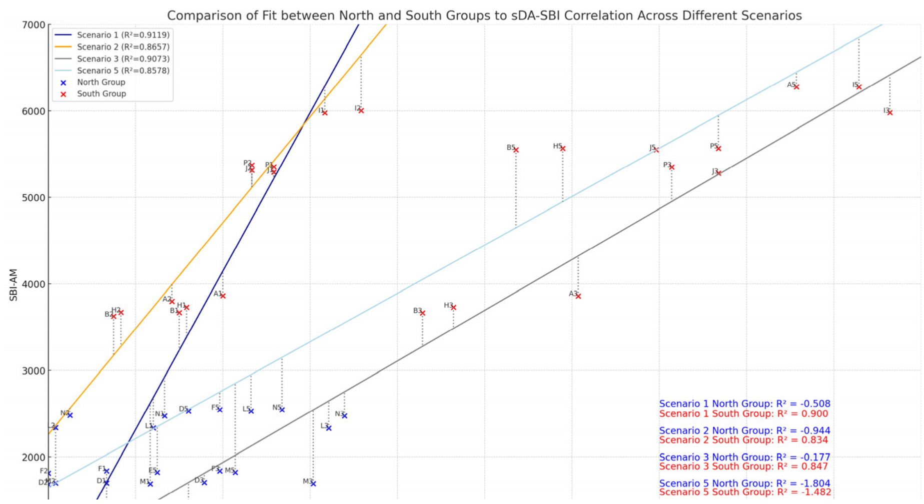

Figure 47： Comparison of linear regression plot of relationship between sDA and SBI-AM in North facing direction and South facing direction

UDI and SBI-AM

In the correlation between UDI and SBI-AM, scenario 3 and 5 exhibit lower coefficients of determination. Notably, only four instances demonstrate a linear relationship between two metrics. Upon comparison of the slopes, it is observed that the slopes of scenarios 1.2 and 4.6 are comparable, suggesting that modifications in the height of window sills and the configuration of combined windows exert small impact on the linear relationship between UDI and SBI-AM, but the number of windows can make a big difference.

Comparing scenario 1(low sill height) to 2(high sill height), they have similar model fit. Scenario 2 has a slightly flatter slope and smaller negative intercept.

Comparing scenario 1(big room) to 3(small room), a reduction in room size disrupts the linear association between the two metrics, as evidenced by the validation of the data from Scenario 5 as well.

Comparing scenario 1(one aperture) to 4(two apertures), Scenario 4 shows a higher model fit. Scenario 4 has a much steeper slope and a significantly large negative intercept.

Comparing scenario 4(square aperture) to 6 (rectangular aperture), both scenarios show strong linear fits, scenario 4 features a steeper slope and lager negative intercept.

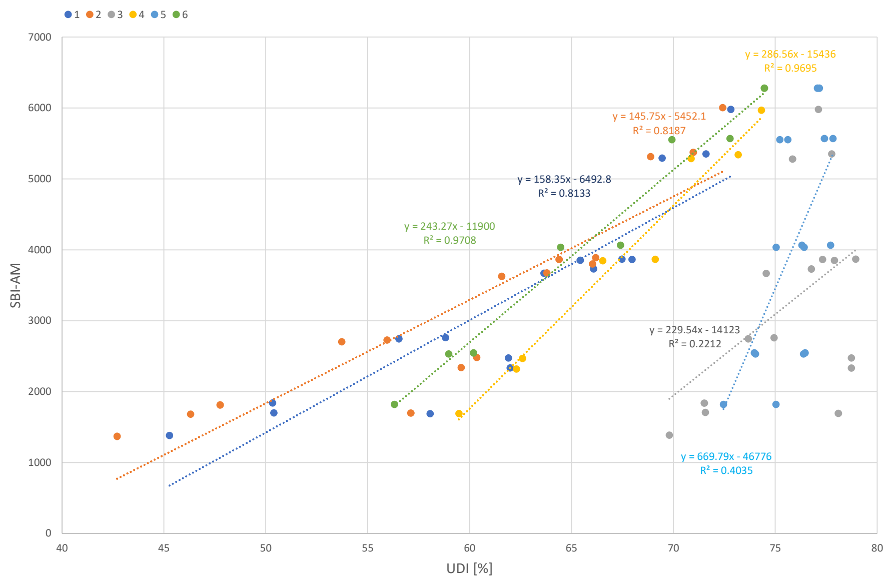

Figure 48: Linear regression plot of Relationship between UDI and SBI-AM

In the analysis comparing north- and south-facing orientations (Figure 49), in all scenarios, the North group has a negative R^2 value and poorer fit than South group, the poor fit is especially pronounced in Scenario 3 and 5, while the South group shows moderate fits in scenario 1 and 2 with positive R^2 values of 0.6086 and 0.6826 respectively. In Scenarios 3 and 5, the fit of South group is still poor but better compared to the North group.

Scenarios 3 and 5 do not adequately fit the data for either group, suggesting that SBI-AM is not a suitable predictor of UDI in some contexts. In contrast, Scenarios 1 and 2 provide better models for the overall relationship between UDI and SBI-AM.

Considering the definition of UDI, which is based on hourly or shorter time-step illuminances over a year and categorizes annual illuminance into three ranges, and exhibits non-linear jumps between categories as values change, the correlation between UDI and SBI-AM is inherently non-linear. This complexity cannot be effectively captured by simple models.

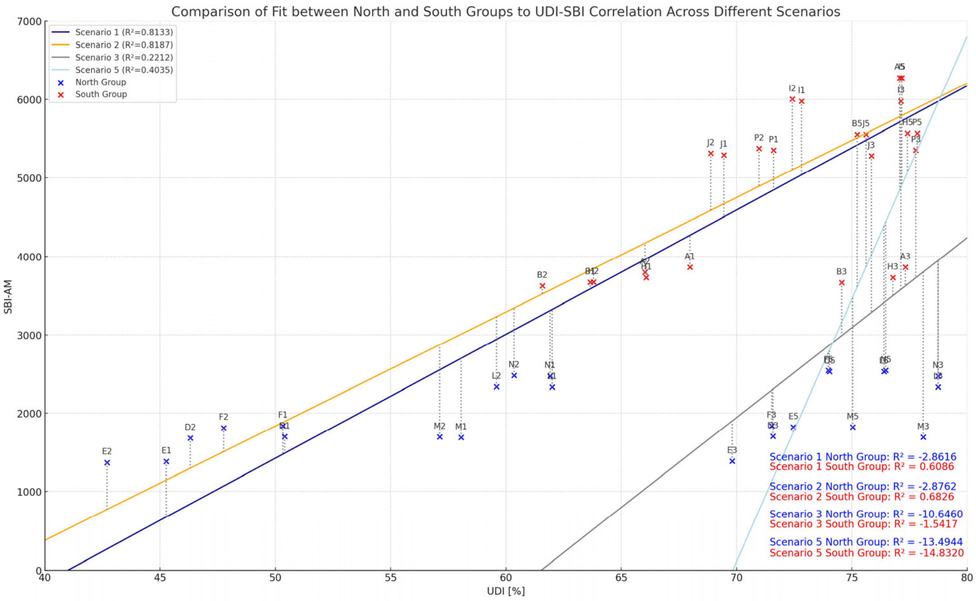

Figure 49: Comparison of linear regression plot of relationship between UDI and SBI-AM in North facing direction and South facing direction

DA and Sky Lumen

Following the evaluation of multiple fitting functions, quadratic regression has been identified as more suitable for modeling the relationships between DA, sDA, UDI, and Sky Lumen, especially influenced by the presence or absence of shading devices. This is likely due to the lower density of residential structures in the experimental setup, similar to conditions at the case study site in Delft. Except for Scenario 1 with shading, which shows a notably low correlation, other scenarios demonstrate good correlations with R^2 values exceeding 0.7 (Figure 50). A comparative analysis of orientation was not conducted due to the dataset division into subgroups based on shading, resulting in limited data in each subgroup.

The graph distinctly segregates into three segments. The upper section, comprising six datasets without shading, shows uniformity with similar vertex values. The lower three datasets, all with shading, also demonstrate comparable vertex values. The middle section is unique, representing Scenario 5 with shading, distinguished by distinct vertex values. Aside from the invalidated Scenario 1 with shading, the relationship lines among the other datasets show a notable degree of similarity, analogous to the patterns observed in the DA and SBI relationship.

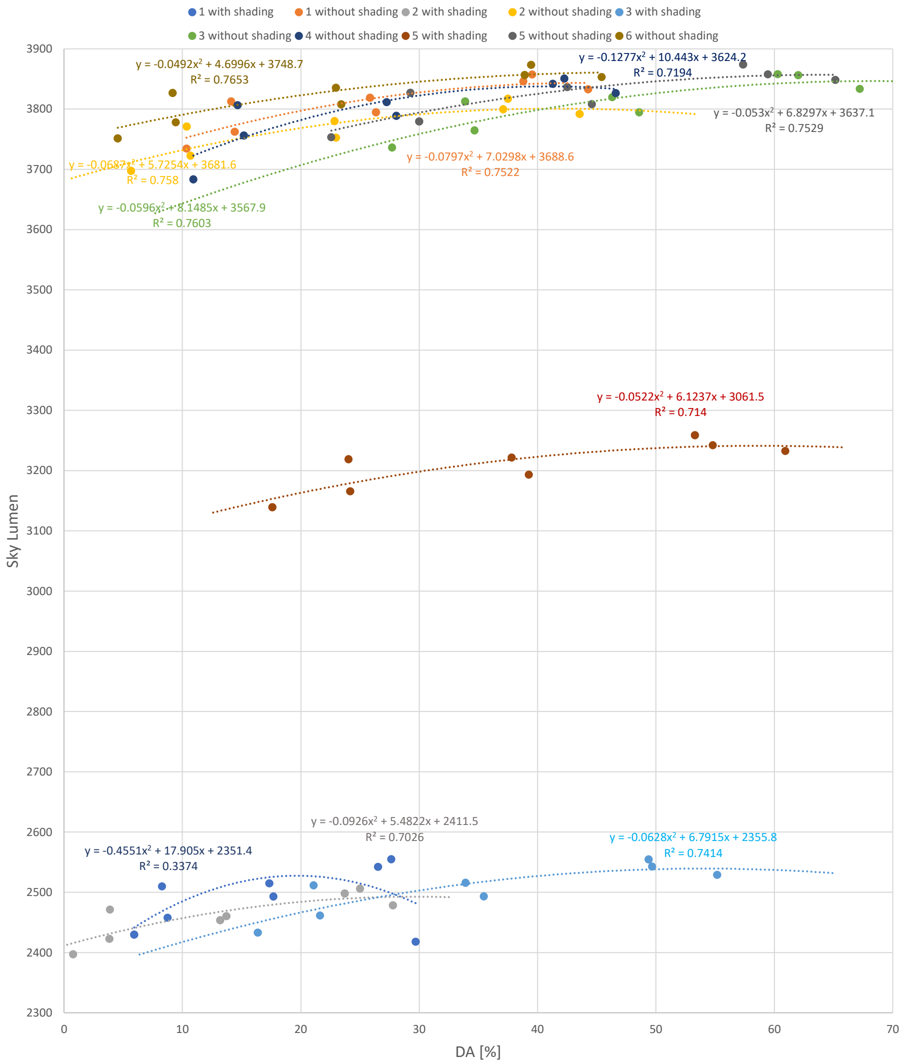

Figure 50: Quadratic regression plot of Relationship between DA and Sky Lumen

sDA and Sky Lumen

In Figure 51, segmented into three distinct parts, Scenario 5 with shading persists as a notably unique case. This scenario continues to stand out distinctly within the dataset. All R^2 values were observed to range between 0.55 and 0.72, indicating a generally lower model fit compared to the relationships between DA and Sky Lumen.

From the analysis of the six data sets without shading, a discernible similarity among scenarios 6, 2, 4, and 1 is evident, as well as between scenarios 3 and 5. These groupings suggest that alterations in the geometric configuration of the room (or room size), serve as another significant moderating factor influencing the relationship between sDA and Sky Lumen apart from the presence or absence of shading.

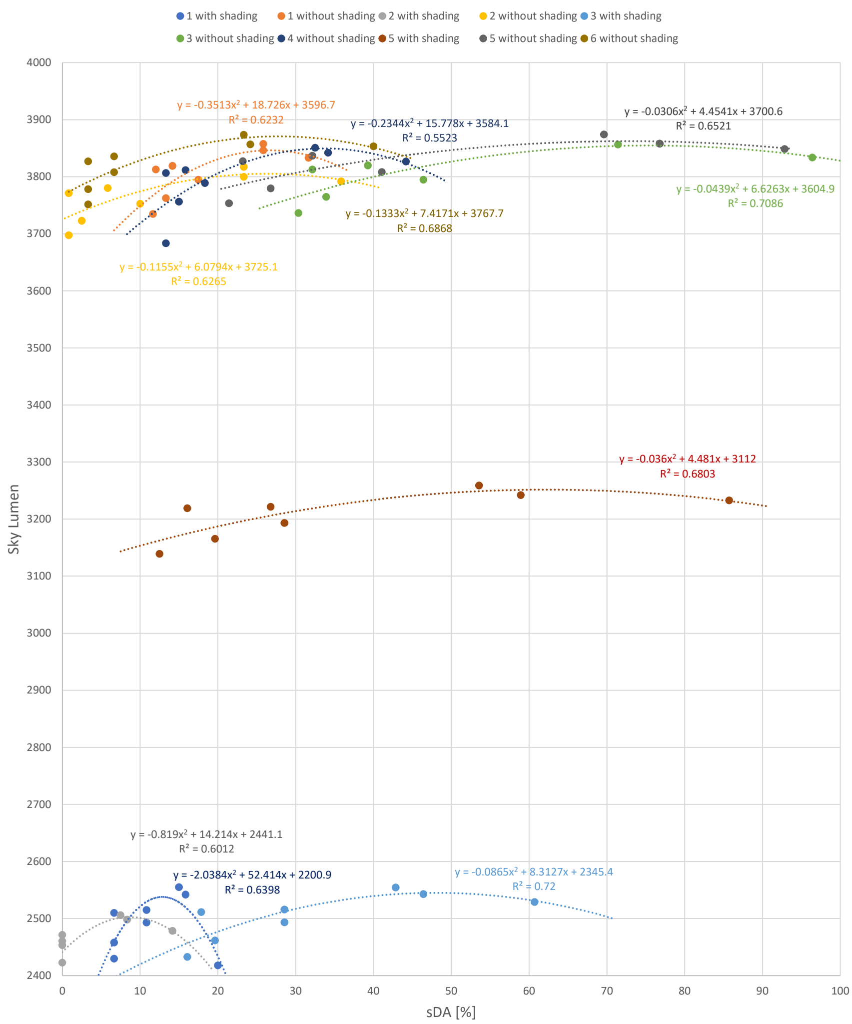

Figure 51: Quadratic regression plot of Relationship between sDA and Sky Lumen

UDI and Sky Lumen

Regarding the correlation between UDI and Sky Lumen, Scenarios 3 and 5 without shading, as well as Scenario 1 with shading, exhibit poor model fits, and the data continues to be categorically segmented into three distinct groups. Furthermore, the patterns of the curves for Scenarios 3 and 5 with shading markedly diverge from the others, indicating that the geometric configuration of the room, or room size, significantly influences this relationship. Alongside the impact of whether shading is present or absent, the spatial configuration of the room emerges as another crucial factor regulating the interaction between UDI and Sky Lumen (Figure 52).

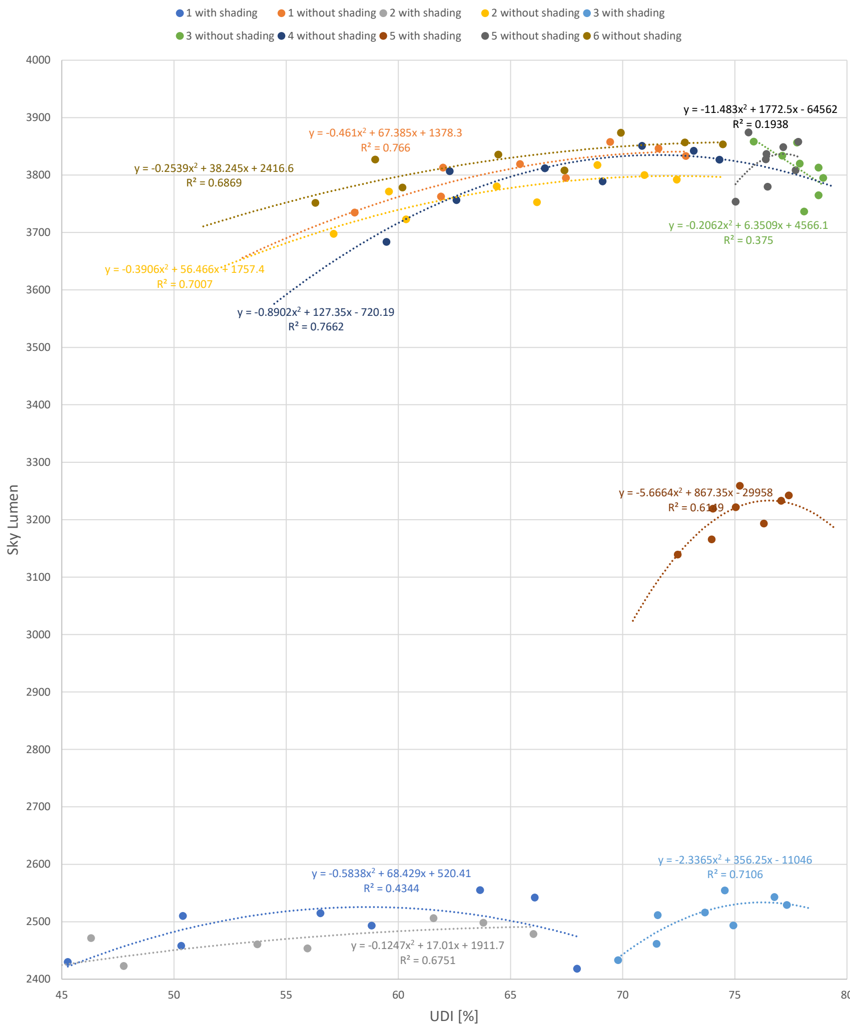

Figure 52: Quadratic regression plot of Relationship between UDI and Sky Lumen

4.3 Daylight Simulation Automation

4.3.1 Element Selection Automation in GH

Given that each execution of Rhino Compute replicates the GH file for processing, no internalized data should exist within the GH script aside from Rhino Compute inputs. On the other hand, directly internalizing geometry leads to attributes loss. To address this issue, Figure 53 illustrates a solution whereby JSON attributes are extracted and added following the internalization of geometry.

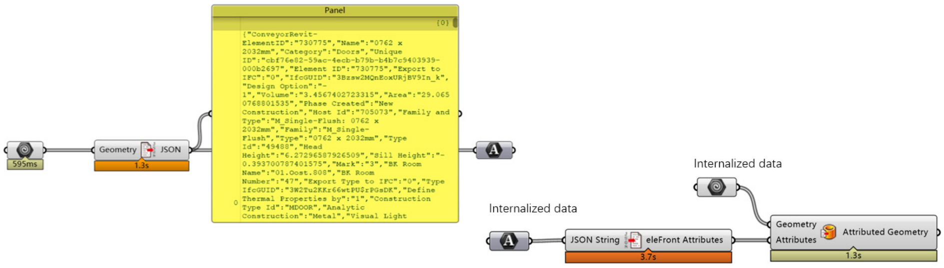

Figure 53: Internalize geometry by adding internalized attributes data

The floor's geometry needs to be reconstructed to ensure uniform grid distribution (Figure 54). Additionally, doors and windows, which often appear as a block, must be separated from their frames and panels to assign the correct materials.

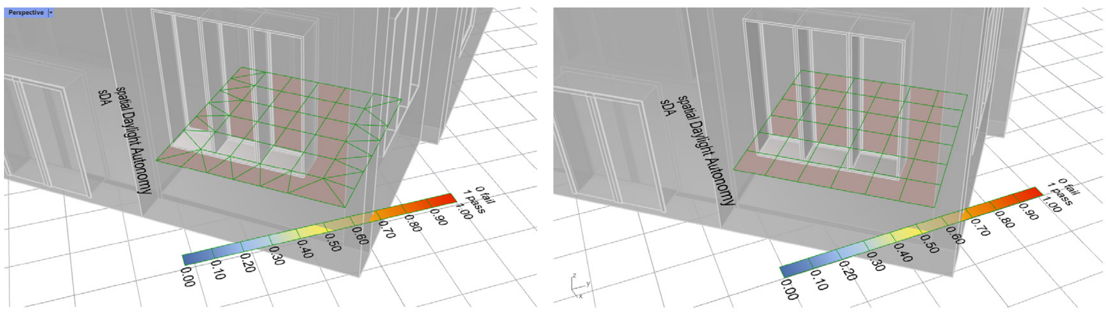

Figure 54: Rebuild floor (a) for evenly distributed sensor grid (b) in GH

4.3.2 Exterior Facade Walls of BIM Building Selection Automation in GH

An additional consideration for daylighting simulations in multi-room buildings is the building's self-shading and the influence of indirect daylight because of its façade system. For instance, the room depicted in Figure 55, situated at a corner and shaded by building segments on both sides of the corridor, also experiences the facade's impact on light. As outlined in Section 6.2, the original BIM model does not distinguish between interior and exterior materials. Nevertheless, to enhance the accuracy of the daylighting simulations, a project parameter called "Exterior" was manually created, with all facade walls assigned a value of 1. Whenever a specific room is selected, not only are the four walls enclosing the room considered, but all facade parts that are not belonging to the room are also selected dynamically as geometry for a new HB Shade component named "Facade". When considering daylighting simulation, surrounding walls in the selected room represents the indoor segment, which were given a white concrete paint material; the remaining facade is treated to represent the impact of external shading and reflection and is designated as exterior red brick material. All the materials can be found in Appendix 11.

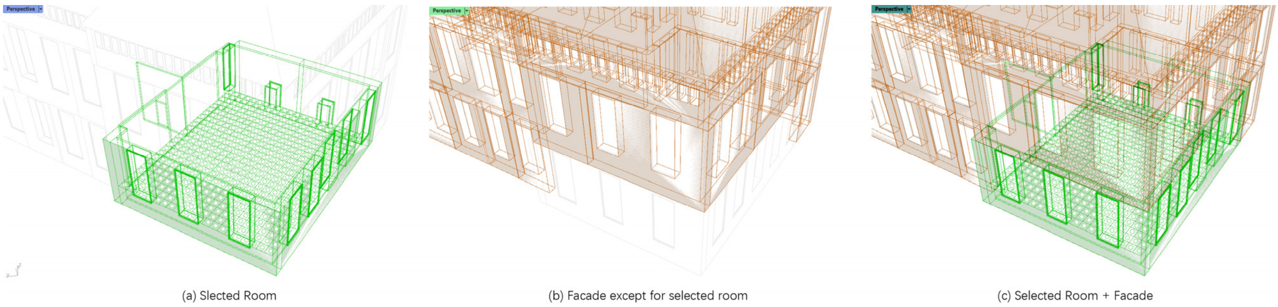

Figure 55: Selected room(a) and the rest of façade considered (b)

Ideally, the analysis should also include windows and their frames, necessitating that the BIM model differentiates between interior and exterior windows, which are typically components of the façade. However, due to the considerable time investment required for such detailed manual modifications, this part is not implemented in the thesis.

4.3.3 Avoid Empty Inputs in GH

The processes of drag and drop, rotation, scaling, and material selection on the Mapbox and dashboard can be segmented into four discrete steps in GH to achieve synchronization of geometric information between frontend and backend. In GH, when the same type of building is present in multiple locations, the duplicate data components were initially used to make duplication at the original site, followed by scaling, rotation, and removal operations. The sequence in which these steps are executed is not critical; however, it is essential to use Scale NU component, which scales the object along the x, y, and z axes respectively, and the Plane input for this component is the XY plane, originating from the initial location. This configuration guarantees precise scaling with each operation.

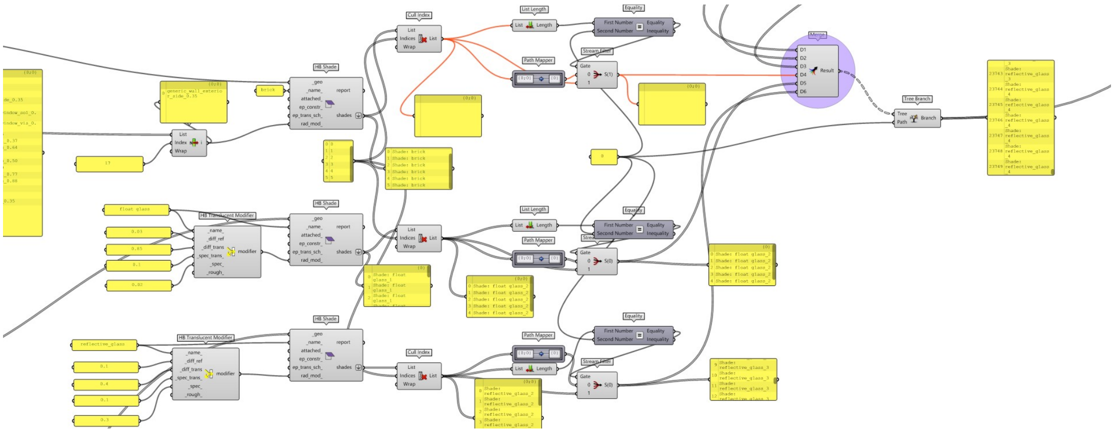

Figure 56: Extracting non-empty data while ensuring no empty inputs in GH workflow

The dispatch component is then employed to filter materials, which are subsequently organized into three categories based on material types. This categorization facilitates the creation of multiple distinct groups of HB shade. In this study, includes three selectable materials as outlined in Section 4.4.2 and Table 16. In instances where not all material types are employed in a scenario (i.e. all added buildings are brick), the input data for this HB Shade component(s) become(s) null, unwanted inputs induce a failure in the daylight simulation. This problem is typically manually rectified within the GH workflow by enabling the component with null output through a middle mouse button click. Nevertheless, for an automated daylight simulation process, a comprehensive solution that accommodates both null and non-null inputs is necessary to ensure robust simulation results.

The strategy is generating an arbitrary geometry at the origin or any coordinate point, and integrating it with the object list containing three materials to circumvent the issue of an empty set. It is important to note that the sequence in which data is accessed affects the functionality of Merge component; this arbitrary geometry must be accessed first. In the case study, a cube is constructed, resulting in six faces. For the HB Shade outputs, the process begins with flattening, followed by the use of the Cull Index component to eliminate the first six items. Subsequent to this operation, the data structure ascends to {0;0}, with the previously empty set of shades reverting to an empty state, and the non-empty set returning to its initial condition. The use of list length and stream filter implements conditional logic: if the set is empty, maintain the path {0;0}; if not, flatten {0;0} to {0}. This adjustment allows the subsequent merge component output to exclusively filter non-empty datasets with the path name {0} using the Tree Branch component (Figure 56). Attention must be devoted to data structures and pathnames during the development of the GH script. The complete GH script is available in Appendix 12.

4.3.4 Rhino Compute Workflow

The simulation results include a compressed mesh simulation grid and numerical results in text format, which are outputs from Rhino Compute. These results are then parsed into the correct format for display on the

Mapbox front-end web page during data processing. It's crucial to ensure that the grid is placed at the correct coordinates upon import. If the user selects the CBDM metric, the latitude and longitude are based on the floor location; if the ABDM metric is selected, they are based on the window location. The height is determined by the room level (as detailed in Section 4.1.3) and the user's chosen simulation height level. The specific implementation process is described in Algorithm 4.

```
Algorithm 4: Rhino Compute of Selected Room
  Input: Simulation Metrics, Selected Room Num, Added Surrounding Building's Info, SiLevel,
  LOD of 3D City Model
  Output: Mesh Simulation Result showing on Mapbox, Numerical Result and comparison on
  Dashboard

  if no Simulation Metrics then
  |  show spinner
  |  remove previous 'rhinoComputeObject_layer'
  |  compute (Simulation Metrics, LOD of 3D City Model)

  procedure compute (Simulation Metrics, LOD of 3D City Model)
     if no Selected Room Num then
     |  display message
     else
     |  start to count Compute Time
     |  Inputs ← Inputs and GH_[Simulation Metrics][LOD of City Model]
     |  send POST request to APP Server
     |  |  JSON.stringify (Inputs)
     |  process response
     |  |  collectResults (responseJson)
     |  |  stop to count Compute Time
     |  |  display result on Mapbox and Dashboard based on Simulation Metrics, LOD

  procedure collectResults (responseJson)
     for every data tree do
     |  for every branch do
     |  |  load Rhino Mesh geometry into doc
     |  |     decode JSON using rhino.DracoCompression.decompressBase64String
     |  |  parseFloat Numerical Result
     load Rhino doc into three.js scene
     load Rhino doc on 'rhinoComputeObject_layer'
     |  at simulationLocation (x, y, z) of Selected Room Num
     |  with rotation: { x: 0, y: 0, z: 180 }
     hide spinner
```

4.4 Interactive User Functionality for Added Building on Mapbox

4.4.1 Rotation & Dragging

The method employed here estimates the variation in the x and y coordinates based on the differences in latitude and longitude observed before and after a positional adjustment. The circumference of the earth is considered 40,075,000 meters. Errors associated with movements in the north-south direction tend to be more substantial compared to those in the east-west direction. But within a limited spatial context, given that the center of the BIM model has been manually established as the center of the world inside GH, discrepancies are negligible for incorporating a new building in proximity to the existing BIM building. As demonstrated in Table 15, the building added in Mapbox and the building synchronized to GH align closely, essentially occupying the same position. The implementation of syncing added building to GH back-end is explained in Algorithm 5.

Algorithm 5: Synchronize Added Buildings Coordinates and Rotation from Mapbox to Rhino

Input: World, BIM Building, Amount of rooms in the BIM Building
Output: Added Buildings' rotation degrees and x, y value in Rhino

rotationList ← [ ]
latitudeList ← [ ]
longtitudeList ← [ ]
for *every childeren* **of** World **do**:
    add rotation.z * (180 / Pi) to rotationList
    add (coordinates[0] - originLongtitude) * (40075000 / 360) to longtitudeList
    add (coordinates[1] - originLatitude) * (cos (originLatitude * Pi / 180) / 360) to latitudeList
rotationList.*remove_first* (Amount of rooms in the BIM Building)
latitudeList.*remove_first* (Amount of rooms in the BIM Building)
longtitudeList.*remove_first* (Amount of rooms in the BIM Building)

4.4.2 Material Selection

In the initial phases of building planning, three alternative materials - float glass, reflective glass, and brick were evaluated for façade application in this case study, providing a representative sample of local materials to effectively demonstrate the potential impact of new buildings. Notably, when implementing reflective glass material, the HB Glass Modifier is not used because it already incorporates predefined reflective properties (Ladybug Tools Forum, 2023), HB Translucent Modifier component is employed instead, which offers diffuse reflectance, transmitted diffuse, transmitted specular, and specular reflection four customizable inputs (HB-Radiance Primer, 2022), enhancing the flexibility of material settings. The brick material is sourced from the library available through the HB Search Modifiers. In cases involving materials with low transparency, such as bricks, the critical parameter is the diffuse reflectance value. For this material, a reflectance value of 0.5 is typically utilized (Figure 57). The default material for all newly added buildings is brick. Besides, the "HB Shade" is the lightest among HB objects since it has no boundary conditions or children (Ladybug Tools Forum, 2020), these material modifiers are also attached to the shade component.

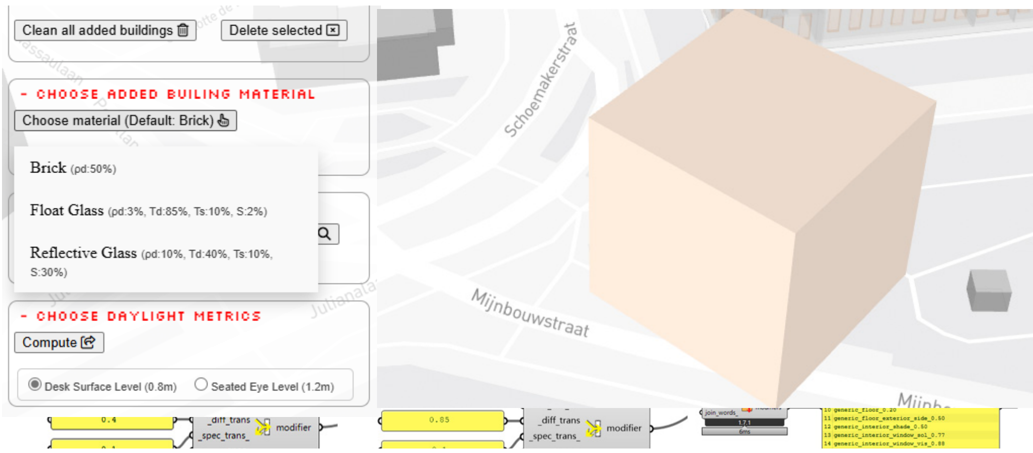

Figure 57: 3 materials settings in GH and user interface on Mapbox

4.4.3 Scaling

From the source code of Object3D.js (Threejs, 2024), object's scale, position, rotation properties are immutable. Threebox inherited this characteristic. This indicates that adjusting the scale of added geometry does not inherently alter its properties, these properties are set only upon the object's importation, and any forced alterations revert to their original state upon the next scene refresh. The approach discussed in this thesis involves the scaling function removing the existing geometry and promptly introducing new geometry. It is crucial to preserve the original geometry's characteristics, position, and material as inputs for the new geometry. Concurrently, with the removal of the old geometry, the associated list of features must also be erased at that particular index (Algorithm 6). From user's end, it straightforward to give dimensions of building being added in meters as inputs, when these dimensions are transferred to GH, scaling factors, which is calculated by dividing the user-entered dimensions by original dimensions (in this case study are established at 25 meters) are employed, due to the necessity of pre-preparing the GLTF for basic typologies as discussed in section 4.1.4, which must then be morphed accordingly. For newly added buildings that do not undergo scaling modifications, the default setting for the scaling factor array remains at [1, 1, 1].

Algorithm 6: Scale Selected Added Buildings

Input: Selected Added Building Object OS, Width, Depth, Height, if_Selected
Output: Scaled building 3D geometry on Mapbox, scalefactorList

```
procedure applyScale
if if_Selected = true then
    scalefactor(x,y,z) ← (Width / originalHeight, Depth / originalDepth, Height /
    originalHeight)
    OS.coordinate(x,y,z) ← unprojectFromWorld (OS.position.x, OS.position.y, 0)
    for every Added Building Info List do
        remove OS.property at OS.index of List
        add OS.property to the end of List
    scalefactorList ← scalefactor(x,y,z)
    load GLTF_OS.type on `custom-add_newbuilding_layer`
        at OS.coordinate(x,y,z) with scalefactor(x,y,z)
        for every surface of the Added Building
            surface.material.color ← OS.color
    re-render the scene
return scalefactorList
```

4.4.4 Remove Selected & Remove All

The functionality to delete selected added buildings and to clear all added buildings offers considerable convenience for users, preventing the need for page reloads. To remove a selected building, the building's index is located by checking the uuid of selected building, and then deletes the corresponding entry from the tracking record's list. It is essential to repaint the map afterwards to update the rendering. For clearing all added buildings, the most efficient approach involves verifying the presence of the layer and then emptying the 'custom-add_newbuilding_layer'. Subsequently, all entries in the tracking record's list should be reset to 'undefined' to erase old data.

4.5 Interactive User Functionality for Per-room Daylight Simulation

4.5.1 Room Query by Name & Clicking

It is convenient for users to have the ability to query rooms by name through a dropdown menu equipped with a search box, in addition to direct selection via clicking. Room names tend to be more recognizable to users compared to room numbers, such as "BG.sOost.050". The list of room names is derived from CSV data exported as detailed in Section 4.1.3. Regardless of the method used for room selection, the input for room selection processed by Rhino Compute remains the room number integer. It should be noted that the bounding box in Threebox is automatically generated upon a hover or click event (Algorithm 7). However, for implementing querying room by name feature, it is necessary to activate the bounding box when importing geometry per room into Mapbox.

Algorithm 7: Room Information CSV Parsing and Room Query Option Generation

```
Input: Room Information CSV File
Output: {room[Num]:Name}, {room[Num]:Level}, [roomName] to show On Mapbox
Room Query Drop Down Menu

fetch 'RoomInformation.csv'
add room 0 to [roomNum] for roof and other elements don't have a room tag
for every line in CSV do
    trim line and split by ','
    if line [0] exist then
        add line[1] to [roomName]
        room[line[1]] ← int line[0]
        room[line[0]] ← line[2]
for every roomName i in [roomName] do
    create option tag ← i
    add i to datalist element
```

Whenever a user selects a room, or conducts a query and opts to "preview Room," the unselected segments of the BIM model are rendered 97% transparent to emphasize the selected room visually (Algorithm 8).

Algorithm 8: Selected Room Preview on Mapbox

```
Input: Selected Room Object (OS) by Clicking / Querying by name
Output: All rooms on Mapbox become 97%transparent except the preview room

procedure roomPreview (OS)
    if OS exist then
        for i in range (length of roomList) do
            if world.children[i].uuid != Selected Room Object.uuid then
                for every component j in room[i] do
                    world.children[i][j].materialTransparent ← true
                    world.children[i][j].materialOpacity ← 0.03
                    world.children[i][j].materialDepthWrite ← false
            else Selected Room Num ← i
        for every component j in Selected Room do
            world.children[Selected Room Num][j].materialTransparent ← false
            world.children[Selected Room Num][j].materialOpacity ← 1
            world.children[Selected Room Num][j].materialDepthWrite ← true
```

re-render the scene
else *display message*

4.5.2 Choose Daylight Metrics & Get Simulation Results

This application incorporates standard annual daylight metrics, including DA, sDA, UDI, and the validated SBI, which has potential to supplant the conventional CBDM standard. Users select these metrics via a dropdown menu on the front-end, with the system recording a sequence number corresponding to the chosen metric and retrieving the appropriate file based on this identifier. Although it is theoretically possible to use a single GH file with the serial number as an input, this methodology is avoided to prevent making the GH file unwieldy. For instance, if the user chooses LOD 1.3 and UDI as the metrics, a metric file named selectRoom_3_1.gh will be selected and executed by Rhino Compute.

When connecting the "text" and "mesh" components in the GH output, it is imperative to maintain the correct sequence to ensure accurate parsing of JSON data, thereby distinguishing between geometric and numeric results. Furthermore, the innertree path names differ among the various metrics. In this workflow, the sequence of connecting the mesh first and then the text is utilized in all GH files. Shading ensures that the number to be parsed consistently remains at index 1.

The legend for each metric appears only after the user makes a selection from the dropdown menu. The coordinates of the mesh grid also differ depending on whether CBDM or ABDM is selected. CBDM is based on the indoor layout and requires floor coordinates, whereas ABDM is based on aperture and necessitates the coordinates of the windows. Given the regular type and distribution of windows in this case study, the window heights can be determined based on the floor heights.

Distinct from general daylight simulation software, this application provides comprehensive explanations for each metric to assist designers in comprehending the implications of the daylight metrics (Table 14).

<table>
<tr><td>Metrics</td><td>DA</td><td>sDA</td><td>UDI</td><td>SBI</td></tr>
<tr><td>Standard</td><td>CBDM</td><td>CBDM</td><td>CBDM</td><td>ABDM</td></tr>
<tr><td>GH Name</td><td>selectRoom_1_2(LOD).gh</td><td>selectRoom_2_2(LOD).gh</td><td>selectRoom_3_2(LOD).gh</td><td>selectRoom_4_2(LOD).gh</td></tr>
<tr><td>Innertree</td><td>{0;0}</td><td>{0;0;0}</td><td>{0;0}</td><td>{0;0}</td></tr>
<tr><td>response Json</td><td>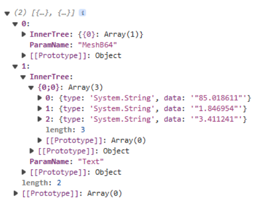
</td><td>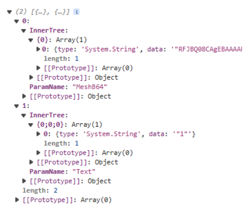
</td><td>
</td><td>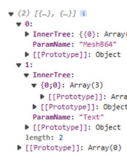
</td></tr>
<tr><td>Coordinates Based on</td><td>Floor</td><td>Floor</td><td>Floor</td><td>Windows</td></tr>
<tr><td>Result Exampleon Application</td><td>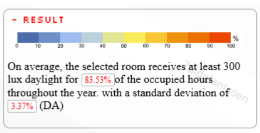
</td><td>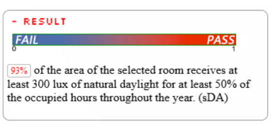
</td><td>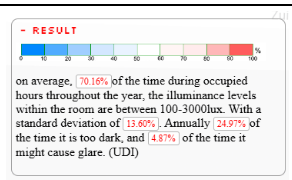
</td><td>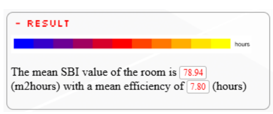
</td></tr>
</table>

Table 14: Different metrics selection and implementation

In Table 15 , the JSON file containing floor coordinates was procured and interpreted as an object, comprising solely latitude and longitude data. To ascertain the altitude information, it is necessary to integrate the simulating surface level with the floor height (Algorithm 9). In Revit, the floor heights for each level can be extracted from the section view, and subsequently combined with the simulating surface level specified in Section 4.5.4.

Algorithm 9: Get Simulation Position for Selected Room

Input: floorCoordinates.JSON, Selected Room, Selected Eye Height
Output: simulationLocation (x, y, z)

fetch ' floorCoordinates.JSON '
parsedObject ← JSONdata
procedure getSimulationLocation
  simulationLocation (x, y) ← parsedObject [Selcted Room] (x, y)
  set different altitude for different room level based on BIM model
  simulationLocation (z) ← selectRoomLevelHeight + selectedSimulationSurfaceHeight

4.5.3 Compare Simulation Results

Common daylighting software typically cannot retain results from previous simulations. In this application, numerical results from each calculation are temporarily recorded for comparison with subsequent simulations. Initially, the result comparison column is blank. When the application is first run, this column remains empty. If it's the first calculation under a specific LOD or grid surface level option, it will display "This is the result of the first simulation in this case." If the LOD or grid surface level changes during the simulation, the results will be re-recorded (Figure 58).

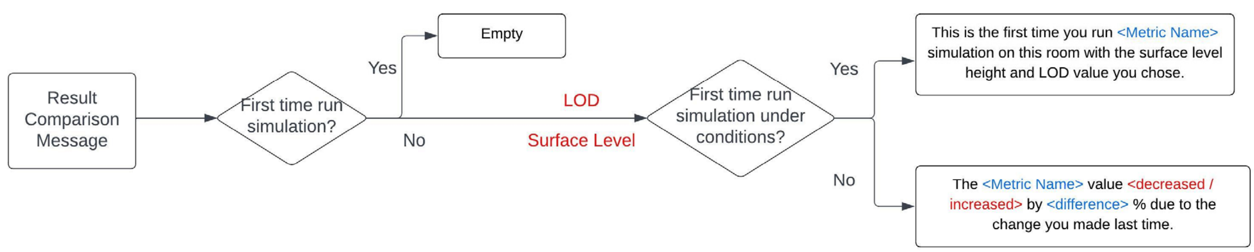

Figure 58: Result comparison message showing in the application

4.5.4 Other Functionalities

The application incorporates other functionalities such as selecting the 3D City LOD, based on data from the 3D Bag website. This application supports LOD options of 1.3 and 2.2, with the default setting at 2.2, which can be adjusted via a radio button interface.

For simulating surface levels for CBDM metrics, two radio buttons are available, offering options of 0.8 meters and 1.2 meters, with the default set to 0.8 meters. A height of 1.2 meters simulates daylight conditions at the average eye level of a seated person, accurately reflecting lighting for tasks like reading or computer work. Conversely, a height of 0.8 meters assesses daylight performance on desk surfaces, helping designers evaluate natural light adequacy for tasks such as writing, reading, or using a computer. When the corresponding simulation grid is imported into Mapbox, the varying heights of the simulation surfaces will be reflected accordingly.

In consideration of potential application scalability, the EnergyPlus weather (EPW) file input feature allows users to navigate to the EPW map website, select the desired location, and copy the corresponding URL (refer to Section 5.2 for further details).

4.6 Workflow Optimization

4.6.1 LOD 1 vs. LOD 2 of 3D City Model

The DA metrics were analyzed to examine the impact of LOD variations on accuracy and computation time. For this analysis, 11 rooms located on the outer part of the BK model were selected to compare the DA metric results.

As shown in Figure 59 and Figure 60, differences in simulation results are minimal across all rooms, indicating that LOD 1.3 closely approximates the results of LOD 2.2. But the percentage differences in simulation time vary significantly, with certain rooms (e.g., Room 35, Room 227, and Room 378) showing

Figure 59: Simulation accuracy and time comparison of LOD 2.2 and LOD 1.3 of static surrounding building models

substantial increases in time required for LOD 2.2 compared to LOD 1.3.

This may be attributed to Delft's characteristics of low housing density, short building heights and minimal urban canyon effect. Despite the prevalence of pitched roofs in Delft, the impact of the building shapes is mitigated by the overall low density. Consequently, this finding might not be applicable to other locations, such as the city center of Amsterdam, where higher density could result in greater variation in simulation results between LOD 1.3 and LOD 2.2.

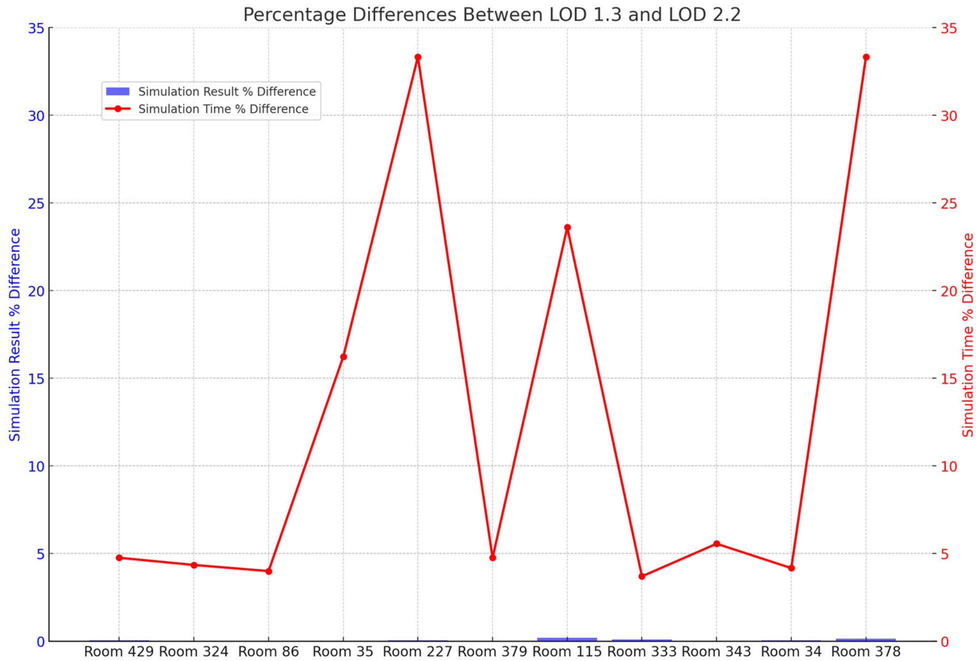

Figure 60: Percentage difference of simulation time and accuracy between LOD 1.3 and LOD 2.2

In conclusion, within this workflow, it is recommended to use LOD 1.3 for simulations as it delivers results comparable to LOD 2.2 without prolonging computational time. Nevertheless, users retain the flexibility to select either LOD 1.3 or LOD 2.2 for the final application.

4.6.2 Load BIM Elements on Mapbox

As discussed in Section 4.1.4, multiple methods exist for integrating a BIM model into Mapbox. To realizing automated daylight simulation on a room-by-room basis, the optimal approach is to categorize it accordingly by room initially and import the model by individual rooms.

4.6.3 Extent of 3D City Model in Daylight Simulation

Seven rooms of differing orientations were selected for the study. The mean DA value for each room was used as the evaluative metric for daylight simulation accuracy. All simulations were conducted with a detail level of 1, a grid size of 0.6m, and a height of 0.8m, using the LOD 1.3 model from 3D BAG. Simulation Results. Figure 61 presents a comparative analysis of the mean DA values and computation times for different range radius.

Across all rooms, the DA mean values are quite consistent regardless of the range radius, indicating that increasing the radius beyond 200m doesn't significantly affect the accuracy of the daylight simulation results. This also suggests that smaller radii might be sufficient for accurate daylight simulations, so in the GH script of all the metrics and LOD options, the 200m radius model is used for regular simulations due to its efficiency in computation time without compromising accuracy.

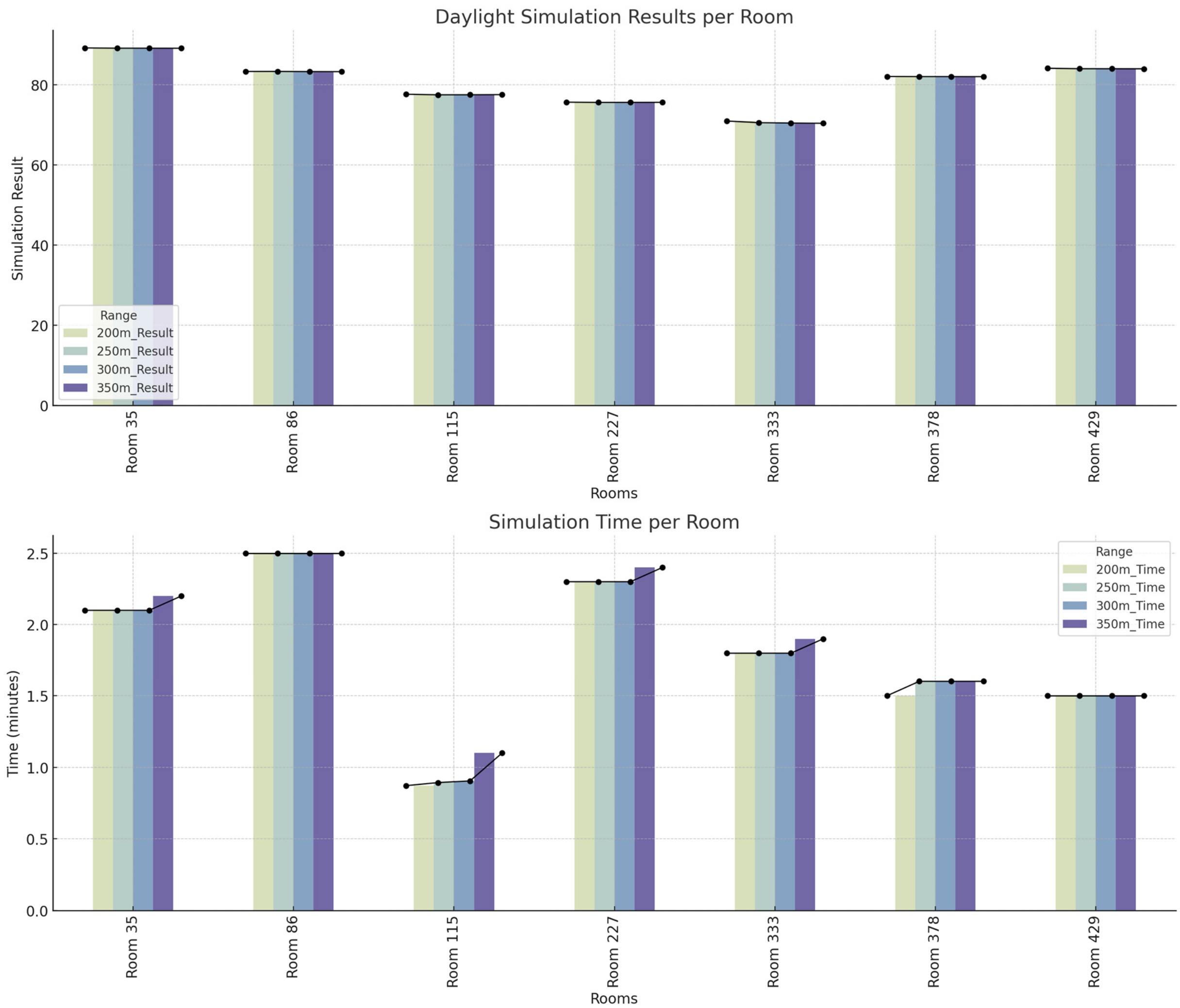

Figure 61: Simulation accuracy and time comparison of different radius of spatial extent of surrounding buildings

As the range radius expands, computation time increase in most of the cases. GH records time with only one decimal place when it is more than 1 minute, potentially obscuring minor variations. Despite this, the overall trend shows a clear upward trajectory, highlighting the increase in computational load as more model details are included.

4.6.4 Other Aspects & Equipment Limitations

HB Shade component is the lightest and meshes can help speed up the computation process (Ladybug Tools Forum, 2020), Complex shapes in the GH script are converted to mesh at the beginning. Owing to the constraints of this thesis, Rhino Compute was only operated on a locally. Consequently, the velocity of the simulation execution is contingent upon the local RAM capacity, and the performance in the plug-in state is notably superior to that observed in power-saving mode computing. The experiments in this section were conducted under computer's optimal efficiency.

5 / Results

5.1 Potential to Utilize SBI & View Lumen

The R^2 value distribution in South orientation and North orientation across scenarios is shown in Figure 62.

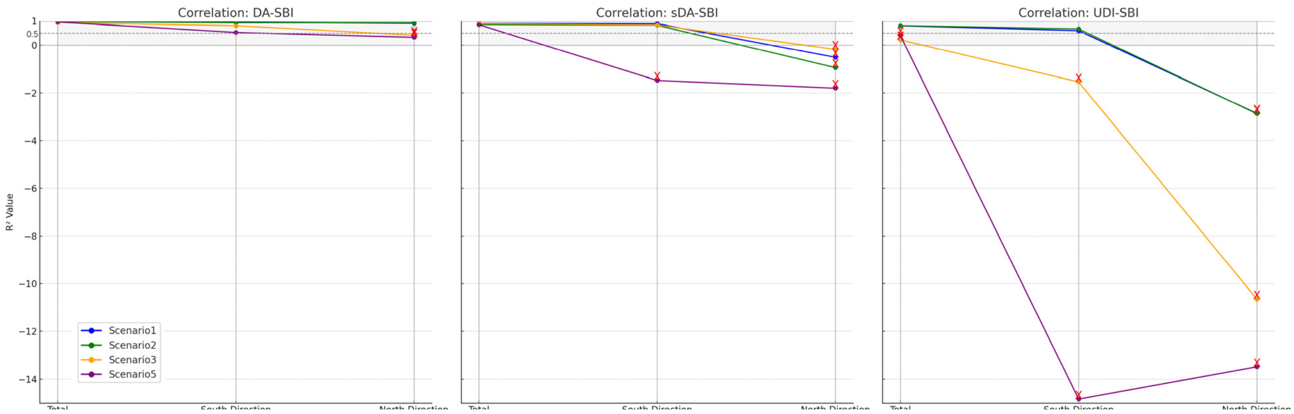

Figure 62: R² value distribution across scenarios: Total, South, and North

The analysis and visualization of values for the correlation metrics (DA-SBI, sDA-SBI, and UDI-SBI) across different scenarios and orientations (South Direction, North Direction) reveal several insights:

1. The combined datasets generally provide a better fit for the regression models due to averaging effect and more data points (16 in total, compared to 6 each for North and South), it captures the variability from both directions, leading to a more accurate fit.
2. For all correlations, the south-oriented scenarios consistently show better fits than the north ones. Orientation is an important moderating variable among the correlations.
3. Red crosses in the plots denote R^2 value less than 0.5. Several north-oriented scenarios for the sDA-SBI and UDI-SBI correlations falls below this threshold too much, emphasizing weak predictive power in these cases.
4. R^2 values across different scenarios implies that specific conditions or configurations play a significant role in determining the strength of the relationship between daylight metrics, for example Scenarios 1 and 2 generally exhibit higher R^2 values for both North and South compared to Scenarios 3 and 5, warranting further investigation into the factors influencing these outcomes.

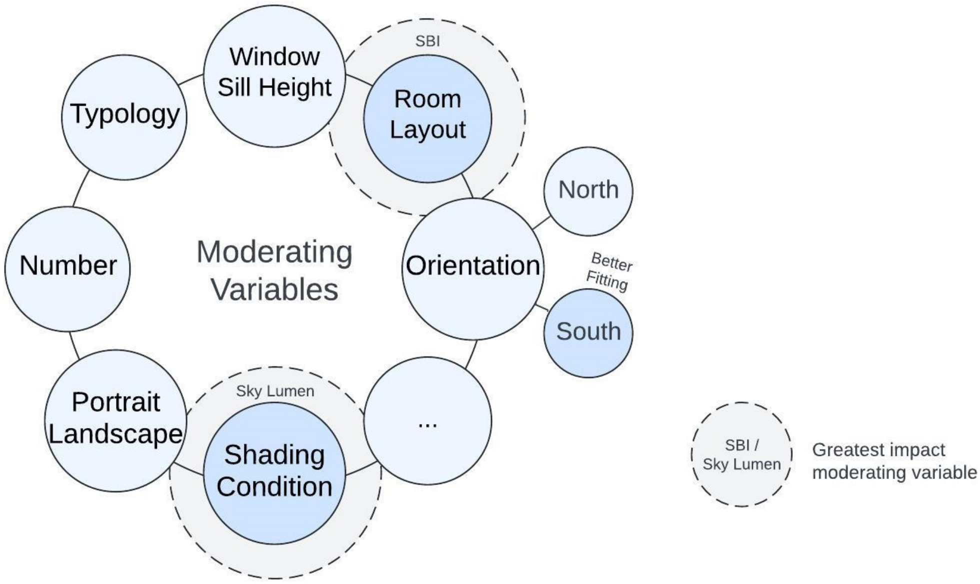

Figure 63: Moderating variables for correlations between CBDM and ABDM metrics

In summary, the analysis of the data from the Section 4.2.2 confirms the initial hypothesis that all the design's moderating variables are valid. Among the metrics correlated with SBI, room layout emerges as the most influential factor, while for sky lumen correlation, the presence or absence of shading as a moderating variable has the greatest impact (Figure 63).

Figure 64 is the boxplot of distribution of the R^2 value of correlations between ABDM metrics and CBDM metrics, by analyzing the median values, DA demonstrates the most robust average effectiveness in predicting variations in SBI and view lumen as dependent variables. Both DA-SBI and DA-view lumen exhibit the greatest consistency across different conditions, as evidenced by the interquartile range comparison. It is important to note the presence of outliers in the sDA-SBI and DA-view lumen distributions, indicating that in real-world scenarios, there may be instances where neither SBI nor view lumen correlate with CBDM measures. The range of R^2 values is most extensive for UDI in its relationships with both SBI and view lumen. Overall, SBI is revealed as the most consistent and predictable metric for assessing general daylight availability in CBDM.

Overall, SBI appears to be a strong candidate for replacing traditional metrics like DA and reasonably effective for sDA but exhibits limited applicability in replicating the performance of UDI. Sky lumen consistently demonstrates lower R^2 values across all metric comparisons, suggesting its limited reliability as an alternative to established daylight metrics such as DA, sDA, or UDI.

Although a robust correlation exists between the SBI values and both DA and sDA values, the practical application of SBI to predict DA and sDA must acknowledge that the relationship can be influenced by varying conditions (such as room characteristics, window features, and obstructions in the surrounding environment). Meanwhile, the correlation lacks strong predictive accuracy in north-facing rooms due to poor data fit. Further research is needed to include additional moderating variables and to establish a definitive quantitative mathematical relationship between these metrics.

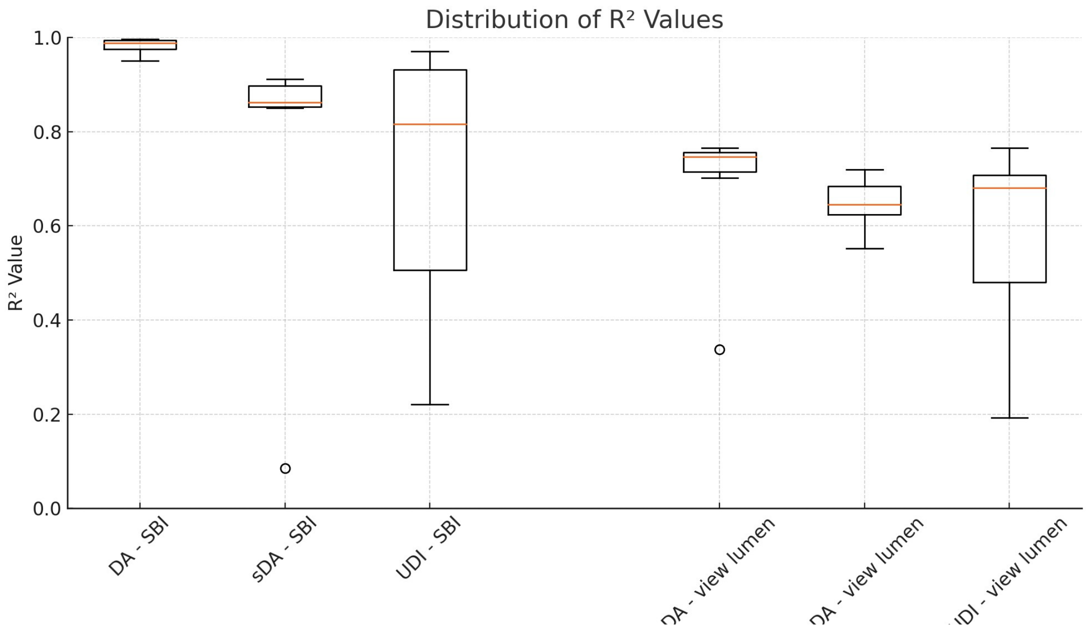

Figure 64: Boxplot of distribution of R^2 value

The SBI metric is implemented on the web application as an option as shown in Figure 65.

Figure 65: SBI as a metric option on web application

5.2 User Interface For Adding Building on Mapbox

User interface design

Part of the functionalities discussed in Section 4.4 involves user interaction via the dashboard, while the other part is performed directly within the Mapbox interface. For instance, actions such as clicking on a room, rotating, dragging and dropping a newly added building, and obtaining a simulation mesh are handled through the Mapbox interface. The dashboard design is depicted in Figure 66.

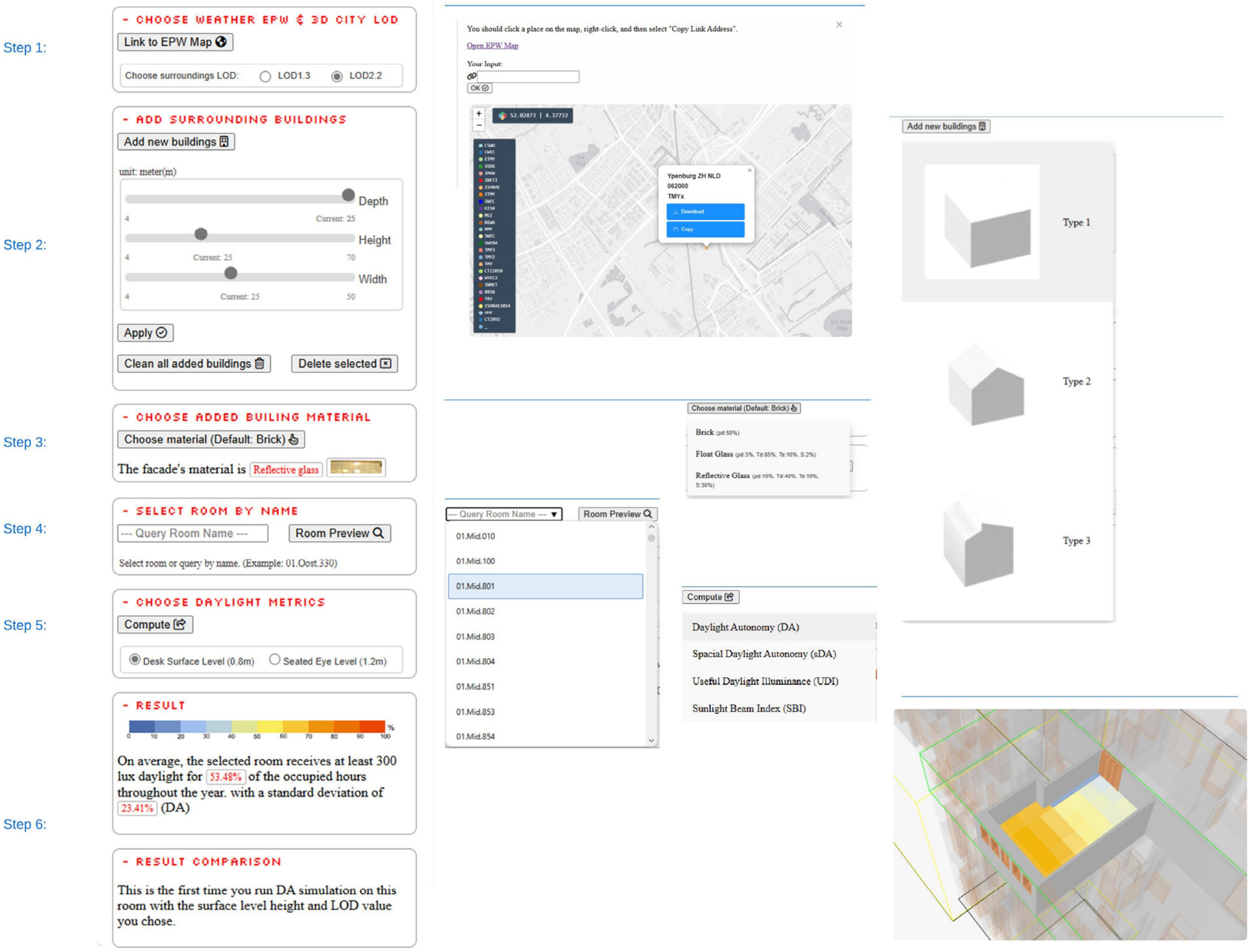

Figure 66: User interface design

The first step involves setting up the static urban environment and EPW data, which are typically site-specific and do not require frequent adjustments. The second step features a drop-down menu offering three prototypes for adding new buildings. These buildings are initially positioned in a default location and can be resized using a slider. Users can preview adjustments by clicking "Apply." There are also two buttons to clear all newly added buildings or delete selected ones. In the third step, users can modify the materials of the newly added buildings, choosing from three available options. Material changes can be previewed in Mapbox, with corresponding color changes. Users can click on any newly added building to view its material information.

The fourth step involves selecting the room for simulation. Users can either click directly on the room or enter its name in the drop-down menu. Clicking "Preview Room" will make the buildings surrounding the selected room translucent. This process can be repeated for multiple rooms. The fifth step requires selecting metrics from a drop-down menu for sunlight simulation and setting the simulating surface height as needed. The sixth and final step involves obtaining the simulation results, along with descriptions and comparisons with previous simulation results under the same conditions.

Table 15 illustrates the detailed steps and corresponding pages for each stage. The blue text represents the pre-settings process, which does not affect the visual representation of the final result but is solely part of the performance or verification process. For example, the initial order of addition is type 3, followed by type 2, and then type 1, with the building list initially recorded as [3, 2, 1]. However, since building 1 remains unchanged and types 2 and 3 undergo sequential scaling, the final building list is reordered to [1, 2, 3]. each modification of the material results in a corresponding change in the building's color. When a building is selected, the currently chosen material is prominently displayed on the dashboard.

Step	Screenshot
Pre settings: Remove extrusion buildings at BIM's location	 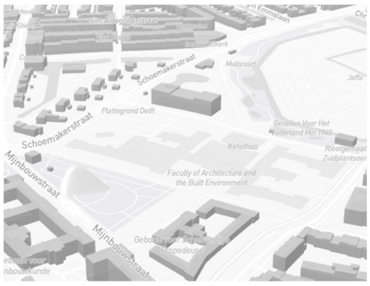
Load in per room	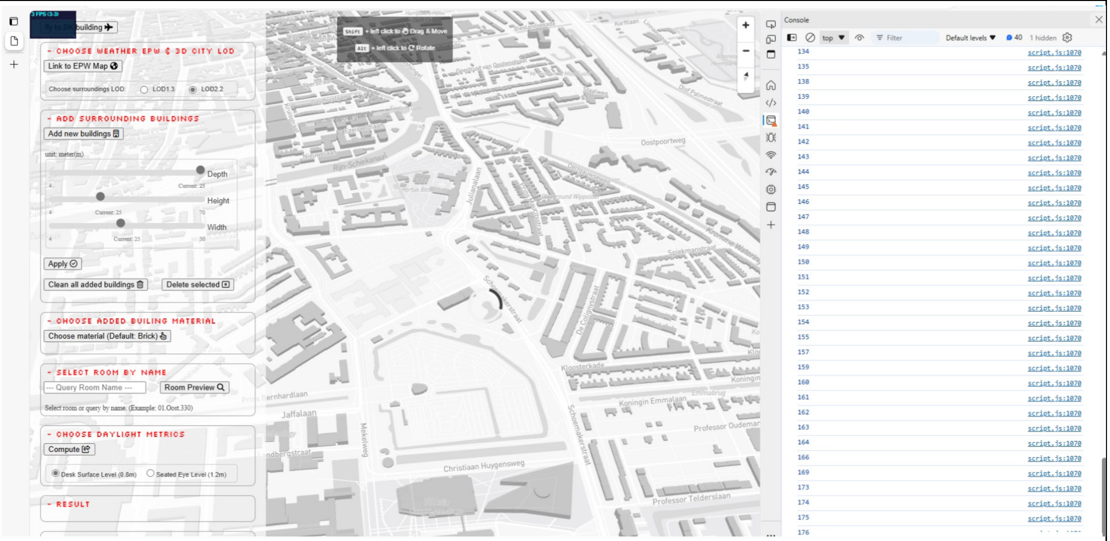
Choose LOD and simulation surface level	 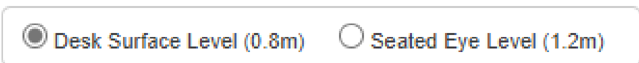

Pre settings: Add Geometry Properties After Setting Mapbox	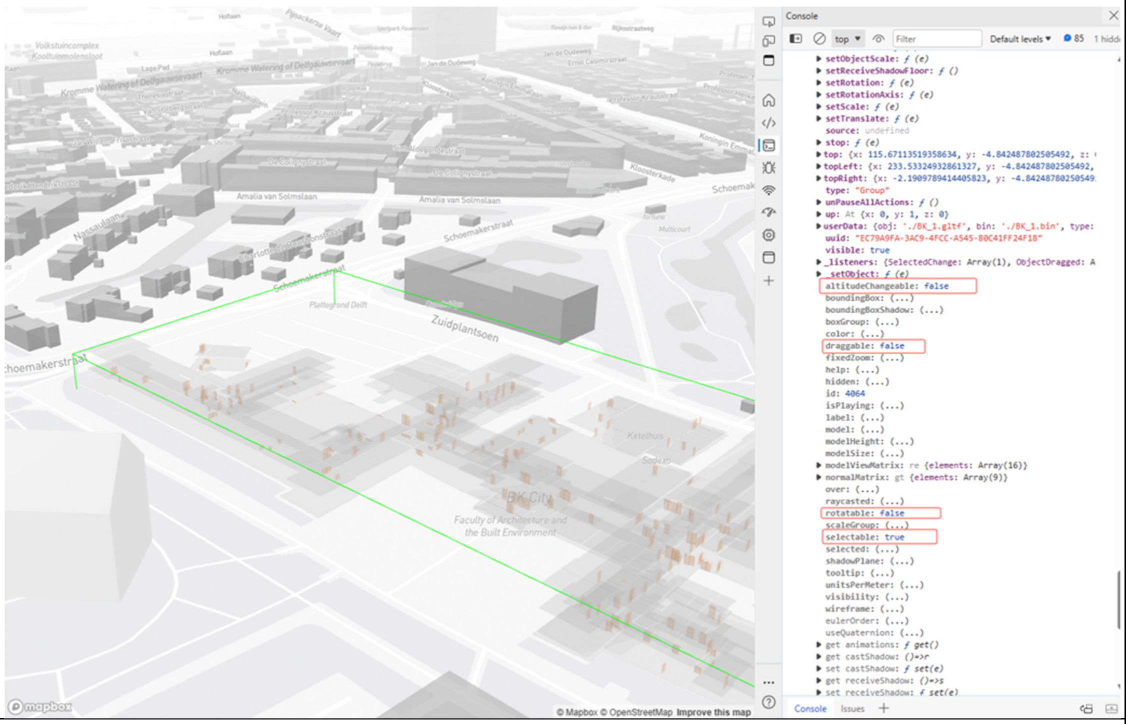
Link to EPW Map webpage and copy the link	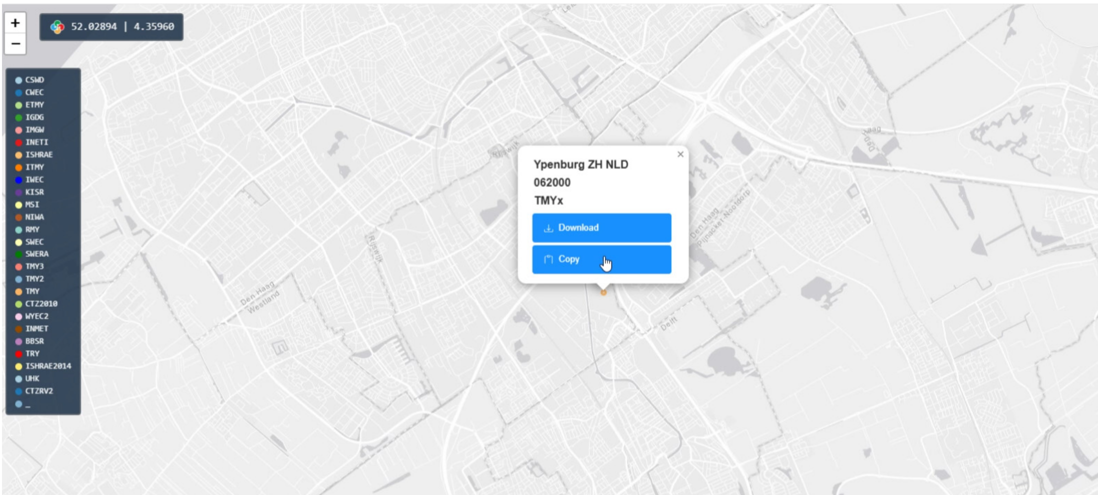
Paste the EPW ur as input	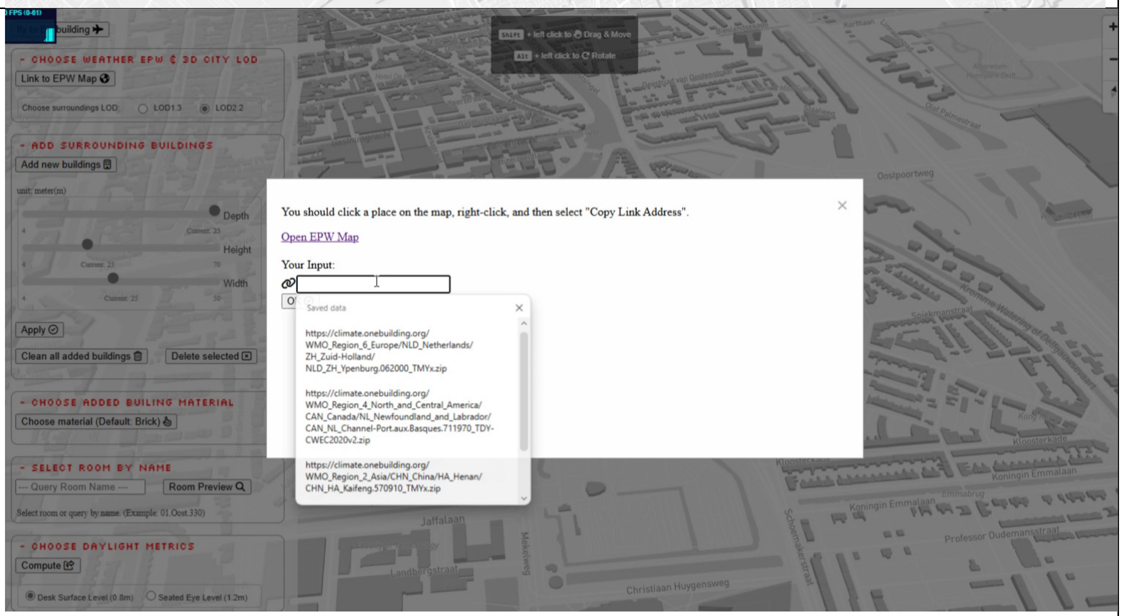

Add new buildings	
Rotating and scaling of added buildings	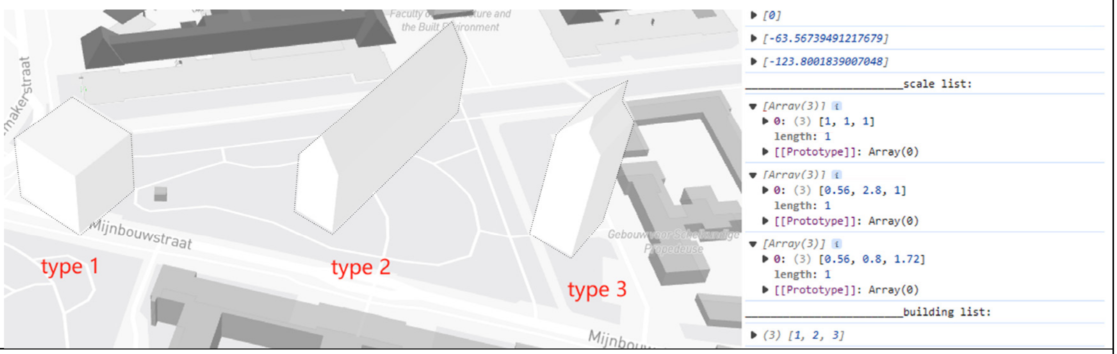
Assign different materials to added buildings and scale according to design	

Pre settings: Added building sync to GH with location, rotation, typology, material	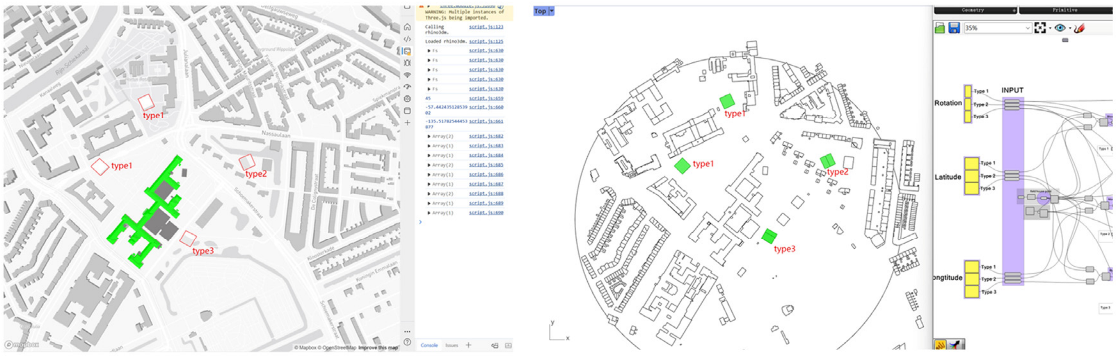
Room query and preview	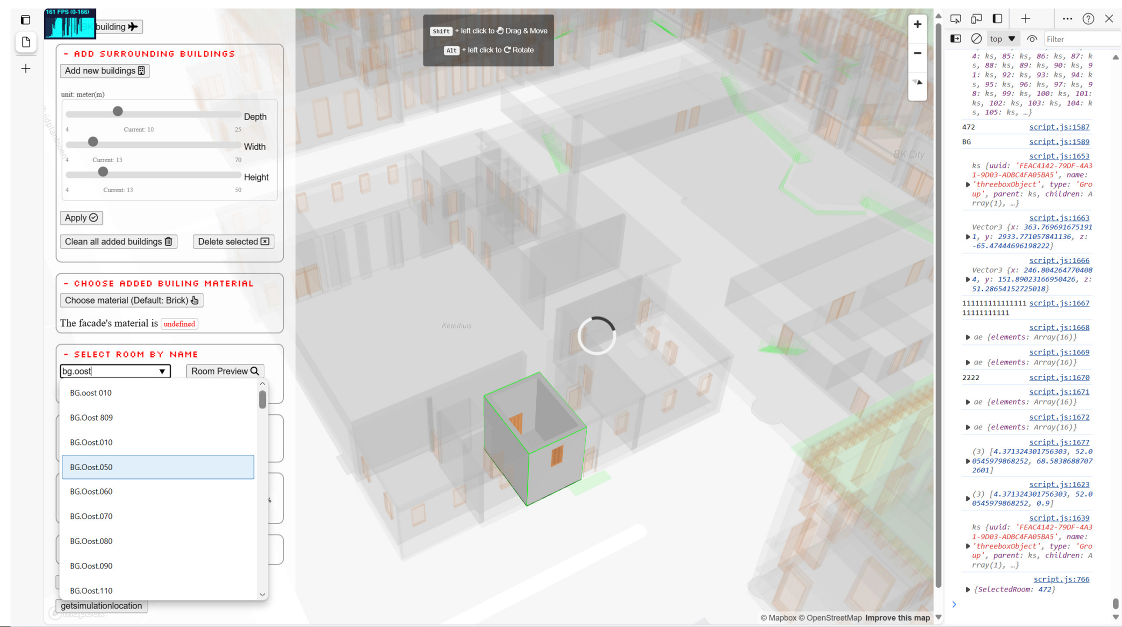
Running Rhino Compute locally	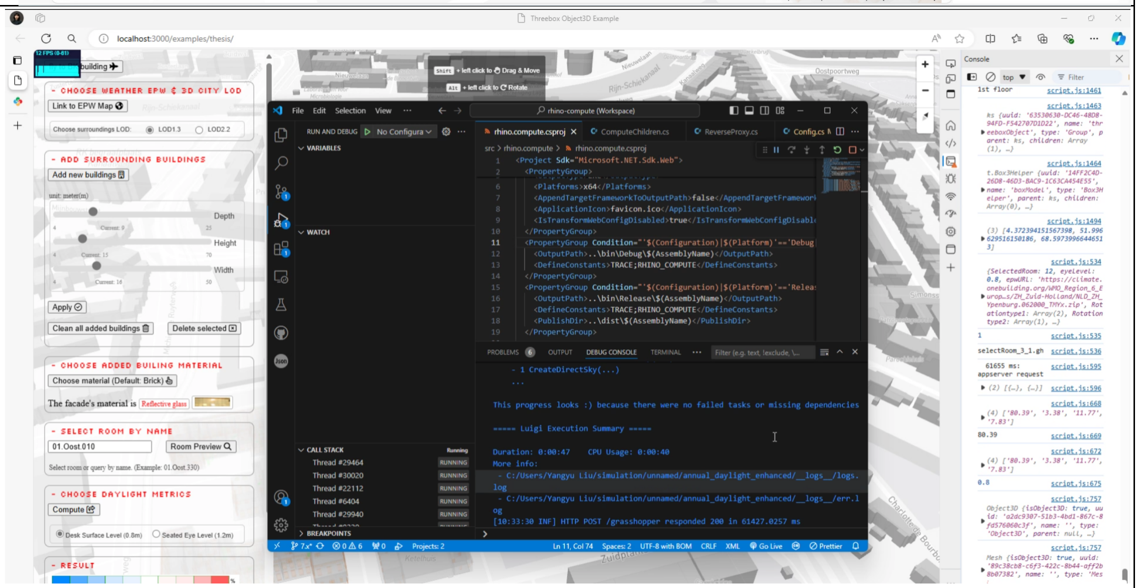

Pre settings: Room coordinate collected the time query / select a room and ready for load in the simulation grid. the coordinate displayed closely aligns with the one in Google map, demonstrating a high degree of accuracy.	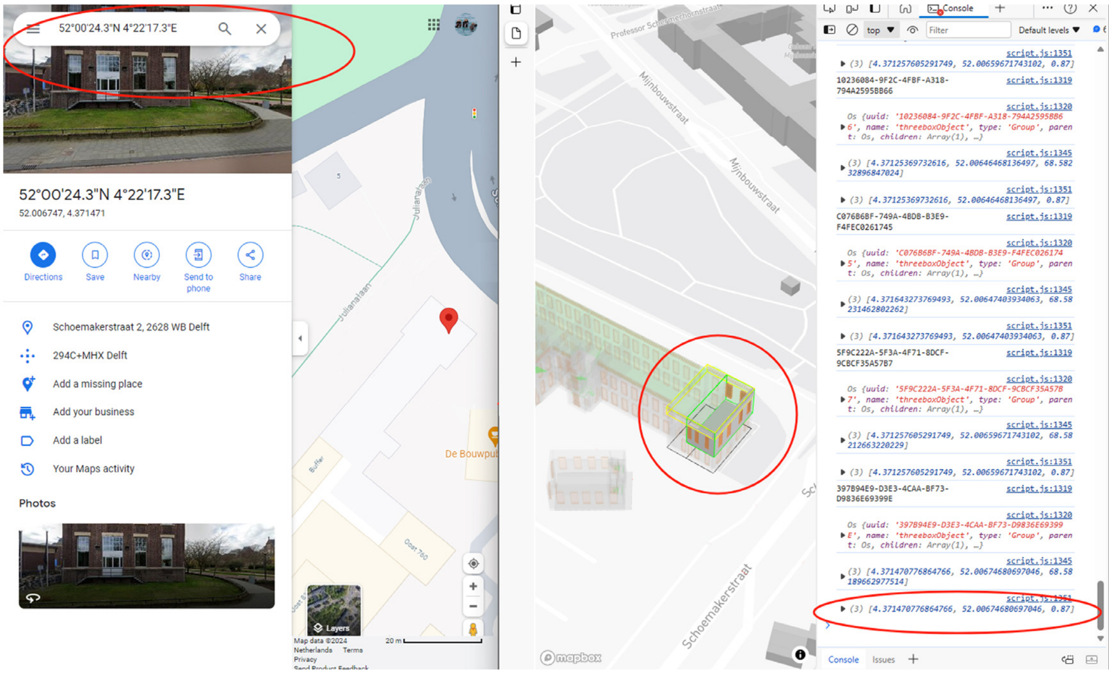
Get simulation result on Mapbox and dashboard	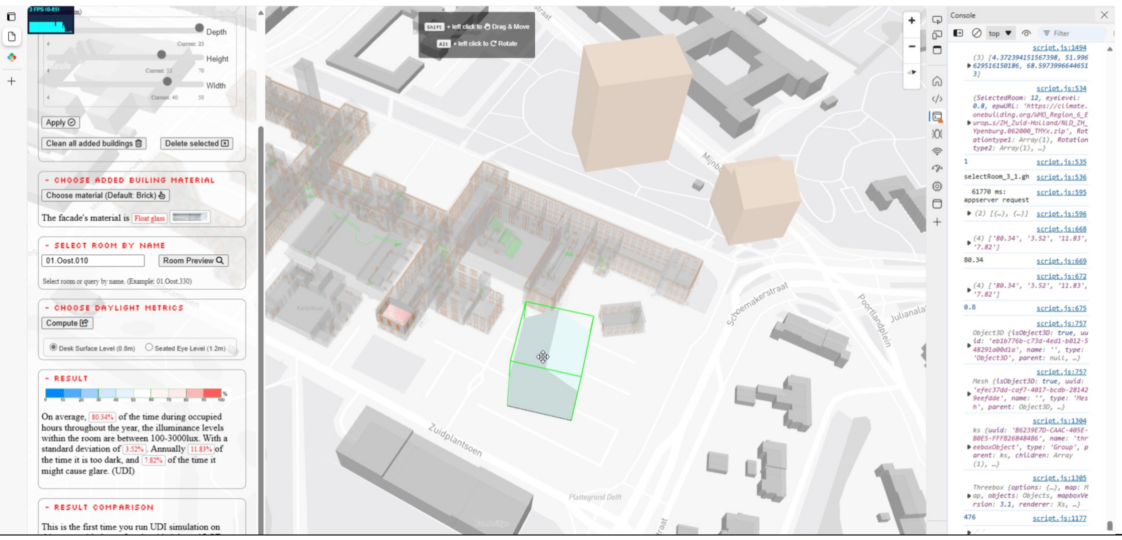

<table>
<tr><td>Result comparison after making changes to the environment</td><td>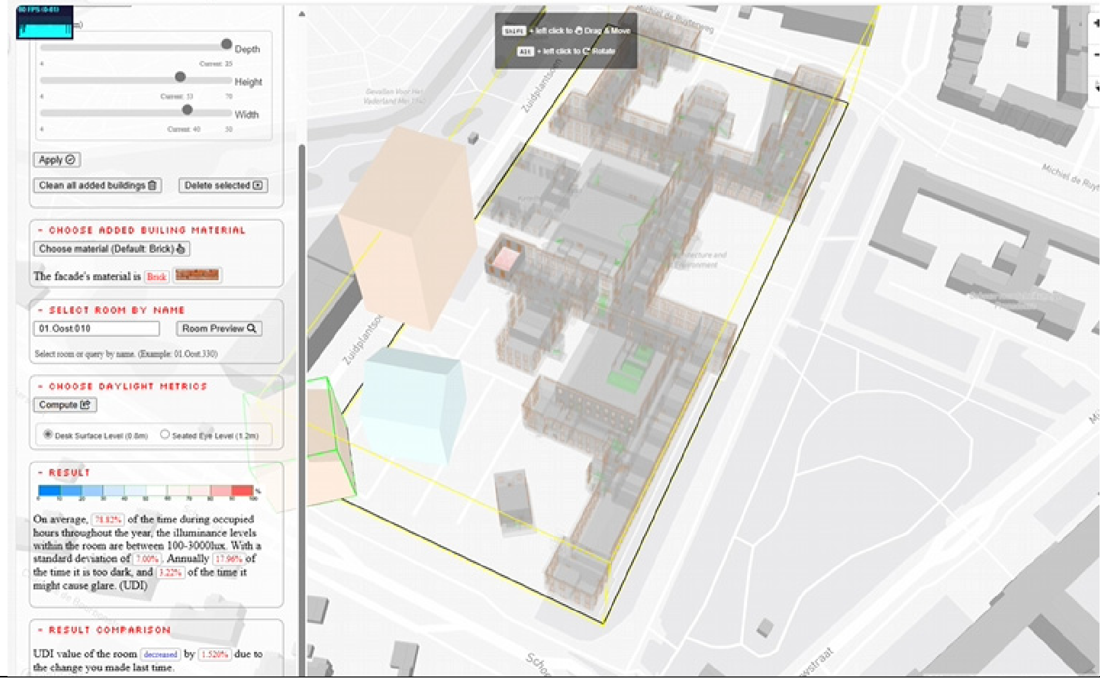
</td></tr>
</table>

Table 15： Results and pre-settings for the application's interface

Material Selection of added buildings

The incorporation of various materials in the newly added building influences the indoor daylight dynamics of BIM model. To empirically demonstrate this effect, an experiment was conducted: A simple room was modeled in Rhino, where a basic box was positioned outside the window to act as an obstruction. Three distinct materials were selected for the box, and the resulting DA variations within the room were recorded. These changes are depicted in Table 16. This indicates that the choice of materials for the facade of a new building is a crucial parameter.

<table>
<tr><td>Material</td><td>Display in the application</td><td>Results
</td></tr>
<tr><td>Float Glass
</td><td>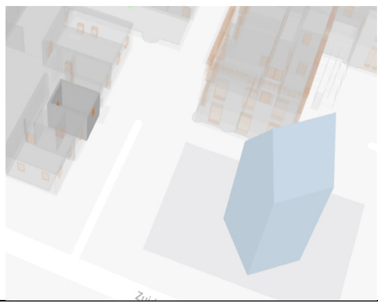</td><td>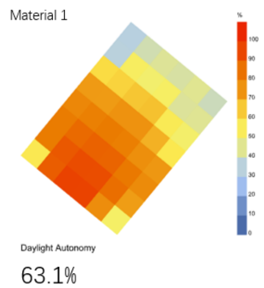
</td></tr>
</table>

Brick 	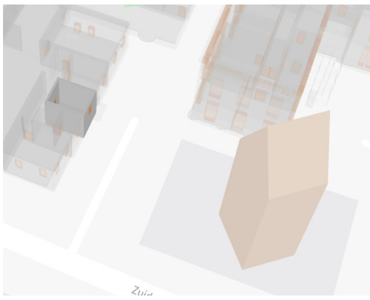	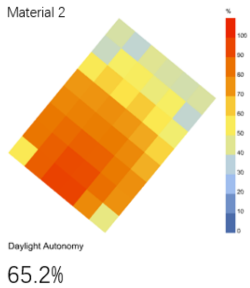
Reflective Glass 	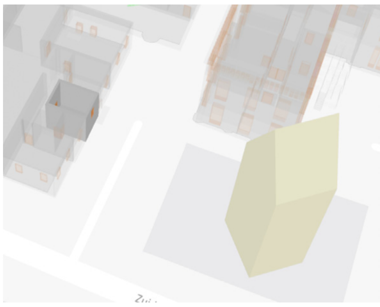	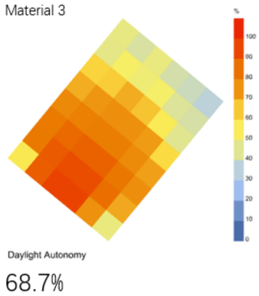

Table 16: Changes of DA value of a room due to material changes of obstruction

5.3 User Interface for Per-room Customized Daylight Simulation

Load in BIM 3D Data on Mapbox & Get Room Coordinates

In Section 4.1.4, it was determined that importing the BIM model by room is the most effective approach. Table 17 illustrates the process of importing the BIM model by individual elements. This method results in a significantly larger page, thereby prolonging the import duration for all elements.

Furthermore, prior to optimization, importing by room directly can lead to errors in element selection, particularly with walls that traverse multiple rooms. These walls necessitate multiple room tags and are treated as common components of several rooms, leading to multiple imports of the same wall. This increases both the import time and the file size, though these increases are still manageable.

The table also demonstrates the process of importing the BIM model by element. By separately importing the floor category to acquire coordinates, a temporary download button was created on the dashboard, the data was saved and subsequently imported it into the official Mapbox page with all categories imported.

Load in per element (only doors)	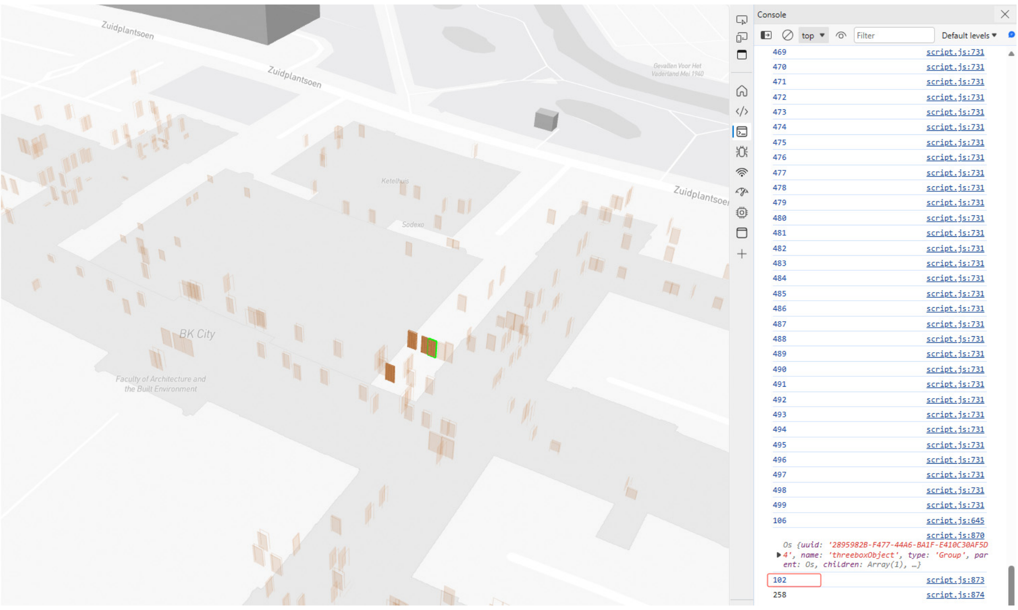
Load in per element + room selection	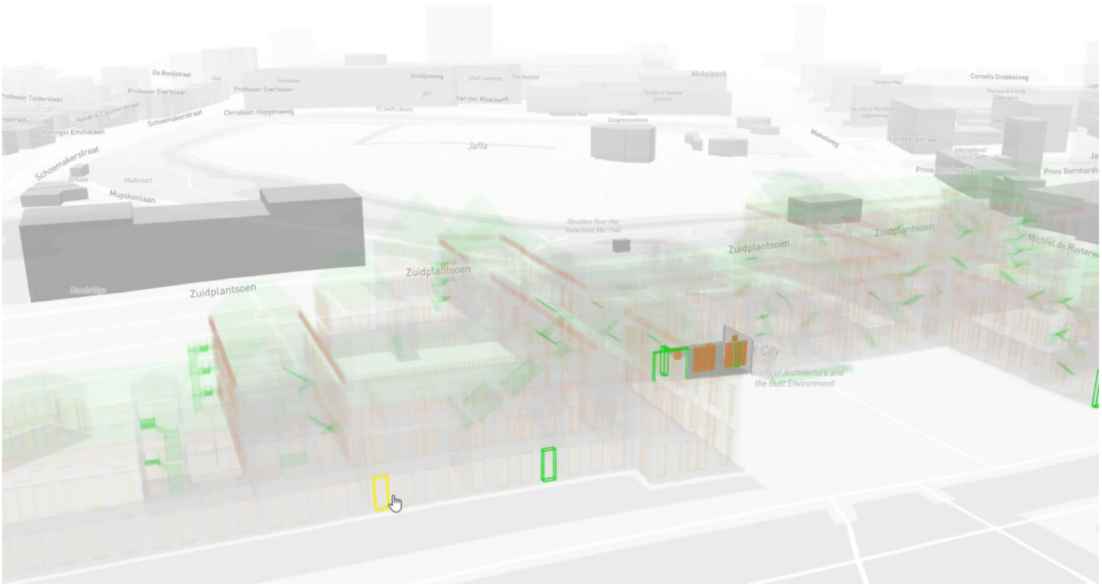
Load in per room without considering roof and exterior BIM elements	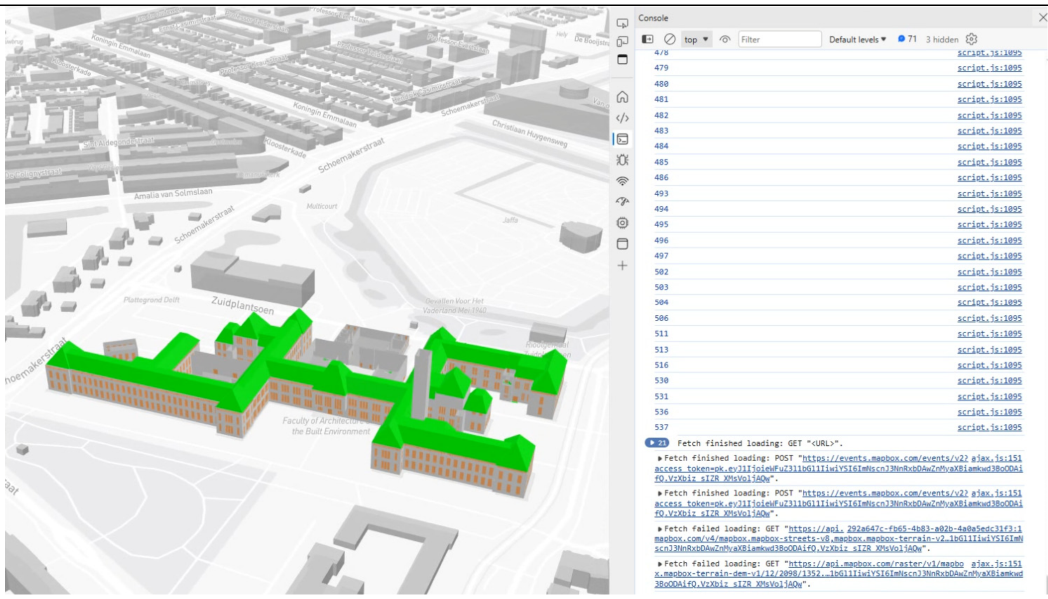

Load in Floor category only	
Load in per room and get coordinates from the above step	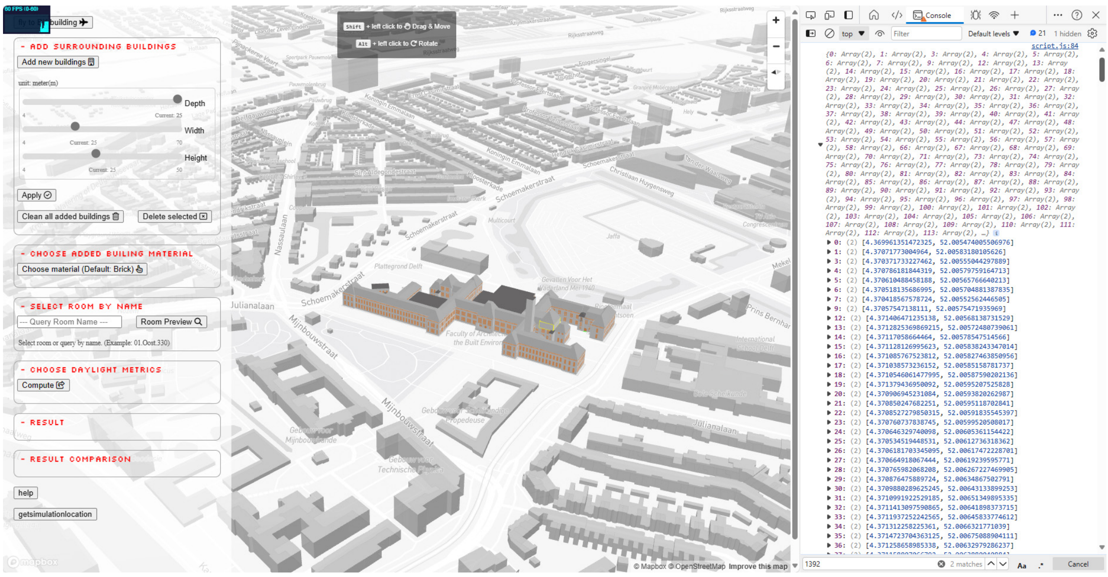

Table 17: Importing BIM models in Mapbox

Get Simulation Results

There are two versions of importing mesh on Mapbox through Rhino Compute Appserver, after trying both the one with brighter colors is chosen. Additionally. Table 18 provides an example of the simulation results for the four metrics. It includes importing the simulation grid into the Mapbox interface (with the SBI based on the window positions) and displaying the numerical results in the result column of the sidebar.

Pre settings: Two ways of getting mesh result, (left) is darker than (right), method	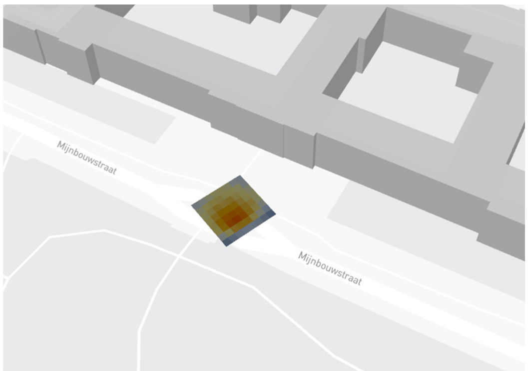 
DA	
sDA	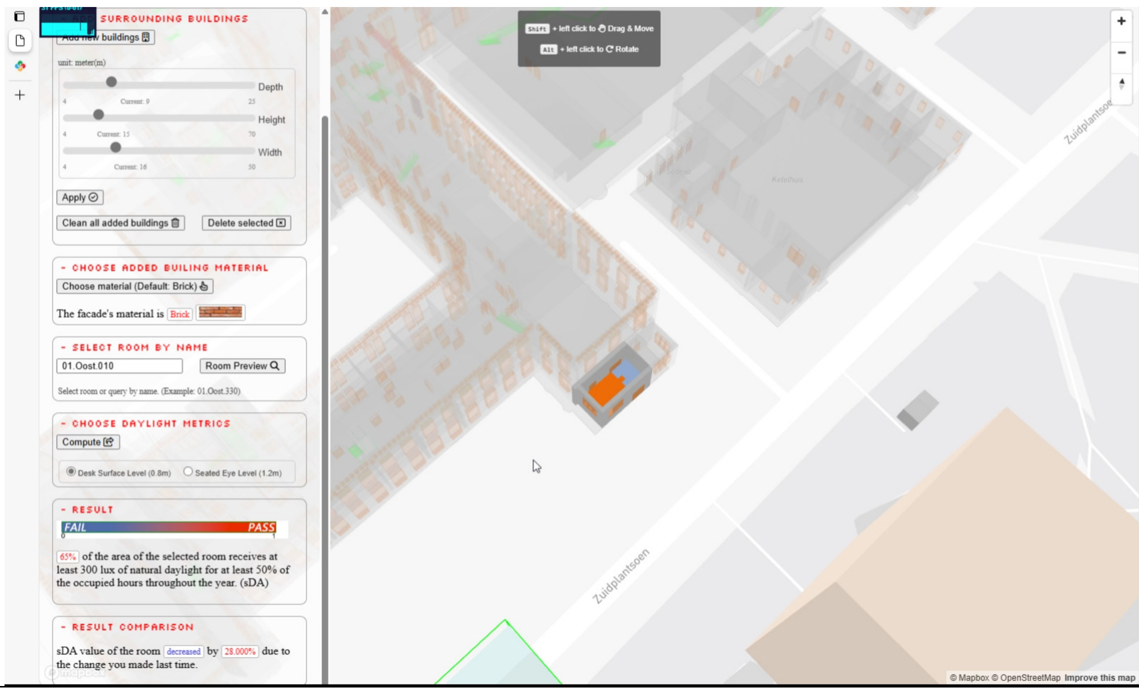

<table>
<tr><td>UDI</td><td>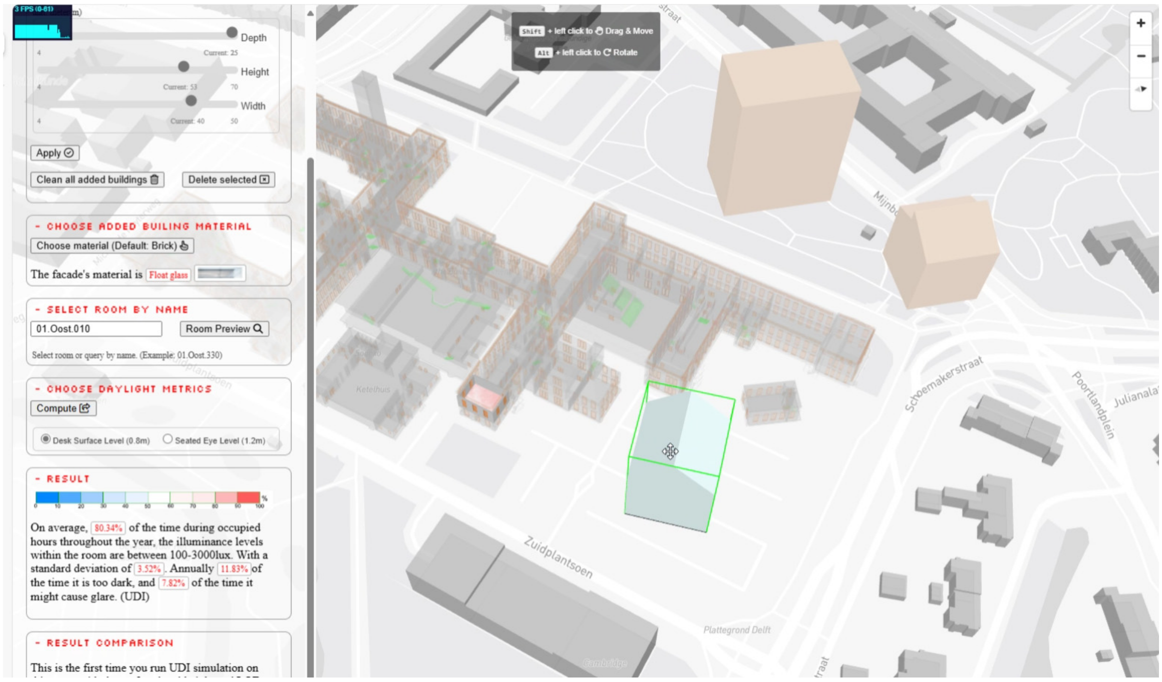
</td></tr>
<tr><td>SBI</td><td>
</td></tr>
</table>

Table 18: Simulation results for different metrics on the application

6 / Conclusions & Discussions

6.1 CONCLUSIONS

The thesis research was about providing a workflow …

1. To what extent can users interact with 3D city models through the interface? How can they be loaded in Rhino and the application for simulation and interaction?

Section 6.3 outlines reasons for not adopting 3D TILE; however, the potential for utilizing 3D BAG 3D TILE to import into MapboxGL and facilitate interaction with the pre-existing built environment is acknowledged. Users have the capability to incorporate new buildings into the web application, manipulate building typology, and perform actions such as rotation, dragging, delete selection, and scaling in three dimensions. Additionally, users can modify façade materials and select the LOD for the surrounding static city model. The 3D BAG model is imported using RhinoJSONCity, with coordinate adjustments made in Rhino before internalizing into GH. Upon initiating an HTTP request, data within the existing Mapbox scene is categorized by building typology and transmitted to the GH backend for geometric modifications: duplicating, rotating, scaling, and moving, to ensure synchronization with Mapbox data, and the final geometry is organized according to the materials to build the HB Shade component. Alterations to the Treebox source code are necessary to add attributes to each imported object, thereby enabling customization of their selectability, rotatability, draggability, and altitude adjustability.

2. How can a BIM model be integrated into Rhino and GIS platform to intelligently identify and segregate components by room, thereby facilitating automatic integration with daylight simulation? How can users interact with BIM room within the application?

Section 4.1.4 details the process for importing BIM models by individual rooms into Mapbox, enabling users to interact with the model through direct clicks or queries by room name, rendering the surrounding rooms transparent for easier previewing. Additionally, users may adjust the simulating surface height height and link to the EPW Map to select appropriate weather files. Dynamo is used within Revit to assign room tags using distinct scripts for various categories. The exported information, retrieved via element IDs, is then incorporated into the glTF file in JSON format. This process includes exporting detailed room information and floor coordinate data. During sunlight simulation, GH script filters and processes elements such as doors, windows, walls, exterior facades, floors, window frames, and ceilings, while also assigning materials that mirror real-life specifications. The numerical and mesh results were then sent back to Mapbox and the dashboard. These results are compared with prior outcomes to visually assess the effects of changes in the external environment.

3. Are the ABDM standards (SBI and view-lumen) appropriate for urban-scale daylight studies aimed at reducing simulation time, as compared to traditional CBDM standards? If applicable, how can these simulations be implemented within the application to enable effective visualization?

Section 4.2.1 introduces GH scripts developed to derive SBI and Sky Lumen outcomes without using ray tracing, based on their physics definitions. Subsequently, Section 4.1.1 establishesd experiments that employ SBI and Sky Lumen as explanatory variables, with DA, sDA, and UDI serving as independent variables to validate a hypothesis that the relationship between these variables is influenced by certain moderating variables. The findings confirm a robust linear relationship between SBI and DA, sDA, and UDI within the experimental settings, with all posited moderating variables notably impacting this linear correlation. Among these, the layout of rooms exerts the most substantial influence, and it also demonstrated much higher fit levels in south-facing rooms, conversely, this linear relationship cannot be used to predict DA, sDA, and UDI through the SBI in north-oriented scenarios. Moreover, a pronounced quadratic relationship exists between Sky Lumen and DA, sDA, and UDI in most instances, with experimentally hypothesized moderating variables, particularly the presence of shading and geometric features of room, significantly affecting this relationship. Overall, SBI emerges as a potent substitute for traditional CBDM metrics like DA and is reasonably effective for sDA, though it shows limited efficacy in replicating UDI's performance. Conversely, Sky Lumen consistently exhibits lower relevance across all comparisons, indicating its restricted reliability as an alternative to CBDM daylight metrics. The final application also incorporates SBI as an option for daylight simulation metrics.

4. What is the impact of varying LODs in 3D city models on computational accuracy and time, and how can the overall workflow be optimized for efficiency?

In this study, using LOD 1.3 and a radius of 200m provides sufficient accuracy and the shortest computation time for daylight simulation when using the Delft BK surroundings as the static urban context. Increasing the LOD and radius results in an obvious increase in computation time with minimal improvements in accuracy. However, this conclusion is specific to Delft, a low-density area with minimal urban canyon effects. In high-density areas like Amsterdam, different LODs may produce more varied results. For example, in New York, different radii may encompass varying intensities of urban canyon effects, leading to more diverse simulation outcomes. The choice of radius is influenced by the BIM scale; in this case study, the BK model represents a larger scale. If a smaller scale BIM model were used, the comparison radius should be adjusted accordingly, for instance, comparing 100m, 150m, 200m, 250m, etc. The optimization of this workflow is thoroughly discussed throughout the full thesis, particularly detailing the methodology for importing the BIM model on a room-by-room basis in Section 4.1.4, and exploring the acquisition of grid 3D coordinates in Section 4.1.3, and HB settings for efficiency.

To what extent can a web application conduct per-room daylight analysis on BIM models to effectively demonstrate the influence of dynamic changes within an urban context?

To encapsulate the key findings of this thesis, the primary research question can be addressed as follows: MapboxGL emerges as a promising GIS platform for integrating BIM models in room-based daylighting simulations, offering a user-friendly interactive system for the efficient manipulation of newly added buildings. The integration of Rhino Compute technology facilitates user interaction, transfer, and access to both geometric and numerical daylighting data seamlessly. Additionally, Rhino Inside technology effectively bridges the gap between Rhino and Revit. In urban-scale studies, the Spatial Brightness Index (SBI) may serve as a suitable alternative to traditional CBDM metrics, potentially accelerating simulation times. The integration of Rhino Compute and MapboxGL, along with the front-end interface setup, establishes a highly user-friendly results interface. Furthermore, the potential utilization of the 3D BAG tiling technique within Mapbox could enhance the control over static built-up urban environments and provide a comprehensive demonstration of the impact of urban context changes on indoor daylighting.

6.2 Requirements for BIM Model as Input

The workflow discussed in the thesis is constrained by the limitations inherent in the Input, specifically the modeling quality of the BIM model and the characteristics of the building itself. Figure 67 illustrates the applicability of workflows to BIM models under various conditions for this workflow, as well as suggestions to enhance the workflow for potential scalability. Ideally, this workflow requires certain standards for modeling quality: all BIM elements must have accurate type classification, include room information, have floor category elements segmented by room, and differentiate between indoor and outdoor materials, which will enable unified selection with Dynamo. A unified logic will be applied to address the articulation of walls and rooms during modeling. For buildings with non-rectangular room geometries, it is necessary to extract the room boundary line using a bounding box-like operation, which requires modifications to the Dynamo script (Appendix 3).

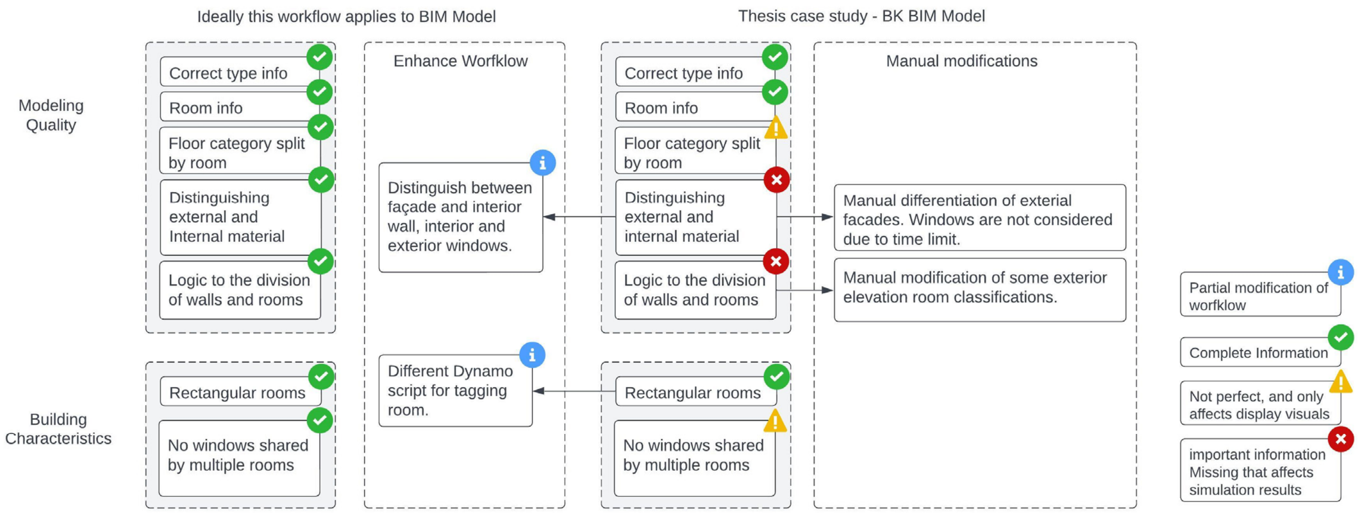

Figure 67: Applicability of workflows to BIM models under different conditions

The BK BIM model used in this case study has some limitations, such as the lack of differentiation between indoor and outdoor materials. Additionally, while the exterior walls are roughly constructed according to the rooms, the articulation between walls is irregular and random (Figure 68), complicating the use of a unified Dynamo script. The final accuracy of the tagging process can be assured to be over 95 percent after some manual adjustments. Furthermore, issues like shared floor geometry across multiple rooms and windows shared by two rooms negatively impacted the visual effect of the application. To ensure the visibility of the ABDM METRICS result grid at the window location, it is essential that all windows in the BIM model are oriented consistently (inside and outside).

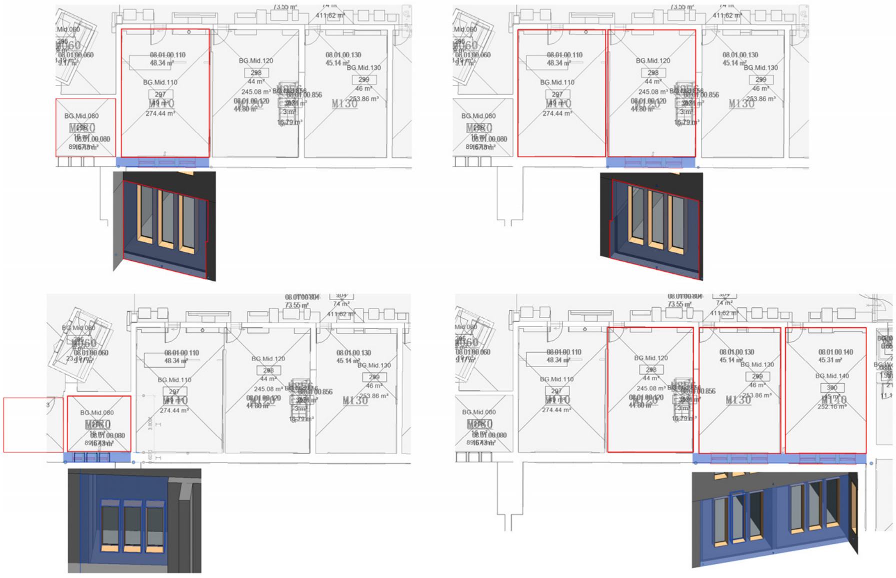

Figure 68: The random joint method of the exterior walls in case study, red box indicates the associated room

6.3 WORKFLOW LIMITATIONS

On March 6, 2024, the release 2.6.0 of pg2b3dm introduced experimental support for Mapbox v3, along with the addition of the --format parameter (defaulting to Cesium) to accommodate Cesium/Mapbox configurations (Geodan, n.d.). At the beginning of the thesis, the conversion of the 3D BAG into 3D tiles and its integration into Mapbox was considered experimental. Concurrently, Company Parallel successfully incorporated the BAG dataset into Mapbox GL, enabling the rendering of 3D buildings across the Netherlands, which were distinctly color-coded based on the age of construction (Netherlands Building Ages, n.d.). Furthermore, FOSS4G has developed a method for handling 3D geo-data within the Mapbox-gl viewer using 3D tiles (Tilburg & Blankert, 2019). Ideally, this thesis would explore interactions with a larger expanse of surrounding buildings, including scalability and the potential to modify façade materials of existing buildings using 3D tile technique. However, due to time constraints, the scope was limited to the addition and modifications of new buildings, as implementing broader modifications involving 3D tile proved challenging.

This thesis only focus on developing features to facilitate the selection of building typology and façade materials, as well as the capabilities for rotation, scaling, dragging, and deletion of newly incorporated buildings.

Considering the cost implications of setting up a production environment with an actual server charged by McNeel company per core per hour, this research runs Rhino compute locally for development and testing, maintaining consistent workflow and principles as running in a real server. The statistical analysis of simulation duration in this study are therefore constrained by computer's RAM capacity and its overall performance. The purpose of comparing computing time is to assess relative timeframes and provide recommendations for optimizing the workflow.

Additionally, it is important to note that while MapboxGL strikes a good balance between user freedom and BIM integration, it may not perform as well as some specialized software in these areas. This limitation should be acknowledged upon completing the research on this workflow. The choice of MapboxGL in this thesis reflects a deliberate tradeoff, balancing various factors to achieve the desired comprehensive outcomes. Exploring alternative software will require adopting a different workflow from the one presented in this research. It is as Celeste et al. discussed in 2022, semantic level BIM/GIS conversion is limited to specific applications, lacking generalization. The most effective integration relies heavily on using multiple commercial software solutions, this is a limitation of this open topic.

For several workflow steps presented in this thesis, there exist numerous approaches, and no single method is universally accepted or considered official. Due to time constraints, this thesis does not enumerate all possible methods and practices. Instead, it highlights general practices that represent a balance between time investment and result accuracy. Examples include the construction of SBI and View Lumen scripts, tagging rooms in Dynamo, the use of surveyors, coordinate conversion, and the transfer of Mapbox data to GH. Occasionally, the methods employed effectively circumvent certain issues. For instance, importing the floor category in advance addresses the problem of relative coordinates in the BIM model. However, the comprehensive solution is also discussed in the thesis.

This thesis does not account for the effects of varies outdoor paving and vegetation on daylighting. Instead, it primarily focuses on the urban canyon effect, enabling users to investigate the impact of adding buildings with different façade materials and changes in urban typology on the indoor daylighting of an existing BIM model. These additional factors should also be considered if sufficient time and open-source databases are available.

6.4 Future Work

This thesis develops a workflow for importing a BIM model into the MAPBOXGL platform to conduct daylight simulations. Given the time and content limitations of this study, not all potential avenues have been fully explored. The following are some promising directions for future research.

1. **Further study of moderating variables affecting the relationship between ABDM and CBDM metrics.** This research does not quantitatively determine the effect of the degree of change in moderating variables on the relationship. To analyze the simulation results more effectively, uniformly varying input dataset needs to be created in GH parametrically.
2. **Implement prediction of traditional metrics with SBI (and sky-lumen).** Analyze the relationship between SBI, sky-lumen, and DA, sDA, and UDI in this case study, and use SBI and sky-lumen to predict data from traditional daylight metrics in the application.
3. **Implement sky lumen metrics in case study** (Figure 70)**.** This may require solving the geometry cutting problem for complex 3D city models. Build view lumen script with the HB glare component might be considered (Figure 69). It is important to note that, with multiple windows, the mesh results are imported at the height of the room's windows.

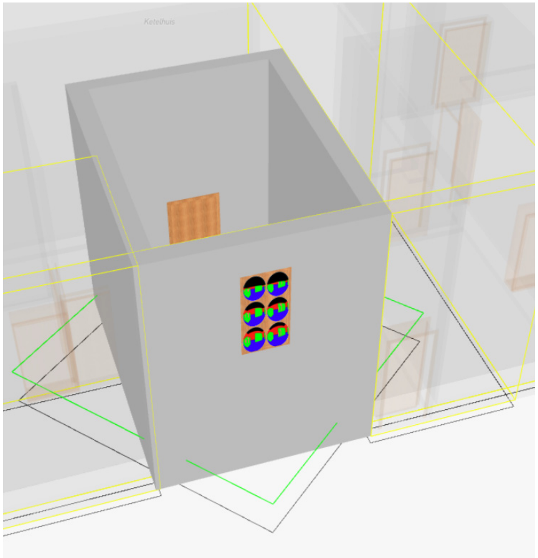

Figure 70: Implement sky lumen metrics in case study

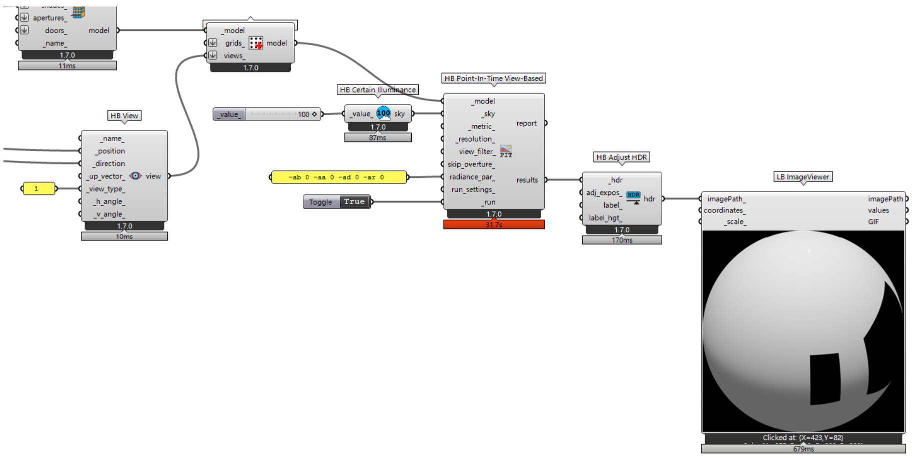

Figure 69: HB View component method of creating hemispherical fisheye

4. **Integration with other open-source databases to consider the impact of ground.** Current daylighting simulations do not typically account for the complexity of outdoor paving. However, the workflow remains largely unchanged, with the primary difference being the need to configure additional materials for the outdoor environment in advance.
5. **Integration with other open-source databases to consider the impact of plants and trees.** Daylight simulating for trees and plants is highly complex but significantly influences the overall insolation results. This aspect needs to be integrated with other workflows for a comprehensive analysis (Figure 71)..

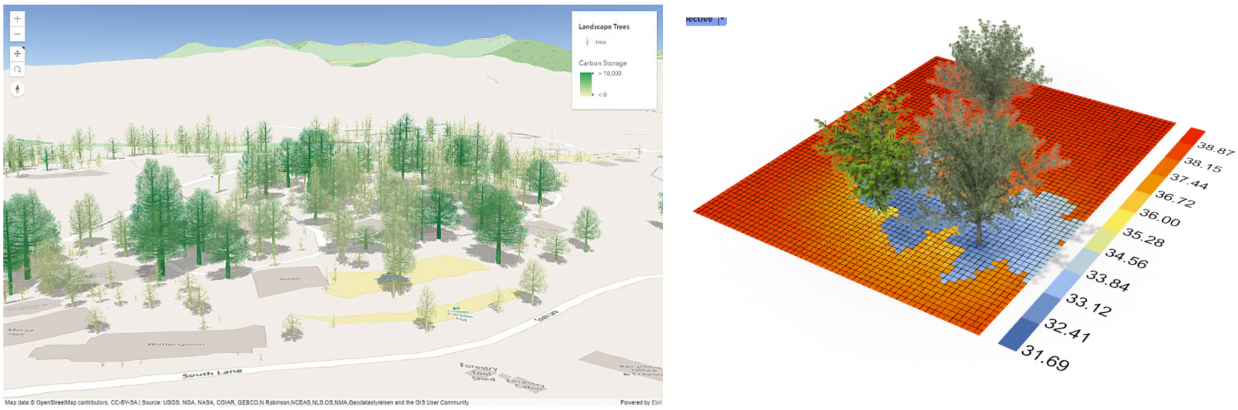

Figure 71: Open-source tree data (left) and Daylight simulation involving trees (right)

6. **Control of static buildings in combination with 3D BAG 3D tile.** 3D BAG Tile and Mapbox are currently in an experimental phase; however, some examples demonstrate the feasibility of utilizing such technique to effect changes (renovations) in the surrounding urban context.
7. **Optimize the way to get room tags in Dynamo.** In this case study, since the room planes are regular rectangles, the bounding box node is primarily used to extract room information from BIM elements. However, this approach is ineffective for irregular geometric planes.
8. **Use Speckle to transfer BIM information to GH.** Speckle, as an open-source plugin, can facilitate the conversion from Revit to Rhino as discussed in this thesis. However, it may be constrained by mesh surfaces, limiting the ability to freely edit geometry later in GH. Attention must be paid to the correspondence between attributes and elements (Figure 72).

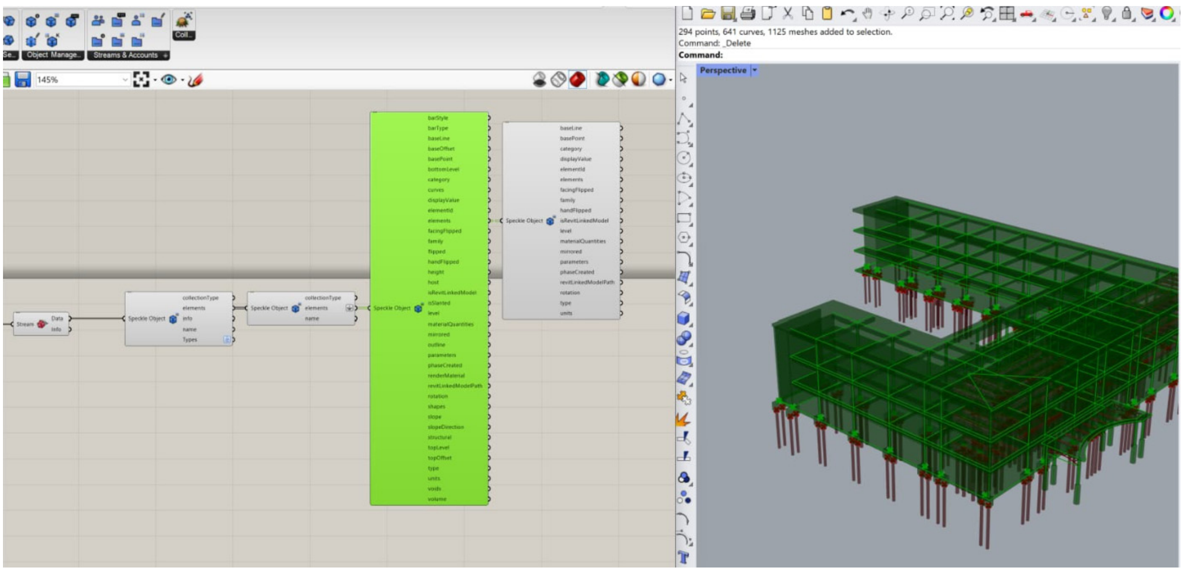

Figure 72: Using Speckle to transfer BIM data to Rhino

9. **Explore other platforms (Autodesk forge / Unity / Unreal Engine).** For a user experience with a higher degree of freedom and better integration with 3DBAG tile, utilizing Unity or Unreal Engine (Rhino Compute C++ library need to be created, Figure 73) as a client for Rhino Compute may be more appropriate option. Additionally, Autodesk Forge offers better integration on the BIM side, but a completely different workflow will be employed.

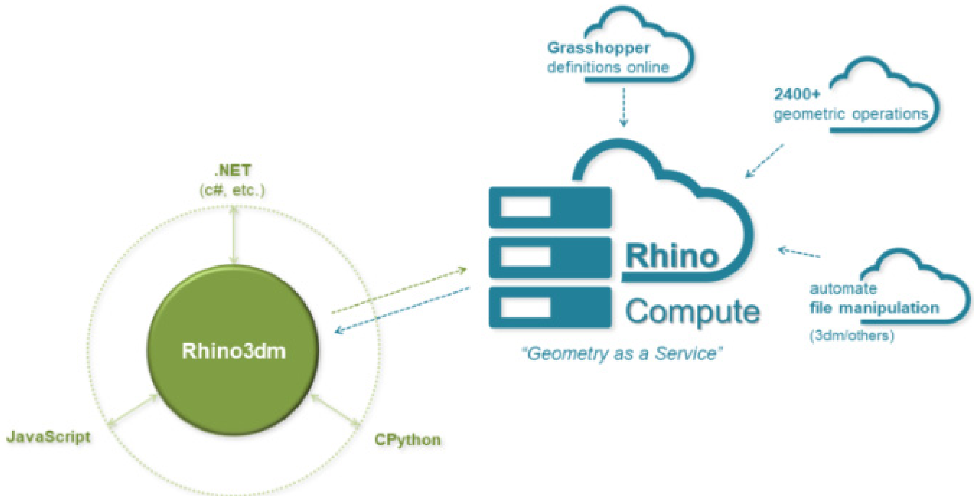

Figure 73: Rhino Compute libraries

10. **Give users more freedom.** Incorporate additional parameters to provide users with greater freedom and more options, while adhering to the same workflow. Or further optimize the workflow to enable users to construct a similar platform with minimal steps. For instance, provide the capability to directly upload a BIM model, select a site, and automatically generate a customized application.
11. **User experience research of the application**. Investigate user satisfaction and ease of use, and refine the user interface based on the feedback received.
12. **Integration with machine learning**. When the application is deployed, it will involve substantial data inputs and outputs. Incorporating machine learning components into the GH Script could assist in data collection, bypass the simulation process to predict data, enable faster responses, or supply data for further research.
13. **Perform different simulations at different degrees of BIM model.** This thesis focuses on daylight simulation at the room level within a BIM model to demonstrate the impact of incorporating new city models. Utilizing the Rhino Compute technique, with some adjustments such as modifying Dynamo scripts for the addition of room information, to manage BIM data effectively. This approach allows for running various simulations (structural, CFD simulations, etc.) with the final results presented in both text and mesh formats.

/ References

A

Azel, N., Pachuca, B., & Wilson, L. (2022). Closing the Gap-Leveraging Rhino Compute and Cloud Computing to Distribute Custom Computational Tools. *Proceedings of the Annual Conference of the Association for Computer-Aided Design in Architecture (ACADIA).* https://papers.cumincad.org/data/works/att/acadia22_128.pdf

B

Biljecki, F., Ledoux, H., & Stoter, J. (2016). An improved LOD specification for 3D building models. *Computers, Environment and Urban Systems*, *59*, 25–37. https://doi.org/10.1016/j.compenvurbsys.2016.04.005

Boersma, F. (2024, February 18). LoD 2 punt 2 Hoezee. *GEOBIMEXPERTS*. https://www.geobimexperts.nl/blog/lod-2-2-hoezee

Boundary elements and stirrup constraints. (n.d.). The Building Coder. https://thebuildingcoder.typepad.com/blog/2021/03/boundary-elements-and-stirrup-constraints.html#3

Bournas, I. (2020). Daylight compliance of residential spaces: Comparison of different performance criteria and association with room geometry and urban density. *Building and Environment*, *185*, 107276. https://doi.org/10.1016/j.buildenv.2020.107276

C

Celeste, G., Lazoi, M., Mangia, M., & Mangialardi, G. (2022). Innovating the Construction Life Cycle through BIM/GIS Integration: A Review. *Sustainability*, *14*(2), 766. https://doi.org/10.3390/su14020766

Cityjson. (n.d.). *GitHub - cityjson/RhinoCityJSON: Rhino/Grasshopper plugin allowing the CityJSON format to be directly used in Rhino 3D and grasshopper*. GitHub. https://github.com/cityjson/RhinoCityJSON

Coordinate systems. (n.d.). https://dirsig.cis.rit.edu/docs/new/coordinates.html

Computational Modelling Group: Publication JOBE-91-109507-. (n.d.). https://como.ceb.cam.ac.uk/publications/JoBE-91-109507-/

Council, U. G. (2013). LEED reference guide for building design and construction. *US Green Building Council.*

D

DiStem Bundle for Autodesk Revit - productivity Revit Plugins by DiRoots. (2024, May 8). DiRoots. https://diroots.com/revit-plugins/distem-bundle-for-autodesk-revit/

F

Fernandez-Antolin, M., Del-Río, J., Del Ama Gonzalo, F., & Gonzalez-Lezcano, R. (2020). The Relationship between the Use of Building Performance Simulation Tools by Recent Graduate Architects and the Deficiencies in Architectural Education. *Energies*, *13*(5), 1134. https://doi.org/10.3390/en13051134

Fernandez-Antolin, M., Del Río, J. M., & González-Lezcano, R. A. (2022). Building Performance Simulations and Architects against Climate Change and Energy Resource Scarcity. *Earth*, *3*(1), 31–44. https://doi.org/10.3390/earth3010003

G

Geodan. (n.d.). *GitHub - Geodan/pg2b3dm: Tool for creating 3D Tiles from PostGIS geometries*. GitHub. https://github.com/Geodan/pg2b3dm

Get the walls, ceiling and floor of a room? (2022, October 5). Autodesk Community. https://forums.autodesk.com/t5/revit-api-forum/get-the-walls-ceiling-and-floor-of-a-room/m-p/9930160#M51824

Grasshopper. (n.d.). Algorithmic Modeling for Rhino. https://www.grasshopper3d.com/

H

Helenkwok. (n.d.). *GitHub - helenkwok/bim-gis-viewer: a submission to IFC.js hackathon*. GitHub. https://github.com/helenkwok/bim-gis-viewer

I

Inanici, M. (2009). *Applications Of Image Based Rendering in Lighting Simulation: Development And Evaluation Of Image Based Sky Models*. https://www.semanticscholar.org/paper/APPLICATIONS-OF-IMAGE-BASED-RENDERING-IN-LIGHTING-Inanici/48f1f521a95aaf70658db1e9b6e224409c9d0baf

InForm - Arup. (n.d.). https://www.arup.com/services/tools/inform

Ingrassia, M. (2021, May 17). *MaCAD Students running their Grasshopper Definitions on the cloud, within the BIM and Smart Construction Module! - IAAC*. IAAC. https://iaac.net/macad_cloudbased_data_management/

Interface, K. U. (2022, January 22). Bridging Data Science and Architectural Practice - KPF Urban Interface - Medium. *Medium*. https://medium.com/@kpfui/bridging-data-science-and-architectural-practice-aceb3f23fd95

Introduction | ELEFront. (n.d.). https://docs.elefront.io/

J

Jscastro. (n.d.). *GitHub - jscastro76/threebox: A Three.js plugin for Mapbox GL JS, with support for animations and advanced 3D rendering.* GitHub. https://github.com/jscastro76/threebox/tree/master?tab=readme-ov-file

Jhorikawa. (n.d.). *GitHub - jhorikawa/GrasshopperPlayerWithRhinoInsideUnityTemplate*. GitHub. https://github.com/jhorikawa/GrasshopperPlayerWithRhinoInsideUnityTemplate

K

Koster, D. (2023). *Integrating urban context in daylighting simulation: The design consequences in Dutch urban areas, regarding visual & non-visual levels of daylight*. https://repository.tudelft.nl/islandora/object/uuid:ec15c377-36d0-412b-8ace-736db2492a5a?collection=education

L

Ladybug Tools | Home page. (n.d.). https://www.ladybug.tools/

M

Mardaljevic, J., & Brembilla, E. (2021). Aperture-based daylight modelling: Evaluating the airmass refinement for the sunlight beam index. *Building Simulation Conference Proceedings*. https://doi.org/10.26868/25222708.2021.30604

Mardaljevic, J., & Roy, N. (2016). The sunlight beam index. *Lighting Research and Technology*, *48*(1), 55–69. https://doi.org/10.1177/1477153515621486

Mardaljevic, J. (2021). The implementation of natural lighting for human health from a planning perspective. *Lighting Research and Technology*, *53*(5), 489–513. https://doi.org/10.1177/14771535211022145

Mardaljevic, J., & Roy, N. (2017, January 1). *Envelope first / Inside later: Aperture sunlight and skylight indices*. Figshare. https://repository.lboro.ac.uk/articles/conference_contribution/Envelope_first_Inside_later_Aperture_sunlight_and_skylight_indices/9430067

Mardaljevic, J. (2019, January 1). *Aperture-based daylight modelling: Introducing the 'View Lumen.'* Figshare. https://repository.lboro.ac.uk/articles/conference_contribution/Aperture-based_daylight_modelling_Introducing_the_View_Lumen_/9458474

MapBox | Maps, navigation, search, and data. (n.d.). https://www.mapbox.com/

Mcneel. (n.d.). *GitHub - mcneel/compute.rhino3d.appserver: A node.js server for solving Grasshopper definitions on Rhino Compute*. GitHub. https://github.com/mcneel/compute.rhino3d.appserver

Mm-Wang. (n.d.). *GitHub - mm-wang/WebApplicationWorkshop: Web application workshop, built for AEC Tech 2019: Seattle*. GitHub. https://github.com/mm-wang/WebApplicationWorkshop

Mesh geometry in LBT 1.0. (2020, October 25). Ladybug Tools | Forum. https://discourse.ladybug.tools/t/mesh-geometry-in-lbt-1-0/11597

N

Nasrollahi, N., & Shokri, E. (2016). Daylight illuminance in urban environments for visual comfort and energy performance. *Renewable & Sustainable Energy Reviews*, *66*, 861–874. https://doi.org/10.1016/j.rser.2016.08.052

Nabil, A., & Mardaljevic, J. (2005). Useful daylight illuminance: a new paradigm for assessing daylight in buildings. *Lighting Research and Technology*, 37(1), 41–57. https://doi.org/10.1191/1365782805li128oa

Netherlands building ages. (n.d.). https://parallel.co.uk/netherlands/#13.3/51.93519/4.43523/0/40

Netherlands topographic map, elevation, terrain. (n.d.). Topographic Maps. https://en-gb.topographic-map.com/map-wpfnh/Netherlands/?center=47.46338%2C-6.45996&zoom=4

NYC Park Study. (n.d.). https://nyc.emptybox.io/

P

Pantazatou, K., Kanters, J., Olsson, P., Nyborg, J. L., & Harrie, L. (2023). Input data requirements for daylight simulations in urban densifications. *Urban Informatics*, *2*(1). https://doi.org/10.1007/s44212-023-00024-6

Proving Ground. (2023, March 30). *Simple Rhino to revit workflow | Conveyor Plugin*. Proving Ground Apps. https://apps.provingground.io/conveyor/

Q

Quek, H. Y., Sielker, F., Akroyd, J., Bhave, A. N., Von Richthofen, A., Herthogs, P., Van Der Laag Yamu, C., Wan, L., Nochta, T., Burgess, G., Lim, M. Q., Mosbach, S., & Kraft, M. (2023). The conundrum in smart city governance: Interoperability and compatibility in an ever-growing ecosystem of digital twins. *Data & Policy*, *5*. https://doi.org/10.1017/dap.2023.1

Question about Radiance Glass Modifer Properties. (2023, July 10). Ladybug Tools | Forum. https://discourse.ladybug.tools/t/question-about-radiance-glass-modifer-properties/22208

R

Radiance. (n.d.). Energy.gov. https://www.energy.gov/eere/buildings/articles/radiance

Rajus, V. S., Risopatron, N. A., O'Brien, W., Wainer, G., & Fai, S. (2022). Mitigating the negative impact of new buildings on existing buildings' user comfort—a case study analysis. *Simulation*, *99*(11), 1095–1115. https://doi.org/10.1177/00375497221101062

REVIT for Architecture & Building Design | AutoDesk. (n.d.). https://www.autodesk.eu/products/revit/architecture

Rhino User Webinar: Daylight Compliance Prediction Web Tool using Rhino.Compute. (n.d.). https://blog.rhino3d.com/2024/02/rhino-user-webinar-daylight-compliance.html

Robert McNeel & Associates. (n.d.). *Rhinoceros 3D*. www.rhino3d.com. https://www.rhino3d.com/

Ronald, D. (2021, December 14). Killer product — A Rhino3D product Analysis - Spatiomatics - medium. Medium. https://medium.com/spatiomatics/killer-product-a-rhino3d-product-analysis-2f90ebfd9465

Robert McNeel & Associates. (n.d.-a). *Compute guides*. www.rhino3d.com. https://developer.rhino3d.com/guides/compute/

S

Shoshev, M. (2022). *From Building Information Models to Building Performance Simulation: Parametric Workflow for High Performance Building Envelope Design for Daylight and Glare Analysis*. [Master's thesis, Politecnico di Torino]. Politecnico di Torino Repository https://webthesis.biblio.polito.it/secure/25167/1/tesi.pdf

Scout. (n.d.). https://scout.build/

Spectral Materials Database: Home. (n.d.). https://spectraldb.com/

Speckle - the platform for 3D data. (2024, May 7). Speckle - the Platform for 3D Data. https://speckle.systems/

Shkundalov, D., & Vilutienė, T. (2020, May 11). *BUILDING MANAGEMENT SYSTEM IN WEBBIM ENVIRONMENT*. http://enviro.vgtu.lt/index.php/enviro/2020/paper/view/725

ShapeDiver <-> Rhino Compute. (n.d.). https://help.shapediver.com/doc/shapediver-rhino-compute

T

Tilburg, Tom van; Blankert, Anne; Vaughan, Rubio: *3D tiles in Mapbox-gl. FOSS4G Bucharest 2019, FOSS4G et al., 2019. https://doi.org/10.5446/43497*

Translucent modifier | HB-Radiance Primer. (n.d.). https://docs.ladybug.tools/hb-radiance-primer/components/1_modifiers/translucent_modifier

three.js docs. (n.d.). https://threejs.org/docs/#api/en/core/Object3D

Three.js – JavaScript 3D library. (n.d.). https://threejs.org/

V

Visual Studio Code - Code editing. Redefined. (2021, November 3). https://code.visualstudio.com/

Van Esch, M., Looman, R., & De Bruin-Hordijk, G. (2012). The effects of urban and building design parameters on solar access to the urban canyon and the potential for direct passive solar heating strategies. *Energy and Buildings*, *47*, 189–200. https://doi.org/10.1016/j.enbuild.2011.11.042

W

Wikipedia contributors. (2023, September 5). *Air mass (solar energy)*. Wikipedia. https://en.wikipedia.org/wiki/Air_mass_(solar_energy)

Larson, G. W., & Shakespeare, R. A. (1998). *Rendering with Radiance: The art and science of lighting visualization*. Morgan Kaufmann Publishers.

Wallabyway. (n.d.). *GitHub - wallabyway/mapboxRevit: View Revit models inside Mapbox*. GitHub. https://github.com/wallabyway/mapboxRevit?tab=readme-ov-file

Wikipedia contributors. (2010, February 18). *File:ECEF ENU Longitude Latitude Relationships.svg - Wikipedia*. https://en.wikipedia.org/wiki/File:ECEF_ENU_Longitude_Latitude_relationships.svg#filehistory

Wedia. (n.d.). *Amsterdam unveils plans to build 20.000 new homes in existing neighbourhoods*. IamExpat. https://www.iamexpat.nl/housing/real-estate-news/amsterdam-unveils-plans-build-20000-new-homes-existing-neighbourhoods

Z

Zheng, Y., Merchant, A., Laninga, J., Xiang, Z. X., Alshaebi, K., Arellano, N., Romaniuk, H., Fai, S., & Sun, D. H. (2023). COMPARISON OF CHARACTERISTICS OF BIM VISUALIZATION AND INTERACTIVE APPLICATION BASED ON WEBGL AND GAME ENGINE. *the International Archives of the Photogrammetry, Remote Sensing and Spatial Information Sciences/International Archives of the Photogrammetry, Remote Sensing and Spatial Information Sciences*, *XLVIII-M-2–2023*, 1671–1677. https://doi.org/10.5194/isprs-archives-xlviii-m-2-2023-1671-2023

3DBAG Viewer. (n.d.). https://3dbag.nl/en/viewer

2D Rotation about a point | Academo.org - Free, interactive, education. (n.d.). https://academo.org/demos/rotation-about-point/

/ Appendix

```javascript
        loadObj: {
            type: null,
            obj: null,
            units: 'scene',
            scale: 1,
            rotation: 0,
            defaultAnimation: 0,
            anchor: 'bottom-left',
            bbox: true,
            tooltip: true,
            raycasted: true,
            clone: true,
            withCredentials: false,
            selectable: true,
            rotatable: true,
            draggable: true,
            altitudeChangeable: true
        },

        Object3D: {
            obj: null,
            units: 'scene',
            anchor: 'bottom-left',
            bbox: true,
            tooltip: true,
            raycasted: true
        },

        extrusion: {
            coordinates: [[[]]],
            geometryOptions: {},
            height: 100,
            materials: new THREE.MeshPhongMaterial({ color: 0x660000, side: THREE.DoubleSide }),
            scale: 1,
            rotation: 0,
            units: 'scene',
            anchor: 'center',
            bbox: true,
            tooltip: true,
            raycasted: true,
        }
```

```javascript
function Threebox(map, glContext, options){
    init: function (map, glContext, options) {
        this.map.on('load', function () {
            this.onMouseMove = function (e) {
```

```javascript
                this.getCanvasContainer().style.cursor = this.tb.defaultCursor;
                //check if being rotated
                if (e.originalEvent.altKey && this.draggedObject && this.draggedObject.rotatable) {

                    if (!map.tb.enableRotatingObjects) return;
                    draggedAction = 'rotate';
                    // Set a UI indicator for dragging.
                    this.getCanvasContainer().style.cursor = 'move';
                    var minX = Math.min(start.x, current.x),
                        maxX = Math.max(start.x, current.x),
                        minY = Math.min(start.y, current.y),
                        maxY = Math.max(start.y, current.y);
                    //set the movement fluid we rotate only every 10px moved, in steps of 10 degrees up to 360
                    let rotation = { x: 0, y: 0, z: (Math.round(rotationDiff[2] + (~~((current.x - start.x) / this.tb.rotationStep) % 360 * this.tb.rotationStep) % 360)) };
                    //now rotate the model depending the axis
                    this.draggedObject.setRotation(rotation);
                    if (map.tb.enableHelpTooltips) this.draggedObject.addHelp("rot: " + rotation.z + "&#176;");
                    //this.draggedObject.setRotationAxis(rotation);
                    return;
                }

                //check if being moved
                if (e.originalEvent.shiftKey && this.draggedObject && this.draggedObject.draggable) {
                    if (!map.tb.enableDraggingObjects) return;

                    draggedAction = 'translate';
                    // Set a UI indicator for dragging.
                    this.getCanvasContainer().style.cursor = 'move';
                    // Capture the first xy coordinates, height must be the same to move on the same plane
                    let coords = e.lngLat;
                    let options = [Number((coords.lng + lngDiff).toFixed(this.tb.gridStep)), Number((coords.lat + latDiff).toFixed(this.tb.gridStep)), this.draggedObject.modelH
                    this.draggedObject.setCoords(options);
                    if (map.tb.enableHelpTooltips) this.draggedObject.addHelp("lng: " + options[0] + "&#176;, lat: " + options[1] + "&#176;");
                    return;
                }

                //check if being moved on altitude
                if (e.originalEvent.ctrlKey && this.draggedObject && this.draggedObject.draggable && this.draggedObject.altitudeChangeable) {
                    if (!map.tb.enableDraggingObjects) return;
                    draggedAction = 'altitude';
                    // Set a UI indicator for dragging.
                    this.getCanvasContainer().style.cursor = 'move';
```

```javascript
            //if the object is selectable
            userScaleGroup.selectable = options.selectable;
            //if the object is rotatable
            userScaleGroup.rotatable = options.rotatable;
            //if the object is draggable
            userScaleGroup.draggable = options.draggable;
            //if the object's altitude can be changed
            userScaleGroup.altitudeChangeable = options.altitudeChangeable
```

```javascript
            let _selectable = true;
            //add selectability property to object
            Object.defineProperty(obj, 'selectable', {
                get() { return _selectable; },
                set(value) {
                    _selectable = value;
                }
            });

            let _rotatable = true;
            //add rotatability property to object
            Object.defineProperty(obj, 'rotatable', {
                get() { return _rotatable; },
                set(value) {
                    _rotatable = value;
                }
            });

            let _draggable = true;
            //add draggability property to object
            Object.defineProperty(obj, 'draggable', {
                get() { return _draggable; },
                set(value) {
                    _draggable = value;
                }
            });

            let _altitudeChangeable = true;
            //add draggability property to object
            Object.defineProperty(obj, 'altitudeChangeable', {
                get() { return _altitudeChangeable; },
                set(value) {
                    _altitudeChangeable = value;
                }
            });
```

src > Threebox.js > Threebox > init > map.on('load') callback > onMouseMove

```javascript
function Threebox(map, glContext, options){
    init: function (map, glContext, options) {
        this.map.on('load', function () {
            this.onClick = function (e) {
```

```javascript
                    let nearestObject = Threebox.prototype.findParent3DObject(intersects[0]);

                    if (nearestObject) {
                        //if extrusion object selected, unselect, clean the selection
                        if (this.selectedFeature) {
                            this.unselectFeature(this.selectedFeature);
                        }
                        //if not selected yet, select it
                        if (!this.selectedObject && nearestObject.selectable) {
                            this.selectedObject = nearestObject;
                            this.selectedObject.selected = true;
                        }
                        else if (this.selectedObject.uuid != nearestObject.uuid) {
                            //it's a different object, restore the previous and select the new one
                            this.unselectObject();
                            if (nearestObject.selectable) {
                                nearestObject.selected = true;
                                this.selectedObject = nearestObject;
                            }
```

Appendix 1: change in Threebox source code for settings

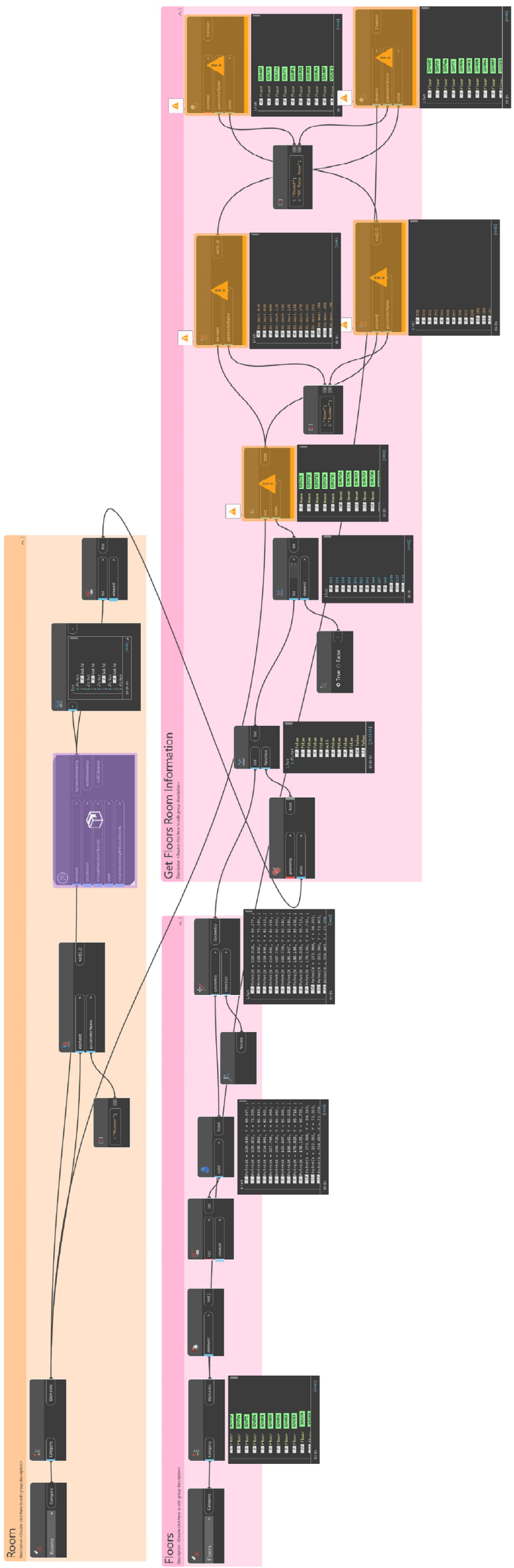

Appendix 2: Dynamo Script for Floor category

Appendix 3: Dynamo Script for tagging Wall category

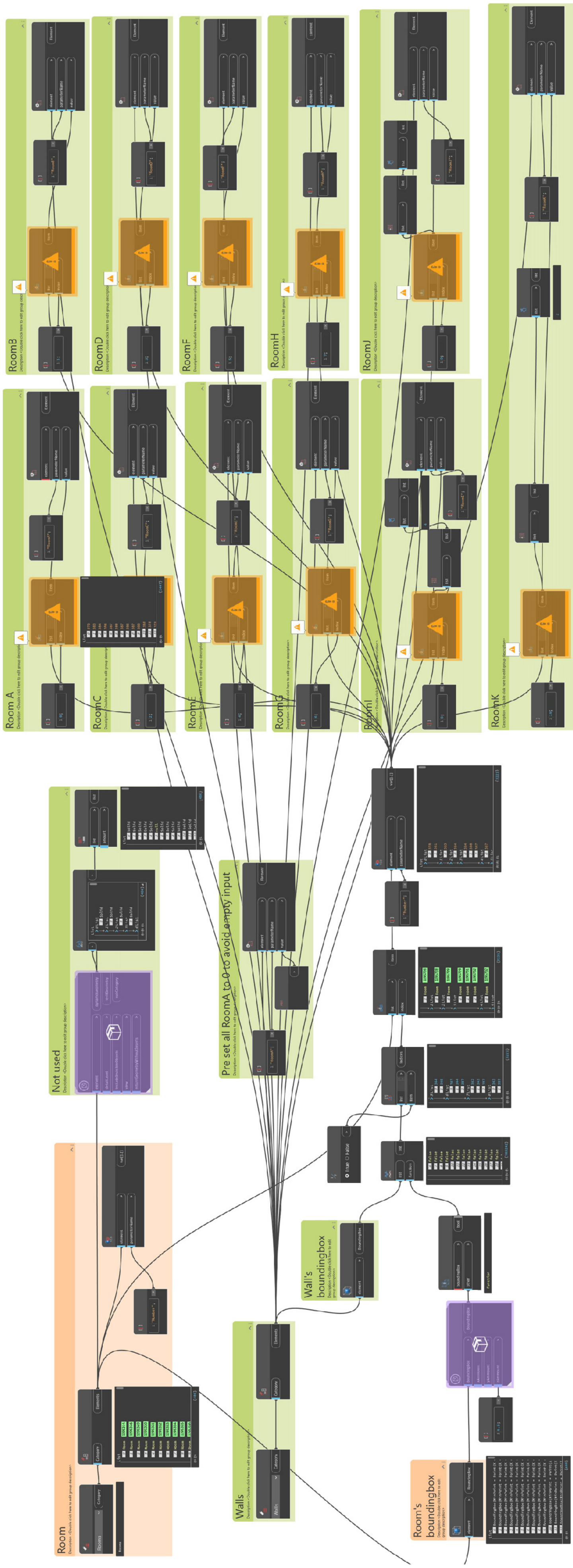

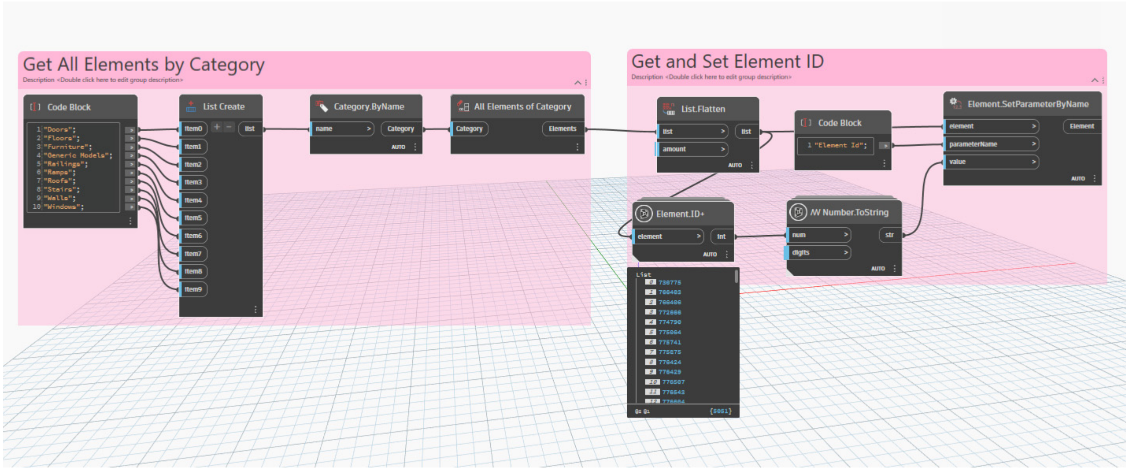

Appendix 4: Dynamo Script for get BIM elements' ID

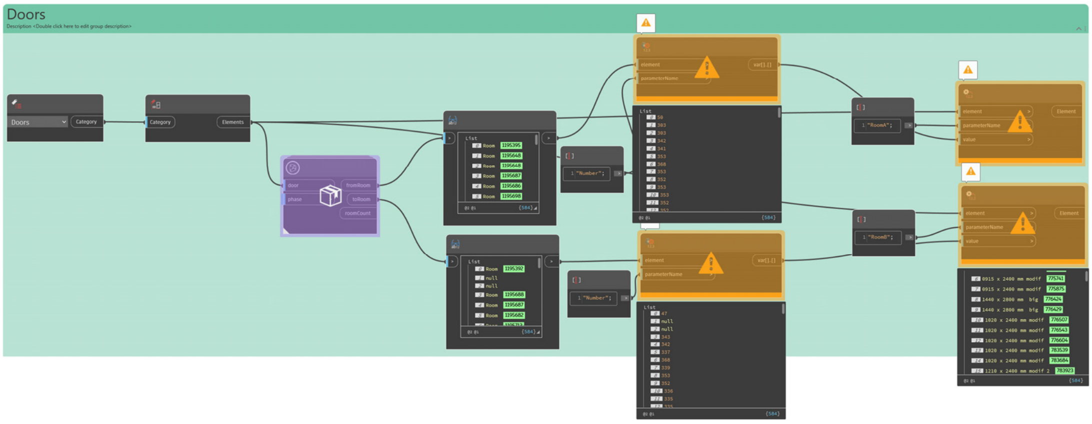

Appendix 5: Dynamo Script for get Tagging Door category

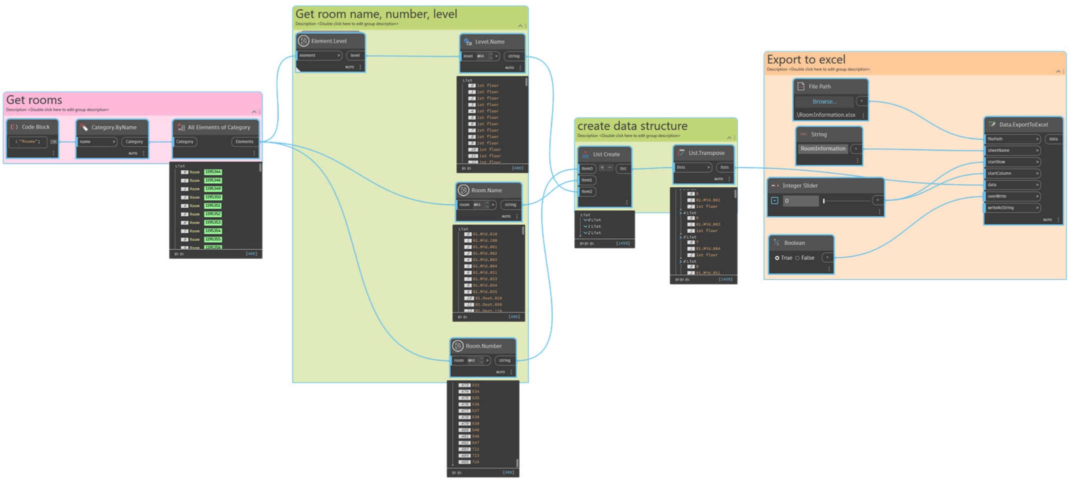

Appendix 6: Dynamo Script for get room information

Appendix 7:

GH Script for SBI-AM

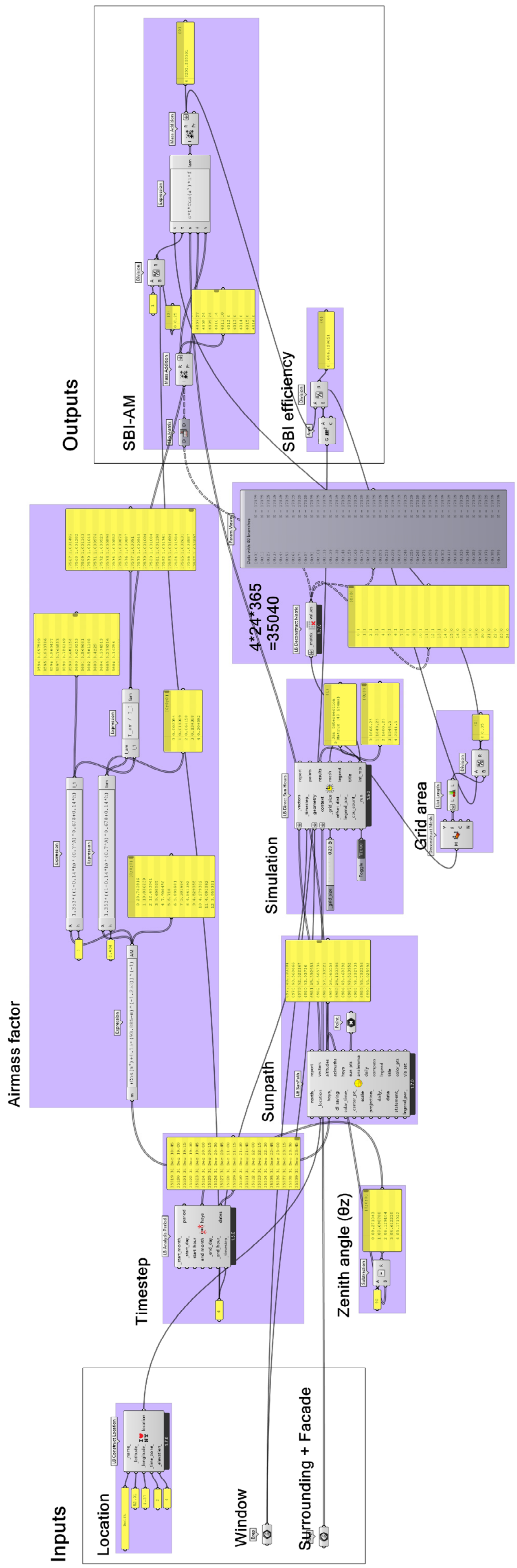

Appendix 8:

GH Script for Sky Lumens

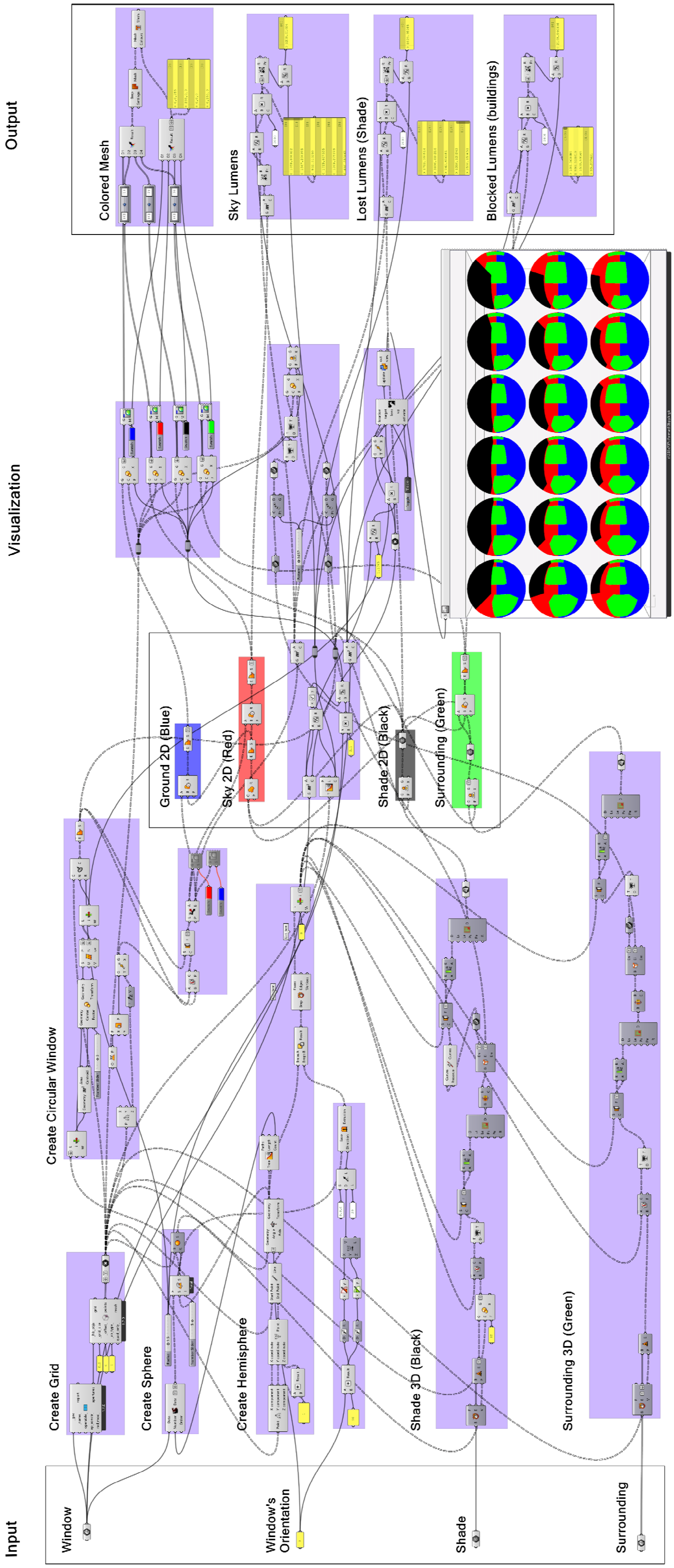

Appendix 9: GH Script for correlation experiments

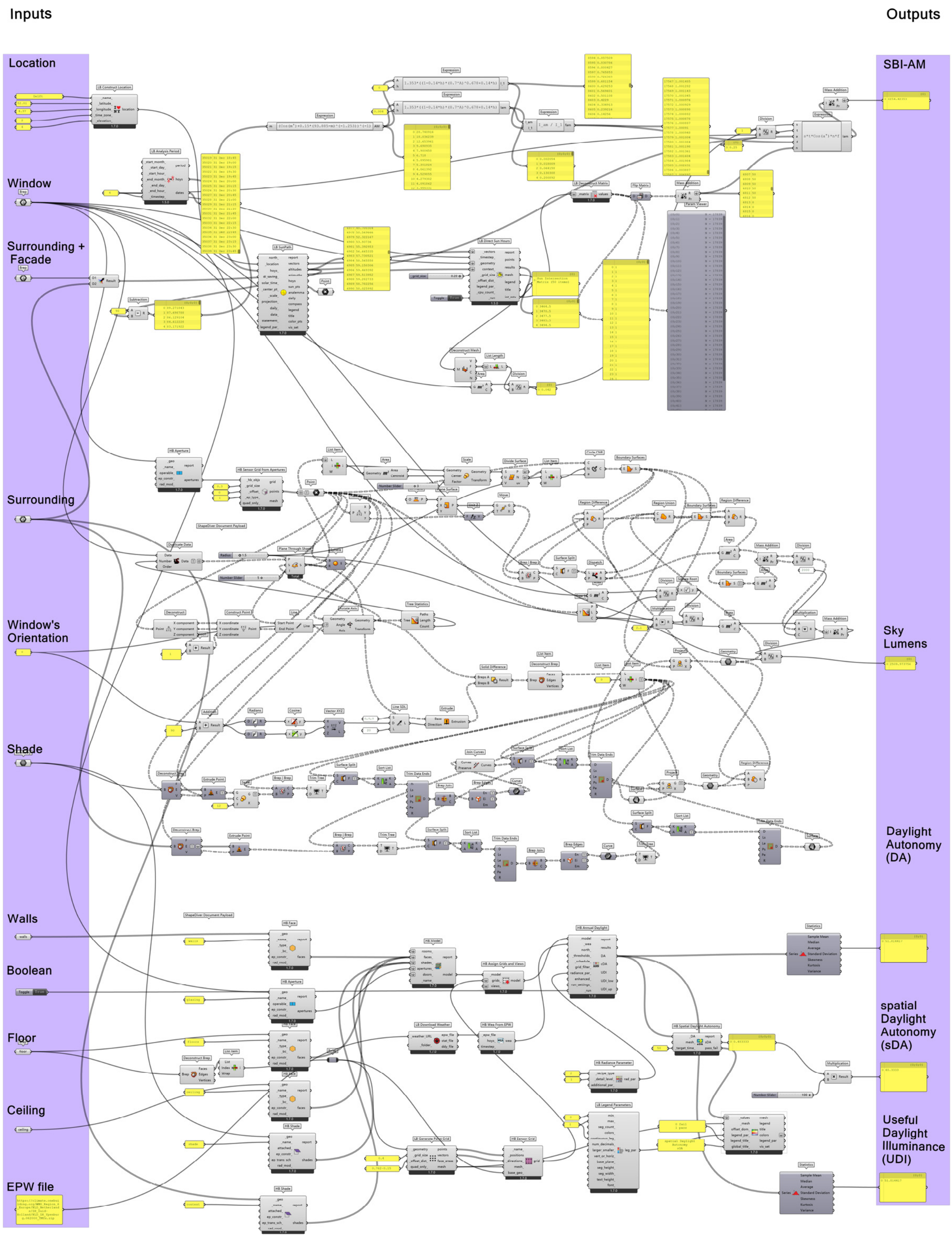

Nun	Name	SBI-AM	view-lumens	DA [%]	sDA [%]	UDI [%]
1	A1	3862.701137	2417.982001	29.704583	20	67.97175
2	A2	3800.177882	2478.422144	27.789833	14.1667	66.028
3	A3	3862.385756	2529.02294	55.169821	60.7143	77.32
4	A5	6278.4478	3232.661164	60.934286	85.7143	77.07375
5	B1	3669.370491	2554.904343	27.64425	15	63.646083
6	B2	3625.663492	2506.023293	25.01	7.5	61.574
7	B3	3667.2939	2554.43865	49.381429	42.8571	74.557321
8	B5	5553.990673	3258.860182	53.3	53.5714	75.223393
9	C1	2744.509117	2514.914103	17.339417	10.8333	56.53
10	C2	2704.062641	2460.438493	13.717167	0	53.722083
11	C3	2744.738745	2515.816073	33.912143	28.5714	73.672321
12	C5	4036.134627	3221.581564	37.818393	26.7857	75.0425
13	D1	1700.11771	2509.912592	8.272167	6.667	50.39725
14	D2	1681.599193	2471.387855	3.871167	0	46.306833
15	D3	1705.306527	2511.442021	21.080179	17.8571	71.568571
16	D5	2530.753	3218.953007	24.035	16.0714	74.030179
17	E1	1382.316212	2429.802876	5.928833	6.667	45.270667
18	E2	1369.217142	2397.154131	0.763833	0	42.69825
19	E3	1387.450782	2432.95982	16.372143	16.0714	69.801964
20	E5	1821.56293	3139.188572	17.593036	12.5	72.457143
21	F1	1838.909329	2457.881975	8.744083	6.667	50.328333
22	F2	1812.84529	2422.715219	3.839833	0	47.75825
23	F3	1838.755359	2461.508648	21.630893	19.6429	71.517321
24	F5	2546.020057	3165.535454	24.18125	19.6429	73.973393
25	G1	2761.591635	2493.001576	17.682167	10.8333	58.814333
26	G2	2727.156784	2453.52048	13.186083	0	55.951083
27	G3	2759.022954	2493.324961	35.4575	28.5714	74.936607
28	G5	4063.876103	3193.13077	39.258036	28.5714	76.301786
29	H1	3730.851668	2542.138246	26.516833	15.8333	66.081917
30	H2	3673.702141	2498.138623	23.722833	8.333	63.79075
31	H3	3729.916304	2542.804427	49.671429	46.4286	76.768929
32	H5	5569.257722	3242.018486	54.803929	58.9286	77.410893
33	I1	5978.529412	3833.108071	44.270417	31.667	72.819167
34	I2	6004.580236	3791.917852	43.5525	35.833	72.41625
35	I3	5979.600559	3833.614732	67.225179	96.4286	77.120536
36	I4	5968.502222	3826.581689	46.605	44.1667	74.319917
37	I5	6278.4478	3848.401559	65.158214	92.8571	77.160893
38	I6	6278.4478	3853.324743	45.422333	40	74.466333
39	J1	5293.188484	3857.479978	39.551167	25.833	69.448417
40	J2	5314.535747	3817.355973	37.49125	23.333	68.8795
41	J3	5279.487203	3858.091344	60.285179	76.7857	75.843393
42	J4	5287.216538	3850.619785	42.264167	32.5	70.867
43	J5	5553.990673	3874.064052	57.360714	69.6429	75.613929
44	J6	5553.990674	3873.412472	39.453583	23.3333	69.921333
45	K1	3852.819915	3818.914163	25.85525	14.1667	65.42725
46	K2	3864.195082	3780.204211	22.859333	5.8333	64.393417
47	K3	3850.595921	3819.838596	46.305179	39.2857	77.900714
48	K4	3846.746056	3811.603852	27.2525	15.8333	66.534667
49	K5	4036.134627	3836.650102	42.503036	32.1429	76.414464
50	K6	4036.134628	3835.608447	22.97475	6.667	64.46375
51	L1	2334.276721	3812.721995	14.11287	12.037	61.995
52	L2	2337.889301	3771.208429	10.366	0.8333	59.587417
53	L3	2332.906842	3812.820429	33.893929	32.1429	78.734643
54	L4	2318.332224	3806.551229	14.666	13.3333	62.293833
55	L5	2530.753008	3827.043698	29.263393	23.2143	76.389107
56	L6	2530.753008	3826.751557	9.176917	3.3333	58.9695
57	M1	1689.250663	3734.473078	10.346917	11.6667	58.058583
58	M2	1697.960887	3697.568948	5.663583	0.8333	57.118167
59	M3	1692.462298	3736.215134	27.71125	30.3571	78.091071
60	M4	1691.934442	3683.44371	10.920083	13.3333	59.475083
61	M5	1821.56293	3753.509914	22.5775	21.4286	75.038214
62	M6	1821.56293	3751.551323	4.539917	3.3333	56.308833
63	N1	2474.283752	3762.5541	14.423917	13.333	61.905083
64	N2	2482.104174	3722.890736	10.681917	2.5	60.346417
65	N3	2474.410343	3764.577417	34.677321	33.9286	78.735357
66	N4	2468.228178	3756.13742	15.187833	15	62.597917
67	N5	2546.020057	3779.694158	30.002143	26.7857	76.465536
68	N6	2546.020056	3778.145807	9.429667	3.3333	60.192417
69	O1	3867.107446	3794.843756	26.34775	17.5	67.4765
70	O2	3889.120015	3752.498472	22.97725	10	66.187083
71	O3	3867.076599	3794.890416	48.579464	46.4286	78.943929
72	O4	3865.113	3788.788227	28.070667	18.3333	69.111917
73	O5	4063.876103	3808.175579	44.582143	41.0714	77.708036
74	O6	4063.876102	3807.889861	23.41425	6.6667	67.407667
75	P1	5353.661041	3846.350433	38.794667	25.8333	71.603
76	P2	5374.321441	3799.932038	37.097417	23.3333	70.973083
77	P3	5352.745379	3856.477585	62.018929	71.4286	77.774464
78	P4	5339.51915	3842.057819	41.292167	34.1667	73.1755
79	P5	5569.257722	3857.746813	59.452857	76.7857	77.831429
80	P6	5569.257722	3856.597647	38.9155	24.1667	72.7765

Appendix 10: Experiments results

Appendix 11: Material Selection

Physical Properties

Property	Value
V(λ) Reflectance	10.39%
M(λ) Reflectance	8.41%
M/P Ratio	0.81
L*	38.05
a*	4.58
b*	7.84
$R_{reflectance}$	12.95%
$G_{reflectance}$	9.67%
$B_{reflectance}$	7.37%
Specularity	0.00%
Roughness	0.30

Red Brick

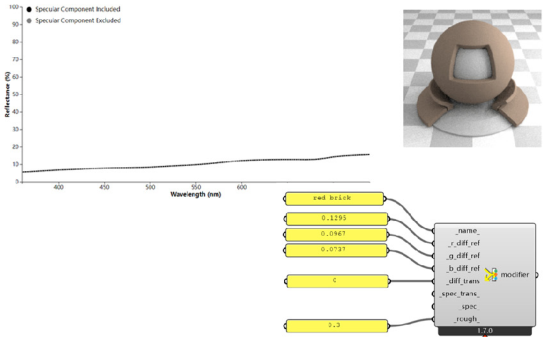

Physical Properties

Property	Value
V(λ) Reflectance	79.66%
M(λ) Reflectance	75.30%
M/P Ratio	0.95
L*	91.46
a*	-1.37
b*	6.14
$R_{reflectance}$	81.49%
$G_{reflectance}$	79.76%
$B_{reflectance}$	70.76%
Specularity	0.10%
Roughness	0.30

White Plaster Wall NL

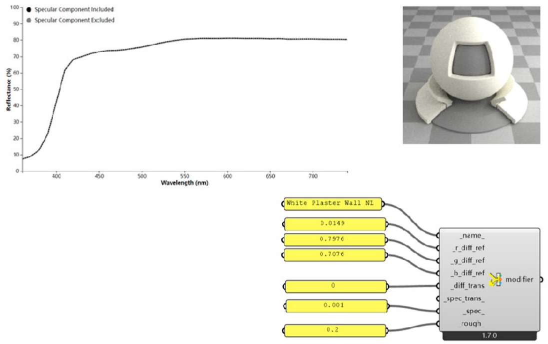

Physical Properties

Property	Value
V(λ) Reflectance	12.31%
M(λ) Reflectance	12.61%
M/P Ratio	1.02
L*	41.79
a*	-1.74
b*	-0.20
$R_{reflectance}$	11.57%
$G_{reflectance}$	12.68%
$B_{reflectance}$	12.59%
Specularity	0.00%
Roughness	0.00

Grey Carpet NL

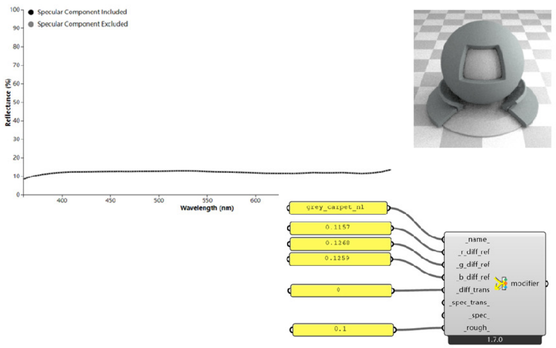

Physical Properties

Property	Value
V(λ) Reflectance	82.92%
M(λ) Reflectance	81.27%
M/P Ratio	0.98
L*	92.94
a*	-0.35
b*	2.44
$R_{reflectance}$	83.94%
$G_{reflectance}$	82.84%
$B_{reflectance}$	79.31%
Specularity	0.09%
Roughness	0.30

White Ceiling Panel NL

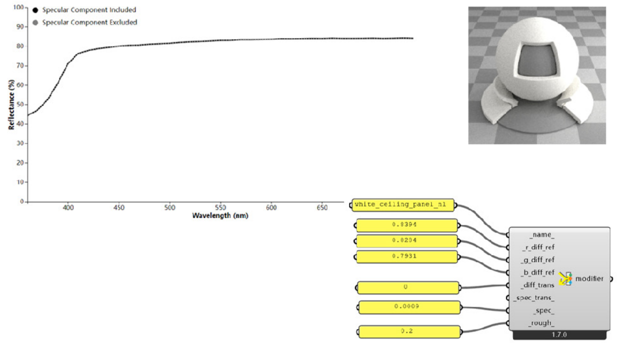

Physical Properties

Property	Value
V(λ) Reflectance	34.50%
M(λ) Reflectance	33.93%
M/P Ratio	0.98
L*	65.31
a*	-0.14
b*	1.47
$R_{reflectance}$	33.70%
$G_{reflectance}$	33.48%
$B_{reflectance}$	32.00%
Specularity	1.60%
Roughness	0.20

Door

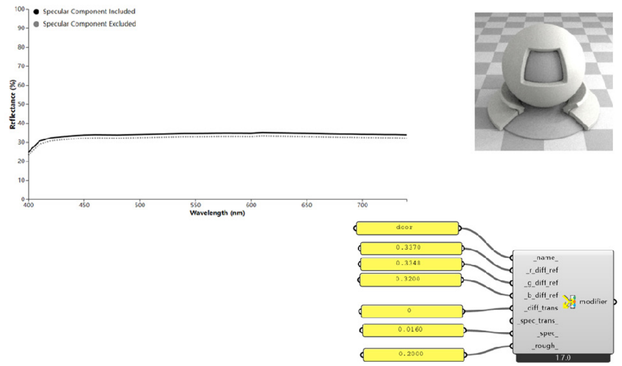

Physical Properties

Property	Value
V(λ) Reflectance	66.44%
M(λ) Reflectance	66.83%
M/P Ratio	1.01
L*	85.25
a*	-1.45
b*	0.57
$R_{reflectance}$	64.87%
$G_{reflectance}$	67.13%
$B_{reflectance}$	65.71%
Specularity	3.99%
Roughness	0.10

Motech Im60 Frame

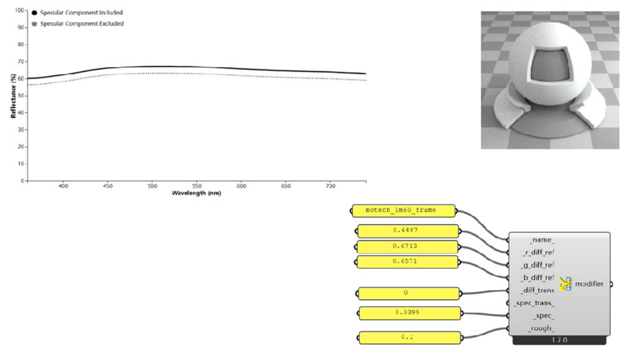

Appendix 12:

Script for Selectroom_1_1 (DA, LOD1.3)

for sDA, UDI, SBI,

Script only needs to be partially changed

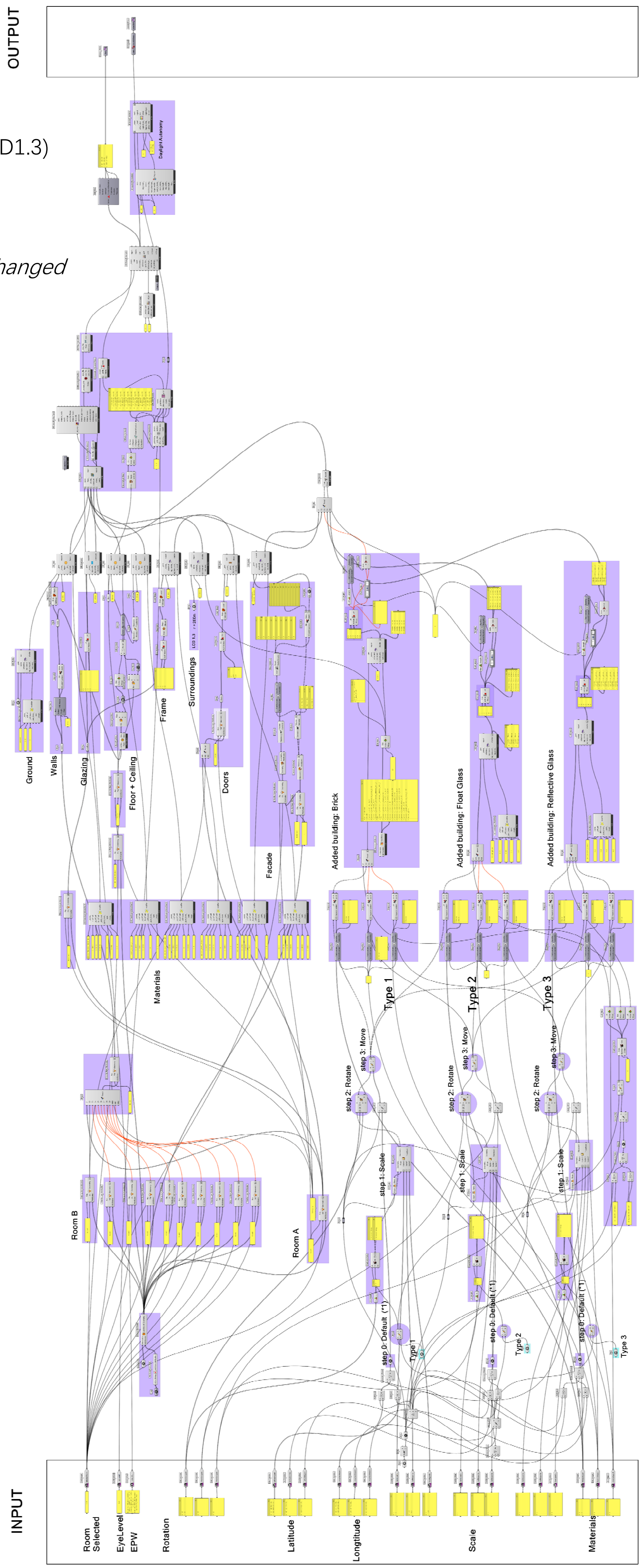

Appendix 13:

Coordinates for rooms

Room Number	Longitude	Latitude	Room Number	Longitude	Latitude	Room Number	Longitude	Latitude	Room Number	Longitude	Latitude
0	4.369957323	52.00546781	118	4.369517725	52.00525762	258	4.370228408	52.00545022	396	4.370421473	52.00533331
1	4.370713702	52.0058256	119	4.369435129	52.00529638	259	4.370164326	52.0052498	398	4.370374617	52.00535726
3	4.370367705	52.00554424	120	4.369502381	52.00520893	260	4.370043863	52.00550668	400	4.370277058	52.00537186
4	4.370782154	52.00579139	121	4.36948481	52.00514452	261	4.369839553	52.00564456	401	4.370277245	52.00529178
5	4.37060646	52.00565147	122	4.369391032	52.00527175	262	4.36978473	52.00560362	402	4.370209129	52.00541072
6	4.370514107	52.00569868	123	4.369420547	52.00518591	263	4.369742023	52.00548023	403	4.370233136	52.00543098
7	4.370414539	52.00551942	124	4.369335718	52.00522895	264	4.369840342	52.00543982	404	4.37021563	52.00532322
9	4.370571443	52.00574852	126	4.370266185	52.0048722	265	4.369797657	52.00540815	405	4.370121556	52.00521169
12	4.371402443	52.00567519	127	4.370333624	52.00492235	266	4.369768677	52.00538672	407	4.370185311	52.00545315
13	4.371278509	52.00571861	128	4.370490799	52.00503887	267	4.369562366	52.00533969	408	4.370119514	52.00548636
14	4.371166558	52.00577928	129	4.370520537	52.00521322	268	4.369428154	52.00521116	409	4.370063158	52.00551513
15	4.371124099	52.00583204	130	4.370286203	52.00533337	269	4.370308015	52.00489535	410	4.370011842	52.00554065
16	4.371081739	52.00582126	131	4.370267901	52.00540843	270	4.370340544	52.00533245	411	4.369954518	52.00557061
17	4.371034545	52.00584539	132	4.370186062	52.00543137	271	4.370282436	52.00538141	412	4.369928758	52.00560649
18	4.371050578	52.0058697	133	4.369986979	52.00548591	272	4.370281388	52.00494675	413	4.369829708	52.00561764
19	4.371375409	52.00594588	134	4.369770796	52.00546704	273	4.37031811	52.005384	414	4.369694968	52.00543956
20	4.370902917	52.005932	135	4.369532953	52.00531304	274	4.370258486	52.00544566	415	4.369845487	52.00544387
21	4.370846219	52.00594499	138	4.370279742	52.00494829	275	4.369888596	52.00548181	416	4.369721484	52.00548873
22	4.3708487	52.00591216	140	4.370315137	52.00538604	291	4.370556721	52.00567688	417	4.369772652	52.00538927
23	4.37075671	52.00598901	143	4.370000242	52.00526132	292	4.370740944	52.00584616	418	4.369649984	52.00545555
24	4.370642301	52.00604741	144	4.370254932	52.00544641	293	4.370659349	52.00578565	420	4.369592784	52.00541283
25	4.370530491	52.00612116	145	4.370232785	52.00542923	294	4.370556064	52.00574299	421	4.369673591	52.00537253
26	4.370614142	52.00616852	147	4.369890611	52.00547991	295	4.370524937	52.00564442	425	4.36947067	52.00532079
27	4.37066089	52.0061862	150	4.370786653	52.00588944	296	4.370454319	52.00566552	426	4.36954976	52.00528048
28	4.370761954	52.00626103	151	4.370730652	52.00584805	297	4.37042964	52.0056156	429	4.369408864	52.00522165
29	4.370872448	52.00634248	152	4.370649387	52.00578843	298	4.370375627	52.00557548	431	4.370264106	52.00490746
30	4.370984001	52.00642514	153	4.370622243	52.0056624	299	4.370320744	52.00553492	432	4.370255392	52.00496117
31	4.371095164	52.0065073	155	4.370532499	52.00568795	300	4.37026743	52.00549532	433	4.370494376	52.00504197
32	4.371137282	52.00641278	157	4.370571753	52.00574854	303	4.370505217	52.0057046	434	4.370519719	52.00521346
33	4.371189697	52.00645214	159	4.370551807	52.00561044	306	4.370571413	52.00574871	435	4.370285274	52.00533331
34	4.37130823	52.00662598	160	4.371033096	52.00584367	308	4.371413693	52.00569912	437	4.370180621	52.00534134
35	4.371468342	52.00674469	161	4.371225669	52.00630005	309	4.37110353	52.00587967	438	4.369540891	52.0051864
36	4.371254631	52.00632359	162	4.371116377	52.00640164	310	4.371370696	52.00565148	439	4.37009871	52.00528485
37	4.371154779	52.0063818	163	4.371127927	52.00638771	311	4.371306431	52.00568988	440	4.370031828	52.0054628
38	4.371089912	52.00632719	164	4.371158417	52.00637452	312	4.371371745	52.00574163	442	4.369872927	52.00556501
39	4.37122452	52.00626047	166	4.370830901	52.00608186	313	4.371268737	52.00570918	444	4.369807577	52.00541662
40	4.37137903	52.00622328	169	4.371315578	52.00621654	314	4.371329441	52.00576345	446	4.369483911	52.00514428
41	4.370872424	52.00609499	173	4.370303386	52.00470826	315	4.371233022	52.00573081	447	4.369510719	52.00529942
42	4.371229263	52.00581376	174	4.370262329	52.00472909	316	4.371184131	52.0057558	449	4.370421704	52.00530986
43	4.371248142	52.00585084	175	4.370223308	52.0047489	317	4.371102958	52.00581243	450	4.370299088	52.00539278
44	4.371014418	52.00589717	176	4.370164208	52.00477924	318	4.371080921	52.0058215	451	4.369999673	52.00526196
47	4.371087952	52.00637467	177	4.370184796	52.00480738	319	4.371034036	52.00584565	452	4.370256491	52.00544843
48	4.371183301	52.00648204	178	4.370194227	52.0048789	320	4.371047753	52.00587078	454	4.369897028	52.00547683
49	4.370831181	52.00608207	179	4.370188367	52.0048924	321	4.371218621	52.00586582	459	4.370682845	52.00561148
50	4.371208498	52.00631297	180	4.370221526	52.00488311	322	4.371281085	52.00583395	460	4.370804899	52.00555112
51	4.371641548	52.00646017	181	4.37030902	52.00482801	323	4.371345801	52.00589951	461	4.370872761	52.00572138
52	4.371677484	52.00652999	182	4.370237167	52.00491692	324	4.371434097	52.00598906	462	4.370916676	52.00575418
53	4.371277606	52.00600796	183	4.370363174	52.00486824	326	4.370899753	52.00593326	463	4.370957177	52.00569995
54	4.370977976	52.00589549	184	4.370380287	52.00495954	327	4.370843305	52.00594664	464	4.371019329	52.00565209
55	4.370868529	52.00590122	185	4.370558437	52.00499789	328	4.370844887	52.00591356	465	4.371063383	52.00568499
56	4.371052399	52.00634833	186	4.370431974	52.00499856	329	4.370755522	52.00598961	466	4.371065429	52.00562098
57	4.371258282	52.00624333	187	4.370483999	52.00503741	330	4.370641822	52.00604748	467	4.371109343	52.00565378
58	4.371251388	52.00646714	188	4.370611192	52.00503707	331	4.370530012	52.00612123	468	4.370626803	52.00541557
66	4.371600232	52.00653358	189	4.370536165	52.00507637	332	4.370656635	52.00618344	469	4.371201274	52.00534665
67	4.371627284	52.00654038	190	4.370656017	52.00508501	333	4.370758118	52.00625859	470	4.3711808	52.0055035
68	4.370207656	52.00477806	191	4.370417951	52.00533685	334	4.37087082	52.0063419	471	4.371264413	52.00549019
69	4.370263897	52.00473005	192	4.370373641	52.00535951	335	4.370983522	52.00642521	472	4.371324302	52.0054598
70	4.370225555	52.00474951	193	4.370203184	52.00544373	336	4.371067663	52.0064874	474	4.371364088	52.0054361
71	4.370191055	52.00476737	194	4.37019809	52.00527459	337	4.371122126	52.00652765	475	4.371408401	52.00540344
73	4.370113522	52.00480671	195	4.369832026	52.00558085	338	4.371156162	52.00642688	476	4.371190799	52.0052169
74	4.370029987	52.00486945	196	4.369846683	52.00544221	339	4.371189167	52.00645153	477	4.37105417	52.00526658
75	4.370197666	52.00485891	197	4.369812669	52.00541702	340	4.371267366	52.00645886	478	4.370915522	52.00531221
76	4.370184767	52.00487247	198	4.369777396	52.00539089	341	4.371278427	52.00661181	479	4.370976814	52.00534075
77	4.370207564	52.00488949	199	4.369649247	52.00535542	342	4.371444168	52.00672749	480	4.37103064	52.00539605
78	4.370228542	52.00490516	200	4.369544407	52.00527776	343	4.371423972	52.00676773	481	4.370973296	52.00542515
79	4.37024952	52.00492083	201	4.370276911	52.00478765	344	4.371172578	52.00632892	482	4.371074426	52.00545662
80	4.370312734	52.00482823	202	4.370197751	52.00486536	345	4.371401933	52.00621166	483	4.37130411	52.00545408
81	4.370368146	52.0048694	204	4.370431354	52.0049466	346	4.371069971	52.006234	484	4.371155494	52.00521394
82	4.37045995	52.00493753	206	4.370164917	52.00481764	347	4.371262736	52.00581046	485	4.370977435	52.00530482
83	4.370551085	52.00500495	213	4.369738932	52.00540813	349	4.371260883	52.00594313	486	4.371090849	52.00548144
84	4.370602691	52.00504349	215	4.370734111	52.00581595	350	4.370978116	52.0058956	493	4.370942374	52.00535822
85	4.370658692	52.00508488	216	4.3706488	52.00570032	354	4.370925603	52.00611449	497	4.369846736	52.00544587
86	4.370783524	52.00512959	217	4.370553813	52.0057494	356	4.371325359	52.00625087	502	4.371426135	52.00566352
87	4.370695266	52.00519156	218	4.370538238	52.00568521	357	4.371154665	52.00606999	503	4.371349893	52.00566765
88	4.370605768	52.00523751	223	4.371259074	52.00574899	359	4.370863508	52.00606812	504	4.371419549	52.0057186
89	4.370516609	52.00528328	224	4.371032988	52.00584635	360	4.371640615	52.00653203	505	4.371307589	52.00568947
90	4.370468736	52.00530774	225	4.371048751	52.0058694	361	4.37169099	52.00652752	506	4.371379849	52.00573875
91	4.370422231	52.00533345	226	4.371248371	52.00585037	363	4.371278056	52.00600808	507	4.371269757	52.00571165
92	4.370378494	52.00532249	227	4.37132638	52.00590884	365	4.370866752	52.00590159	508	4.371336527	52.00576108
93	4.370375745	52.00535704	228	4.370736743	52.0060158	367	4.371112859	52.00635922	509	4.371229599	52.00573273
94	4.370336387	52.00534105	229	4.370886543	52.00591786	368	4.371234083	52.00647592	510	4.371074994	52.00581346
95	4.370277474	52.00529131	230	4.370850105	52.00590916	370	4.370994789	52.00615147	511	4.371046472	52.005866
96	4.370201619	52.00533191	231	4.370481485	52.00611393	373	4.371652745	52.00645449	512	4.371045578	52.00585873
97	4.370201914	52.0054149	232	4.370534939	52.00615364	374	4.371598687	52.00649753	513	4.371015495	52.00583137
98	4.370116016	52.00521415	233	4.370779566	52.00624928	375	4.371599159	52.00654044	514	4.371223711	52.00586323
99	4.370234374	52.00545702	234	4.370992552	52.00640642	376	4.371625135	52.00653814	515	4.371194806	52.0063336
100	4.370121669	52.00548457	235	4.371223245	52.00657017	377	4.370232148	52.00545727	516	4.371175739	52.00643852
101	4.370064634	52.00551368	236	4.371151398	52.00642439	378	4.370303852	52.00472925	517	4.37090924	52.00610227
102	4.370010794	52.00554136	237	4.371181886	52.00644716	379	4.370124515	52.00482131	518	4.371278434	52.005776
103	4.369954578	52.00557023	238	4.371444487	52.00672645	380	4.370185966	52.00487379	519	4.371103809	52.00587988
104	4.369841813	52.00561114	239	4.371257297	52.00628558	381	4.370312645	52.0048288	521	4.370872704	52.0060952
105	4.369779264	52.00553273	243	4.370870125	52.005899	382	4.370201467	52.00489452	530	4.370409606	52.0053253
106	4.369844627	52.00544238	244	4.371223374	52.00648048	383	4.370367188	52.00486953	531	4.370448354	52.00535317
107	4.369720466	52.00548924	245	4.370167278	52.00479855	384	4.370433399	52.00491855	532	4.370374838	52.00535785
108	4.369807536	52.00541489	246	4.37022341	52.00481515	386	4.370498351	52.00496663	533	4.369926429	52.00561539
109	4.369649674	52.00545553	247	4.370190327	52.00483194	387	4.370550686	52.0050055	534	4.36984104	52.00556716
110	4.369781773	52.00539586	248	4.370155008	52.00485003	388	4.37063298	52.00506653	535	4.369809785	52.00541849
111	4.369762443	52.00538164	249	4.37011955	52.00486803	389	4.370782985	52.00513004	536	4.369771804	52.0053897
112	4.369655011	52.00535951	251	4.370465364	52.00496583	390	4.3709209	52.00510408	537	4.369633632	52.00539333
113	4.369593733	52.00541376	252	4.370279734	52.00487445	391	4.370867726	52.00506458	538	4.369887513	52.00559058
114	4.369584604	52.00530736	253	4.370242543	52.00491051	392	4.370692691	52.00519305	539	4.369780682	52.00544378
115	4.369536892	52.00537173	254	4.370619076	52.00521233	393	4.370606616	52.00523708	540	4.369781352	52.00549641
116	4.369545975	52.00527872	256	4.370415448	52.00535285	394	4.370518504	52.00528214	546	4.370965912	52.00567306
117	4.369480192	52.00532982	257	4.370242275	52.00530865	395	4.370468426	52.00530773	547	4.37064215	52.00543129

Appendix 14:Room tag for Wall category

Element Id	RoomA	RoomB	RoomC	RoomD	RoomE	RoomF	RoomG	RoomH	RoomI	RoomJ	RoomK	Category
325651	381											Walls
325726	383											Walls
325984	384											Walls
326468	386											Walls
326530	387											Walls
326601	388											Walls
329007	387	388	433									Walls
329053	386	387	433									Walls
329057	387	433										Walls
329067	388	433	434									Walls
329446	388	389	434									Walls
376892	378											Walls
376897	378											Walls
376906	378											Walls
376910	378	379										Walls
376915	379											Walls
376919	379											Walls
376990	391											Walls
376995	391											Walls
376999	389	391										Walls
377054	384	386	433									Walls
377059	384	386										Walls
377063	383	384	432	433								Walls
377068	383	384										Walls
377072	383	430	432									Walls
377077	379	381	430									Walls
377081	381	383										Walls
378091	378	379	381									Walls
378538	392	434										Walls
378546	392											Walls
378797	379	380	430									Walls
379331	382											Walls
379336	380											Walls
379350	380	382	430									Walls
379988	390											Walls
379993	390											Walls
379997	389	390	391									Walls
380001	389	390										Walls
380026	389											Walls
380030	389	392										Walls
380410	389											Walls
380977	392	393	434									Walls
380982	393											Walls
380987	393	434										Walls
381411	394											Walls
381416	393	394	434									Walls
381421	394	434										Walls
381432	394	395										Walls
381443	395											Walls
381448	395	434	449									Walls
381453	395	396										Walls
381686	396											Walls
381694	396	449										Walls
381704	396	449										Walls
381709	396	435										Walls
381714	396	398										Walls
381723	398											Walls
381727	398	399	435									Walls
381732	398	435										Walls
381873	400	435	450									Walls
381878	400	436	450									Walls
381882	400	435	436	450								Walls
381887	400	436	450									Walls
381914	401											Walls
381918	401	435										Walls
381937	405											Walls
381942	401	404	405									Walls
381953	405	406										Walls
381966	406	451										Walls
381970	406											Walls
381975	406											Walls
381980	406											Walls
381984	405											Walls
381993	401	404	435									Walls
381997	404	435										Walls
383655	406	439	451									Walls
383822	403	407	452									Walls
383837	304	403	436	452								Walls
383841	402	403										Walls
383924	377	403	407	452								Walls
383932	377	407										Walls
383936	377	407										Walls
383988	377	407										Walls
383992	403	407										Walls
383996	403	407										Walls
384008	402	407										Walls
384238	407	408										Walls
384267	408	440										Walls
384271	408	409										Walls
384279	408	409										Walls
384287	408	409										Walls
384291	409	408										Walls
384299	409	410										Walls
384307	409	410										Walls
384316	409	410										Walls
384324	409	410										Walls
384332	409	410										Walls
384336	410											Walls
384340	410	411										Walls
384376	411											Walls
384390	411	412										Walls
384395	412											Walls
384399	412	413	453									Walls
384403	412	413										Walls
384407	413	442	453									Walls
384415	413											Walls
384419	413											Walls
384426	414	440	442	443								Walls
384430	414	442	443									Walls
384438	414											Walls
385704	413	414										Walls
387305	443	445										Walls
387309	414	416	443									Walls
387313	416	418	540									Walls
387428	415											Walls
387432	415	443	454									Walls
387440	415	443										Walls
387454	420	445										Walls
387459	420	445										Walls
387469	420	445										Walls
387480	420	445	458									Walls
387485	420											Walls
387489	420	445										Walls
387500	423	425	447									Walls
387505	423	425										Walls
387510	423											Walls
387514	425											Walls
387518	427											Walls
387522	425	427	447									Walls
387527	427	429	447									Walls
387532	427	447										Walls
387537	425	447										Walls
387550	424	447										Walls
387555	424											Walls
387560	426	447										Walls
387565	426											Walls
387570	426	428	429	447								Walls
387575	429											Walls
387605	429											Walls
387609	429											Walls
387622	429											Walls
387657	429											Walls
387664	438											Walls
387668	438											Walls
387672	429	438										Walls
387676	438	446										Walls
387682	446											Walls
387690	429	446										Walls
387694	446											Walls
387700	421	443	445									Walls
387710	421	445										Walls
387715	421	445										Walls
387719	421											Walls
387730	418	445										Walls
387740	418	420	445									Walls
387745	416	418										Walls
387755	417	443	444									Walls
387759	417											Walls
387763	417	419	443	445								Walls
387767	417	443	445									Walls
387777	419	443	445									Walls
387781	419	421	445									Walls
387785	419											Walls
392249	407	408										Walls
393329	300	304	377	407	408	452						Walls
393333	299	300										Walls
393341	299	300										Walls
393346	299											Walls
393358	298											Walls
393362	297	298										Walls
393366	297											Walls
393374	296	297	302									Walls
393605	408											Walls
394480	296											Walls
394515	293											Walls
394524	292	293	301									Walls
394529	292	293	301	302	498							Walls
394538	292											Walls
394543	291	292										Walls
394552	291	292										Walls
394556	291	301	327	328	350	365						Walls
394560	291	301										Walls
417846	480	482										Walls

Element I	RoomA	RoomB	RoomC	RoomD	RoomE	RoomF	RoomG	RoomH	RoomI	RoomJ	RoomK	Category
394757	326	350	351									Walls
394761	326	350										Walls
394765	326	327	328									Walls
394769	326	327										Walls
394773	326	327	351									Walls
394782	326	351										Walls
394791	326	327										Walls
394970	326	350										Walls
395218	327	328										Walls
395446	327	351										Walls
395547	328	365										Walls
395557	327	329	351									Walls
395561	329	330	351									Walls
395565	329											Walls
395569	329	330										Walls
395580	330											Walls
395594	330	351										Walls
395660	331											Walls
395672	331											Walls
395688	331											Walls
395696	333	334	352									Walls
395704	334											Walls
395708	333	334	352									Walls
395712	333											Walls
395716	333	352										Walls
395720	332	333	352									Walls
395724	332											Walls
395728	332	351	352									Walls
395732	331	332										Walls
395736	331	332										Walls
396083	291											Walls
398941	330	331	332	351								Walls
399157	335	352	353									Walls
399161	335	336	353									Walls
399165	334	335	352									Walls
399169	335											Walls
399175	336	337	353									Walls
399179	336	337										Walls
399187	336											Walls
399214	337	341	353									Walls
399218	337	341	353									Walls
399222	337											Walls
399994	341											Walls
400002	341											Walls
400010	341	342										Walls
400023	342											Walls
400043	342											Walls
400047	342											Walls
400058	343											Walls
400062	343											Walls
400066	342	343										Walls
400070	342	343										Walls
401138	340											Walls
401143	368											Walls
401153	340											Walls
401209	339											Walls
401229	338	339										Walls
401233	338	339	353	355								Walls
401243	338	355										Walls
401247	338	344	355									Walls
401255	338											Walls
401260	338											Walls
401264	338											Walls
401268	339											Walls
401273	339											Walls
401340	344	355	356									Walls
403973	345											Walls
403983	345											Walls
404198	318	319										Walls
404202	309	319										Walls
404219	319											Walls
404227	319											Walls
404235	319											Walls
404259	317	318	347									Walls
404264	309	318	347									Walls
404273	318											Walls
404281	318											Walls
404289	318	319										Walls
404293	318											Walls
404297	317	318										Walls
404301	318											Walls
404305	317	318										Walls
404310	317	318										Walls
404331	309	319	320									Walls
404335	309	320										Walls
404344	319	320										Walls
405629	318											Walls
405633	318											Walls
405637	318											Walls
406025	317	347										Walls
406030	316	317										Walls
406107	315	316										Walls
406116	316											Walls
406120	316	317	347	518								Walls
406200	313	315										Walls
406205	315	347										Walls
406383	311	313										Walls
406388	308	311	313	347								Walls
406392	313											Walls
406418	308	311										Walls
406432	311											Walls
407639	308											Walls
407648	308											Walls
407856	312											Walls
407860	308	312	314	347								Walls
407864	312	314	347									Walls
407970	314											Walls
407974	314	347										Walls
407978	314	347										Walls
408078	322											Walls
408090	322											Walls
408094	322	347										Walls
408255	321	322	347									Walls
408643	323											Walls
408655	321	323	348	349	514							Walls
408761	324											Walls
408765	324											Walls
408770	323	324	325	349	363							Walls
409158	324											Walls
409444	324	325										Walls
409824	462											Walls
409828	461	462										Walls
409832	461	462										Walls
409836	461											Walls
409848	461											Walls
409905	463	465										Walls
409913	463	464	465									Walls
409917	463	465										Walls
409921	463	464										Walls
409925	464											Walls
409933	466	467										Walls
409937	464	466	467									Walls
409941	464	466										Walls
409945	464	466										Walls
409991	467											Walls
409999	467											Walls
410003	464	465	467									Walls
410130	461	463										Walls
410134	462	463										Walls
410138	461	462	463									Walls
410265	468											Walls
410269	468											Walls
410273	468											Walls
410277	468											Walls
410305	470											Walls
410309	469	470	471	483								Walls
410313	482	470										Walls
410317	470											Walls
410335	471											Walls
410343	471	483										Walls
410352	472	474	483									Walls
410356	472											Walls
410360	472	483										Walls
410364	472	483										Walls
410676	474											Walls
410688	473	474	483									Walls
410789	473	483										Walls
410793	473	483										Walls
410905	475											Walls
410909	475											Walls
410917	473	474	475	483								Walls
410921	475	483										Walls
411205	475	483										Walls
411321	469											Walls
411330	469	483										Walls
411472	469	479	480	482								Walls
411670	469	475	483									Walls
413357	476											Walls
413409	484											Walls
413413	476	484										Walls
413417	484											Walls
413425	476	484										Walls
413429	476	484										Walls
413501	476	484										Walls
413649	477	484										Walls
413653	469	477	485									Walls
413658	477											Walls
413662	477	485										Walls
414426	477											Walls
415268	469	477										Walls
416369	469	477										Walls
417518	469	477										Walls
493606	444											Walls

Element Id	RoomA	RoomB	RoomC	RoomD	RoomE	RoomF	RoomG	RoomH	RoomI	RoomJ	RoomK	Category
417850	460	480	481	482								Walls
418057	479	480	481	493								Walls
418061	480	481										Walls
418085	460	481										Walls
418103	479	493	494	495	496							Walls
418137	478	479	496									Walls
418141	478											Walls
418145	478											Walls
418166	493											Walls
418170	494											Walls
418174	495											Walls
418178	496											Walls
418186	493	494										Walls
418202	494	495										Walls
418232	460	482	487									Walls
418998	495	496										Walls
422766	124											Walls
422770	124											Walls
422774	123	124	135									Walls
422779	122	124	135									Walls
422892	123											Walls
422912	120	121	123									Walls
423058	121											Walls
423062	121											Walls
423066	120	121										Walls
423518	122											Walls
423527	119	122	135									Walls
423531	122	135										Walls
423606	117											Walls
423610	117	119	135									Walls
423618	117	135										Walls
423722	115											Walls
423726	115	117	135									Walls
423730	113	115	135									Walls
423734	115	135										Walls
423975	119											Walls
423987	119	135										Walls
423996	120											Walls
424012	120	123	135									Walls
424130	107	134										Walls
424142	107											Walls
424148	107	109	113	134	135							Walls
424152	107	109										Walls
424156	109	113										Walls
424160	109											Walls
426605	107	134										Walls
426862	113											Walls
426874	113	135										Walls
427088	105											Walls
427092	104	105	134	195								Walls
427096	105	107	134									Walls
427100	103	104	105	133	134	146	195					Walls
427828	104											Walls
427850	104											Walls
427859	104											Walls
427876	102	103										Walls
427881	103											Walls
427912	102											Walls
427921	101	102										Walls
427960	100	101										Walls
427964	100	101										Walls
427972	100	132	193									Walls
429022	99	132	144	193								Walls
429444	96											Walls
429458	95	96										Walls
429554	95											Walls
429841	98											Walls
429849	98											Walls
429854	98											Walls
429859	143											Walls
429863	143											Walls
429889	143											Walls
430723	90											Walls
430737	89	90										Walls
430782	89											Walls
430792	88	89										Walls
430866	87											Walls
430964	87	88										Walls
431417	88											Walls
431956	86											Walls
431960	86	87	129									Walls
431965	85	86	128	129	139							Walls
431969	86											Walls
432307	86											Walls
435154	73	74	125									Walls
435158	74											Walls
435162	74											Walls
435166	74											Walls
435234	73											Walls
436197	3	100										Walls
436201	3	7	99	100	131	132	144	193				Walls
436232	6											Walls
437731	20	21										Walls
437736	20	22	55									Walls
437745	20	44	55									Walls
437754	22	55										Walls
437764	21	22										Walls
437796	1	21	23	45	150							Walls
438125	23	24	45									Walls
438130	23											Walls
438134	23	24										Walls
438144	24	45										Walls
438149	24											Walls
438176	24	25	27	45	46							Walls
438180	25											Walls
438184	25	26	27									Walls
438735	25											Walls
439102	27	28	45	46								Walls
439111	26	27										Walls
439115	26	27										Walls
439124	26											Walls
439144	27	28										Walls
439148	27											Walls
439618	29											Walls
439622	28	29	30	46								Walls
439626	28	29										Walls
439630	28	46										Walls
439785	28											Walls
439936	27											Walls
440168	30											Walls
440172	29	30										Walls
440180	30	46										Walls
440581	31	46	48									Walls
440585	30	31	46									Walls
440589	31											Walls
440690	34											Walls
440698	34											Walls
440702	34											Walls
440710	34											Walls
440714	34											Walls
440718	34											Walls
440940	342											Walls
441813	342											Walls
442046	34											Walls
442054	35											Walls
442058	35											Walls
443724	33											Walls
443728	58											Walls
443737	32	33	48									Walls
444346	32											Walls
445059	37	164										Walls
445276	36	161										Walls
445371	40	161	724									Walls
445381	40	724										Walls
447163	17	18	42	44	160							Walls
447178	16	17	160									Walls
447188	16	42										Walls
447192	15	16										Walls
447196	14	15	16									Walls
447205	15	16	42									Walls
447209	14	15	42									Walls
447214	14	16										Walls
447747	14	42										Walls
447755	13	14										Walls
447764	13	42										Walls
447768	13											Walls
447772	13											Walls
449142	13	14										Walls
449303	12	13	42									Walls
449308	12											Walls
449312	12											Walls
449316	12											Walls
450204	19	53										Walls
450208	19	53										Walls
450227	19											Walls
450238	19											Walls
450243	19											Walls
450247	19											Walls
450680	19	53										Walls
479839	98											Walls
489601	423	445	447									Walls
491455	424	445										Walls
491740	445	447										Walls
491921	445											Walls
492138	445											Walls
492193	443	445										Walls
492197	443	445										Walls
493598	415	443	444									Walls
529177	502	504	518									Walls
529181	502	504	518									Walls
529185	504	506	518									Walls
529205	506											Walls
529213	347	506	518									Walls

Element I	RoomA	RoomB	RoomC	RoomD	RoomE	RoomF	RoomG	RoomH	RoomI	RoomJ	RoomK	Category
494611	402	403	435	436	440							Walls
495936	304	436	450									Walls
495940	398	450	532									Walls
495949	435	437										Walls
495953	398	399	450	532								Walls
495957	398	399	435	450								Walls
496112	434	435										Walls
496120	404	405	439									Walls
496124	437											Walls
496128	437	439										Walls
496132	439											Walls
496136	405	439										Walls
496145	439	451										Walls
496149	439	451										Walls
497795	411	453	534	538								Walls
497924	440	442										Walls
499023	439	451										Walls
499027	451											Walls
499031	451											Walls
499203	451											Walls
500169	435											Walls
500295	434											Walls
501102	389	434										Walls
501630	433											Walls
501635	432	433										Walls
501639	432											Walls
501644	432											Walls
501668	432											Walls
501677	430	432										Walls
501681	430	431	432									Walls
501690	380	430										Walls
501695	430	431										Walls
501710	431											Walls
501945	382	430										Walls
502167	430	431										Walls
502287	432											Walls
502710	382	431										Walls
503317	431	432										Walls
503406	304	460										Walls
503426	302	459	460									Walls
503430	302	304										Walls
503438	302	459	460									Walls
503442	302	459	460									Walls
503446	302	459	460									Walls
503454	301	460										Walls
503459	301	350										Walls
503467	301	302										Walls
503471	294	302	303									Walls
503479	294											Walls
503483	294	303										Walls
503487	303											Walls
503495	302											Walls
505014	296	302										Walls
506447	296	302	303									Walls
506546	296	303										Walls
507519	302	304	460									Walls
507692	302	459	460									Walls
509501	301	302	460									Walls
510216	326	350	365									Walls
510229	350	365										Walls
511469	350	351										Walls
514829	418	443	445	537								Walls
514833	537											Walls
514837	445	537										Walls
514841	445	537										Walls
514845	445	537										Walls
514849	537											Walls
515180	537											Walls
515517	497											Walls
515521	443	497										Walls
515525	443	497	535	539								Walls
515529	443	497	539									Walls
515533	536											Walls
515541	536											Walls
515545	443	536	539									Walls
515803	443	445	536	539								Walls
515965	443	445	536	539								Walls
516622	535											Walls
516630	443	535	536	539								Walls
516634	443	535	539									Walls
516760	443	535										Walls
516853	443	535	539									Walls
517815	411	533	538									Walls
517819	533											Walls
517823	413	533										Walls
517827	413	533	538									Walls
517831	411	413	453	534	538							Walls
517835	411	440	453	534								Walls
517839	413	414	440	443	534	540						Walls
517843	413	534										Walls
518237	411	538										Walls
518241	413	538										Walls
518577	413											Walls
518811	395	434	449	530	531							Walls
518815	530	531										Walls
518823	434	435	449	530								Walls
519312	531											Walls
519316	435	530	531	532								Walls
519324	531											Walls
519332	395	531										Walls
519556	435	532										Walls
519883	298	299	499									Walls
520099	297	298	499									Walls
520103	297	298	307	499								Walls
520766	292	293										Walls
520988	292	301										Walls
521125	292	293	498									Walls
522083	460	546										Walls
522087	460	546										Walls
522091	460	546										Walls
522095	460	546										Walls
522172	460	547										Walls
522176	460	547										Walls
522180	460	547										Walls
522184	460	547										Walls
522574	516											Walls
522578	353	368	516									Walls
522582	353	516										Walls
522917	515											Walls
522922	352	353										Walls
522926	352											Walls
522930	352											Walls
522935	352											Walls
522939	352											Walls
523185	352	353	355	516								Walls
523496	354	359										Walls
523504	354	359										Walls
523508	354											Walls
523517	359											Walls
523521	359											Walls
523525	359											Walls
523531	0											Walls
523553	0											Walls
524019	346	517	528									Walls
524027	346	517	521									Walls
524031	346	517	521									Walls
524081	346	517	521	528								Walls
524093	346	370	517	528								Walls
524097	346	370	517									Walls
524101	346	517										Walls
526070	350	364	513									Walls
526074	511	512	513	722								Walls
526082	513											Walls
526090	513											Walls
526094	511	722										Walls
526098	511	512	722									Walls
526102	511	512										Walls
526106	511	512										Walls
526118	350	364	511									Walls
526122	511	519										Walls
526140	350	519										Walls
526148	510	513	722									Walls
526152	317	347	510	518	722							Walls
526156	510											Walls
526160	317	347	510	518	722							Walls
526164	510											Walls
526168	510											Walls
526182	317	347	518	722								Walls
526198	518	722										Walls
527816	323	514										Walls
527824	514											Walls
527828	322	347	514	518								Walls
528422	316	509										Walls
528426	347	509	518									Walls
528430	315	316										Walls
528434	507	509										Walls
528438	313	507										Walls
528442	347	507	518									Walls
528446	505	507										Walls
528599	503											Walls
528604	505											Walls
528608	503	505	518									Walls
528612	502	503	518									Walls
528616	347	505	518									Walls
528688	507											Walls
529082	502	503										Walls
529102	502											Walls
529106	502											Walls
529110	502											Walls
529173	504											Walls
665397	185	188	204									Walls
665401	128	184	186	187	189	204						Walls
665406	185	204										Walls

Element Id	RoomA	RoomB	RoomC	RoomD	RoomE	RoomF	RoomG	RoomH	RoomI	RoomJ	RoomK	Category
529219	347	506	508	518								Walls
529223	508											Walls
529227	347	508	518									Walls
529231	347	506	508	518								Walls
530517	350											Walls
530707	322	347	514	518	519							Walls
530777	518	519										Walls
530781	317	347	518	722								Walls
530785	322	347	518									Walls
530789	347	518										Walls
530802	322	347	518									Walls
530866	502	518										Walls
535132	518	347										Walls
535136	317	347	518									Walls
535145	321	347	348									Walls
535153	348	349										Walls
535170	321	348										Walls
536032	349	363										Walls
537060	348											Walls
538614	309	319	320	350	364							Walls
538618	350											Walls
541644	352	355										Walls
541648	352	355										Walls
541652	352	355										Walls
541656	352	353	355									Walls
544148	368											Walls
544459	339	368										Walls
544698	341	368										Walls
544984	339	368										Walls
546354	344	355	356									Walls
546414	355	356										Walls
546810	40	345	357	724								Walls
602392	127	128	138									Walls
602397	82	83	84	85	128							Walls
602402	128											Walls
602407	128	129										Walls
602778	7	131	140									Walls
602790	130	132										Walls
602794	95	96	130									Walls
602799	91	92	93	94	130	131	191	192				Walls
602902	129	130										Walls
602907	129											Walls
602912	87	88	89	90	91	129	191					Walls
603742	129	130										Walls
604370	132											Walls
604409	99	132	144									Walls
604413	132	145										Walls
604536	100	132	133	193								Walls
605861	100	101	102	103	133							Walls
606413	132	133										Walls
606885	133	134										Walls
607195	133											Walls
607396	133	147										Walls
608420	112	114	116	118	120	134	135	199	200			Walls
608551	120	123	135									Walls
608555	123	135										Walls
608806	4	44										Walls
608815	4	460										Walls
608836	7	460										Walls
610287	43											Walls
610291	19	43										Walls
610299	43											Walls
610308	42											Walls
611010	42	43										Walls
611560	42											Walls
611691	42	44										Walls
611745	44	45	357									Walls
611800	44											Walls
611859	44	45										Walls
614067	46	47	56									Walls
617258	25											Walls
618119	424	426	428									Walls
618529	112	114	135									Walls
618608	114	116	135									Walls
618775	116	118	135									Walls
618824	118	120	135	149								Walls
619325	199											Walls
619339	135	199	200									Walls
619344	200											Walls
619352	120	135	149	200								Walls
619836	120											Walls
621892	112	114	116	118								Walls
634908	110	111	134									Walls
634912	110	111										Walls
634917	111											Walls
634921	110	134										Walls
634926	111	134										Walls
635191	108	110	134									Walls
635196	108	110										Walls
635283	106											Walls
635291	106	108	134	147	196							Walls
635296	106	108										Walls
635434	197	198										Walls
635444	197	198										Walls
635449	198											Walls
635471	196	197										Walls
635475	197											Walls
635492	197											Walls
635497	196	197										Walls
635502	196											Walls
635507	147	196										Walls
641547	134	135										Walls
642072	112	134	135									Walls
646764	104	195										Walls
646768	104	195										Walls
648058	193											Walls
648067	144	145	193									Walls
648077	145	193										Walls
648082	193											Walls
648494	193											Walls
648498	99	144	193									Walls
648811	97	132	145									Walls
648815	97	132										Walls
648819	97	130	131	132								Walls
649050	7	97	131	132	144	145	193					Walls
649986	194											Walls
649990	98	141	142	194								Walls
649994	194											Walls
649998	194											Walls
650044	95											Walls
650429	98											Walls
650557	98											Walls
651039	98											Walls
651131	98											Walls
655894	90	191										Walls
655919	191	192										Walls
655944	192											Walls
656371	91	92	93									Walls
656375	91	92										Walls
656379	92	93										Walls
656383	91	93										Walls
656642	90	91										Walls
658387	128	187	189	204								Walls
658392	128	186	187	204								Walls
658404	187											Walls
658514	128	189										Walls
658519	189											Walls
658713	190											Walls
658718	188	190	204									Walls
658722	128	129	189	190								Walls
658727	86	129	139	190								Walls
658916	188											Walls
658926	185	188	204									Walls
659217	185											Walls
659649	128											Walls
661083	186											Walls
661087	128	184	186	204								Walls
661092	184											Walls
662361	183											Walls
662371	181	183										Walls
662391	181											Walls
662680	173											Walls
662690	173											Walls
662695	125	173	174									Walls
662705	174											Walls
662710	125	174	175									Walls
662720	175											Walls
662725	125	175	176									Walls
662742	176											Walls
662748	73	176	206									Walls
662753	125	176	177									Walls
662758	73	176	177	206								Walls
663274	73	125	176	206								Walls
663374	125	176	177	206								Walls
663447	73	125	176	206								Walls
663590	78	79	182									Walls
663703	180	182										Walls
663713	180	202										Walls
663839	179	180	182									Walls
663844	76	77	178	179								Walls
663854	125	178	202									Walls
663859	178	202										Walls
663864	178	179	180	202								Walls
663869	178	179										Walls
665389	188	204										Walls
665393	188	204										Walls
891698	46	48										Walls
951843	406	451										Walls
951903	406											Walls
982777	108											Walls
989213	91	93	191	192								Walls
989220	93	94	131									Walls
989224	93	94										Walls

Element I	RoomA	RoomB	RoomC	RoomD	RoomE	RoomF	RoomG	RoomH	RoomI	RoomJ	RoomK	Category
665410	204											Walls
665415	183	203	204									Walls
665420	184	203										Walls
665424	181	203										Walls
665434	180	182	203									Walls
665455	138	182										Walls
665463	138											Walls
665468	125	176	201	206								Walls
665473	125	173	174	175	176	177	201	206				Walls
665478	201											Walls
666021	138											Walls
666782	125	202										Walls
666988	125	201	202	203								Walls
667621	125	181	201	203								Walls
667679	85											Walls
667684	84	85										Walls
667703	84											Walls
667708	83	84										Walls
667725	82	83										Walls
667729	83											Walls
667877	82											Walls
668237	81	82										Walls
668246	80	81										Walls
668250	81											Walls
668337	80											Walls
668491	72	73	125									Walls
668495	71	72										Walls
668505	72											Walls
668577	70	71										Walls
668589	71	70										Walls
668593	69	70										Walls
668605	69											Walls
668609	68	69										Walls
668613	68											Walls
668621	68											Walls
669268	68	69	70	71	72	125						Walls
669572	125											Walls
669579	125											Walls
669661	80	125										Walls
669889	81	82	127									Walls
669893	80	81	126									Walls
669902	127	138										Walls
669907	75	76	77	78	79	126						Walls
670043	125	126										Walls
670200	75	76	125									Walls
670552	76	77										Walls
670561	75	76										Walls
670580	75	76										Walls
670831	74	125										Walls
671234	79	138										Walls
671309	77	78										Walls
671313	78	79										Walls
672158	138											Walls
673091	153	159										Walls
673101	4	153	154	155	159							Walls
673106	153	159										Walls
674728	159											Walls
674732	159											Walls
674981	7	11	159									Walls
675012	6	7	155	159								Walls
675780	6											Walls
676111	6	155	723									Walls
676116	6	155	723									Walls
676120	6	155										Walls
676124	6	155										Walls
676129	3	6	155									Walls
681037	6	10										Walls
681532	6	723										Walls
682526	723											Walls
682923	5	6										Walls
684103	459	460										Walls
684291	5	6	7	460								Walls
685307	3	6										Walls
685662	3	6	7									Walls
686197	6	723										Walls
686541	6	151	152	154	155							Walls
686545	151	152										Walls
686549	6	152	723									Walls
686554	152											Walls
686559	150	151	154									Walls
686563	150	151										Walls
686572	8	150	154									Walls
686582	150											Walls
687783	4	44	154									Walls
687788	8	21	22	23	55	150						Walls
687814	6	154	155									Walls
688073	1	4	5	153	154	155						Walls
688582	1	4	8	55								Walls
688605	1											Walls
688649	1	6	10									Walls
689787	151											Walls
691549	16	160										Walls
691558	44	54	160									Walls
692025	17	18	44									Walls
692030	17	18										Walls
692034	17	18										Walls
692038	17	44	54									Walls
692047	16	17										Walls
694630	161	169										Walls
694643	57	161										Walls
694648	57	161										Walls
696151	40	50	57									Walls
700377	45	46	56	346	351	352	355					Walls
700397	45	346	351	352	357							Walls
701442	161	164										Walls
701452	161	164										Walls
701457	161	163	164									Walls
701462	161											Walls
701467	161											Walls
701478	161											Walls
701588	32	161	162									Walls
701593	32	162										Walls
701598	32	161	162	163								Walls
701706	32	161	162	163								Walls
701716	161	163										Walls
701721	32	161	163									Walls
701726	32	161	163									Walls
701731	32	161	162	163								Walls
702262	161	169	724									Walls
702272	161	169										Walls
702277	161	169										Walls
702282	57	161	169									Walls
702323	56	161										Walls
702328	32	56	161									Walls
702391	161	163										Walls
703006	32	37	47									Walls
703010	32	37										Walls
703524	47	50	56									Walls
703842	37	47	50									Walls
705073	47	50										Walls
705090	38	50										Walls
705193	36	37	50									Walls
705224	36	40										Walls
705229	36	40										Walls
705234	36	40										Walls
705244	36	40	50									Walls
705708	39											Walls
705718	39	57										Walls
705898	39	50	57									Walls
706176	50	57										Walls
706304	36	50										Walls
706353	36	50										Walls
706370	36	40	50									Walls
722689	33	48										Walls
726068	32	46	47									Walls
730390	38	50										Walls
754964	483											Walls
756279	485											Walls
756283	478	479	485									Walls
756287	485											Walls
756292	469	479	485									Walls
765586	0											Walls
765933	0											Walls
765972	0											Walls
766210	0											Walls
776275	352	353										Walls
778579	344	355	356									Walls
779038	344	356										Walls
779333	344	355	356									Walls
779736	355	356	515									Walls
784527	351	352										Walls
797349	308	347										Walls
811483	460	546										Walls
811943	460											Walls
812305	481											Walls
812758	460											Walls
812857	460											Walls
812887	0											Walls
813161	460	482	487									Walls
813427	460											Walls
813796	0											Walls
817890	483											Walls
826010	443	540										Walls
826143	414	416	455	540								Walls
830856	443	444										Walls
836624	440	443										Walls
890151	34	35										Walls
891283	31	34	48									Walls
1285536	268											Walls
1290701	260	263	264	275								Walls
1290903	260	262	263									Walls
1291387	134	198	199	213								Walls
1291676	198											Walls

Element Id	RoomA	RoomB	RoomC	RoomD	RoomE	RoomF	RoomG	RoomH	RoomI	RoomJ	RoomK	Category
989228	93	94										Walls
989238	94	131										Walls
997767	310											Walls
997772	308	310										Walls
997871	310											Walls
1072818	321	322	323	514								Walls
1073107	321	323	348									Walls
1074372	308	310	311									Walls
1074875	308	312										Walls
1075044	321	322	347	362								Walls
1075940	293	294	302	306	498							Walls
1077101	302											Walls
1077373	302	459	460									Walls
1077615	297	298	299	300	302	304	499					Walls
1077742	302	304										Walls
1078748	368											Walls
1079550	341	353	368									Walls
1082701	345	356										Walls
1083078	515	516										Walls
1083217	344											Walls
1088905	315	316	347	509	518							Walls
1096225	477											Walls
1096297	469	477										Walls
1096803	477											Walls
1096912	469	477										Walls
1096947	469	477										Walls
1097207	477											Walls
1098110	471	483										Walls
1099383	475	483										Walls
1099551	475	483										Walls
1100724	402	407	440									Walls
1104060	419											Walls
1104771	440	454										Walls
1104969	443	454										Walls
1105217	454											Walls
1106383	409	410	411	440	442	453	534					Walls
1106815	442	453										Walls
1108094	413	414	442									Walls
1109324	532											Walls
1110850	404	435	437									Walls
1111512	433	434										Walls
1112809	379											Walls
1118768	38	56										Walls
1119825	1	8	21	22	55							Walls
1131901	99	132										Walls
1132543	96											Walls
1135539	126	127										Walls
1135656	138											Walls
1144077	3	6										Walls
1150774	20	21	45									Walls
1153717	34	48										Walls
1153876	34	48										Walls
1154830	50	57										Walls
1155949	40	724										Walls
1157303	45	46										Walls
1174717	4	153	460									Walls
1176508	41	49	346	517								Walls
1176512	41	346										Walls
1176516	41	63	346									Walls
1176559	41	166	517									Walls
1176563	41	166										Walls
1176567	41											Walls
1181289	309	347	348									Walls
1181905	350	357										Walls
1182220	309											Walls
1184562	373											Walls
1184566	361											Walls
1184570	360	361	372	373	374	376						Walls
1184574	360	374	375									Walls
1184578	374											Walls
1184582	373											Walls
1184586	361	372	373									Walls
1184590	360	361	372	373								Walls
1184594	372											Walls
1184598	361											Walls
1184602	360	361	372	373	376							Walls
1184606	360	361	373	376								Walls
1184610	376											Walls
1184614	360	375	376									Walls
1184623	375											Walls
1184627	360	374	375	376								Walls
1184631	375											Walls
1184635	360											Walls
1184713	373											Walls
1185239	51											Walls
1185243	51											Walls
1185247	51											Walls
1185251	51	52	65	66	67							Walls
1185255	66											Walls
1185259	66											Walls
1185263	67											Walls
1185267	52											Walls
1185271	52											Walls
1185280	51	52	65	66	67							Walls
1185284	51	65	66	67								Walls
1185288	51	65	66	67								Walls
1187969	373											Walls
1188109	373											Walls
1188113	373											Walls
1188117	373											Walls
1197956	140											Walls
1198347	132	144	145									Walls
1198423	147											Walls
1206970	432											Walls
1209792	460											Walls
1210180	460											Walls
1210458	0											Walls
1228334	238											Walls
1228338	238											Walls
1228342	235	238										Walls
1228346	238											Walls
1228373	235											Walls
1228378	235	244										Walls
1228382	235	244										Walls
1228386	235	244										Walls
1228390	235											Walls
1228516	234	235	239									Walls
1228626	235	236	237	239								Walls
1228654	244											Walls
1228659	244											Walls
1229062	244	237										Walls
1230906	268											Walls
1230910	268											Walls
1230918	267	268										Walls
1230932	268											Walls
1230936	268											Walls
1230940	268											Walls
1233800	251											Walls
1233804	251											Walls
1233808	272											Walls
1233812	251	254										Walls
1233816	251											Walls
1233861	251	272										Walls
1234312	259											Walls
1234316	257	259										Walls
1234321	259											Walls
1234325	259											Walls
1234616	257											Walls
1234624	257											Walls
1234639	257	271										Walls
1234643	254	257	270									Walls
1234648	254	257										Walls
1234653	254											Walls
1234830	263	267										Walls
1234841	267											Walls
1234845	263											Walls
1234855	263	264	265	266								Walls
1234876	264	275										Walls
1234880	266											Walls
1234884	264	265										Walls
1234888	265	266										Walls
1234892	265	266										Walls
1234896	265	266										Walls
1234905	266											Walls
1234910	265											Walls
1234921	264											Walls
1284440	260	275										Walls
1284444	275											Walls
1284569	262											Walls
1284574	261											Walls
1284579	260	261	262									Walls
1284583	260	261										Walls
1284587	260	262										Walls
1284591	261											Walls
1284608	260											Walls
1284612	260											Walls
1284666	260											Walls
1284706	258	260										Walls
1284711	258	260	271									Walls
1284715	260	271										Walls
1284720	260	271										Walls
1284724	260	271										Walls
1284913	258	260										Walls
1285524	267											Walls

Element I	RoomA	RoomB	RoomC	RoomD	RoomE	RoomF	RoomG	RoomH	RoomI	RoomJ	RoomK	Category
1313961	272											Walls
1313985	253											Walls
1313990	250											Walls
1313995	245	247	248	249	250	251						Walls
1313999	251	253	269	272								Walls
1314078	250	251	252	253								Walls
1314083	250	251	252									Walls
1314089	251	252	253	269								Walls
1314117	251											Walls
1314123	251	269										Walls
1314128	251	252	269									Walls
1314134	251	252										Walls
1314139	251	252										Walls
1314419	245	246	247	251								Walls
1314430	245											Walls
1314438	245	249										Walls
1314448	245	248	249									Walls
1314452	245	248	249									Walls
1314457	245	248										Walls
1314461	245	247	248									Walls
1314465	245	247	248									Walls
1314509	245											Walls
1314513	245											Walls
1314517	245											Walls
1314684	245											Walls
1314805	245	246										Walls
1314810	245	246	247									Walls
1314831	245	246	247									Walls
1315627	245											Walls
1316005	251											Walls
1316318	245	251										Walls
1331483	254											Walls
1331488	254											Walls
1331493	254											Walls
1331497	254											Walls
1331501	254											Walls
1331532	254	255										Walls
1331536	254	255	256									Walls
1331543	254	256	270									Walls
1331861	256	270	271									Walls
1331865	270	271										Walls
1331869	271											Walls
1331930	256	270										Walls
1338003	227											Walls
1338007	226	227										Walls
1338011	227											Walls
1338015	227											Walls
1382282	219											Walls
1382286	219	258	260									Walls
1382369	260											Walls
1382555	258	260	271									Walls
1382559	258	260	271	274								Walls
1382563	260	271	274									Walls
1382567	258	260	274									Walls
1382571	258	260										Walls
1382788	219	260	271									Walls
1382843	219	258	260	271	274							Walls
1383404	219											Walls
1383408	218	219										Walls
1383413	218											Walls
1383419	218											Walls
1383423	217	218	723									Walls
1383427	217	218										Walls
1383431	215	216	217	218								Walls
1383435	217											Walls
1383439	216	218										Walls
1383443	216	218										Walls
1383455	216											Walls
1383744	215											Walls
1383749	215											Walls
1383754	215	241										Walls
1383809	223											Walls
1383814	223											Walls
1383818	223											Walls
1383822	223											Walls
1383827	223											Walls
1383831	223	224	240									Walls
1383858	224											Walls
1383862	224	225	241									Walls
1383867	224	225										Walls
1383872	224	225	240									Walls
1383877	224	240										Walls
1383882	225	240	241									Walls
1383886	224	225	241									Walls
1383897	240	241										Walls
1383902	240											Walls
1383906	241											Walls
1383910	241											Walls
1383914	228	229	241	243								Walls
1383938	228											Walls
1383942	228	229										Walls
1383976	228	229										Walls
1383980	228	229	230	243								Walls
1383984	228	230	243									Walls
1384010	228	230										Walls
1384016	226											Walls
1384026	226											Walls
1384123	228											Walls
1384372	215	228										Walls
1384535	215	228	230	241	243							Walls
1385322	54	241										Walls
1385661	233											Walls
1385689	228											Walls
1385693	228											Walls
1385697	231											Walls
1385702	228	231	232									Walls
1385707	228	232										Walls
1385712	232	233										Walls
1385716	231	232										Walls
1385720	231	232										Walls
1385724	231	232										Walls
1385835	231											Walls
1385840	232											Walls
1385961	228	232	233									Walls
1386245	233											Walls
1386302	233	234										Walls
1386306	234											Walls
1386341	239											Walls
1386346	234											Walls
1386350	234	235	236	239								Walls
1386430	239											Walls
1386435	239											Walls
1386440	236											Walls
1386445	237											Walls
1386457	235	236	239									Walls
1386467	235	236	237									Walls
1389603	256	255										Walls
1389743	271											Walls
1391116	223											Walls
1393442	313											Walls
1403346	262											Walls
1487729	106	147										Walls
1501705	363											Walls
1501714	363											Walls
1501723	363											Walls
1502295	53											Walls
1502299	53											Walls
1502394	53											Walls
1506327	340	368										Walls
1507908	58											Walls
1507914	58											Walls
1508311	33	48	58									Walls
1526552	482											Walls
1532125	345	356										Walls
1532453	345	356										Walls
1532458	345	356										Walls
1535501	345	346	352	355	356	357						Walls
1537637	294	306										Walls
1537641	294	306										Walls
1538454	344	355										Walls
1538464	344	355										Walls
1538630	344	355										Walls
1539005	295	302										Walls
1539009	295	302										Walls
1539013	295	302										Walls
1539017	295	302										Walls
1541124	302	303										Walls
1542188	352	355										Walls
1543095	403	407										Walls
1544150	36	50										Walls
1545070	6	9										Walls
1545074	6	9										Walls
1545078	6	9										Walls
1545082	6	9										Walls
1545728	294	306										Walls
1547229	41	166	517									Walls
1548418	6	152	155									Walls
1548841	6	9	155	157								Walls
1548846	6	157										Walls
1548851	6	9	155	157								Walls
1548856	6	155	157									Walls
1549185	6	155	723									Walls
1549844	6	152										Walls
1575271	293	305	498									Walls
1614994	38	39	40	46	56	57	161	169	346	357	724	Walls

/ Reflections

Reflection

Relation with Master's program

Building technology track always encourages us to create smart buildings that are sustainable, comfortable and environmentally intelligent, this research is focusing on automating workflows, enabling cloud capabilities, enhancing integration with urban information, and creating user-friendly interactive daylight simulation tools. It helps lowering the barrier of simulating indoor daylight performance and get the result in a faster way, and can provide designers an option to directly see how the change on urban context influence indoor daylight performance at the early stage of designing and planning. How to integrate and manage built environment information and data is also one of the main goals from Design informatics studio, this research tries to communicate between several software and pass data from one to the other, with primary focus of integrating BIM into the GIS platform for room-level control and computation, and together makes the final program user-friendly.

Research Influences

This research primarily focuses on the relevance of ABDM and CBDM, as well as on the choices within the workflow that may impact its efficiency. The former is addressed in Section 4.2 of the thesis, while the latter is discussed throughout the thesis. The experiments revealed a strong linear relationship between SBI and DA, sDA, and UDI, establishing SBI as a viable daylight metrics option on the application. Regarding workflow efficiency, the application adopts time-saving and accurate practices validated by the author, such as retaining the city model within a 350-meter radius, maintaining LOD 2.2, importing the BIM model on a room-by-room basis, and importing the floor first to obtain latitude and longitude coordinates. These optimized practices are integrated into the overall workflow.

Work assessment

Firstly, based on the requirements for user interaction interface design, various functionalities were added: adding new buildings, drag-and-drop, rotate, scale, delete, select and preview materials, change the LOD of the surrounding static city model, link to the EPW Map for weather data selection, adjust the height for sunlight analysis, query rooms by name, click on rooms to change transparency for preview, and select daylight metrics. In the final dashboard, users can view the mean value and compare results from different sunlight analyses, visualizing the differences for the same room. After conceptualizing the user operations, each function and button was implemented. Consideration was given to both the front-end user interface and the backend processes, such as transferring data formats, tracking data information, and synchronizing with the GH script. This ensured data structure integrity and avoided empty inputs until Rhino Compute returned the simulation results, which were then presented in Mapbox (geometrical) and the interface (numerical). During the preprocessing of the Revit model, different elements were labeled as rooms according to their category. The GLTF data was rewritten with the Element ID to serve as a bridge for obtaining room coordinate information. When importing the BIM model, the time, accuracy, and interactivity of multiple importing methods were compared. For daylighting simulation, the impact of the BIM model on its own façade was considered, along with the automatic selection and reconstruction of individual daylighting components (glazing, doors, window frames, floors, roofs).

This thesis details the development of GH scripts for SBI and sky lumen based on their physical definitions. It sets up experiments to quantitatively analyze the relationships between two new metrics (SBI and sky lumen) and traditional metrics (DA, sDA, UDI). Key factors considered include window sill height, room spatial configuration, aperture typology (portrait and landscape), individual and combined aperture distributions, aperture orientation and shading conditions. These factors were treated as moderating variables, and a preliminary qualitative analysis was performed through sequential comparison. The R^2 value for these six relationships across scenarios were compared using boxplots to evaluate the accuracy and stability of the predictive models. If time permits, further experimentation with more detailed quantitative analyses of these moderating variables needs to be carried out. This would require the parameterization of setup variables in GH and the use of larger data sets.

Furthermore, multiple rooms at LOD 1.3 were selected to compare the radius of the surrounding urban model for insolation considerations. Simulation time and accuracy were assessed for radii of 200m, 250m, 300m, and 350m. Subsequently, the daylight simulation time and accuracy for multiple rooms at LOD 1.3 and LOD 2.2 were compared, with the radius fixed at 350m. These steps were taken to optimize the urban model input for daylight simulation.

Mentoring and feedback

I received a significant amount of direct and instructive feedback from my meetings with both advisors, which was crucial to the development of my thesis. This was particularly important in the early stages, when the scope was still very broad and my understanding of the geomatics field was limited. My first advisor and I met weekly to discuss my progress, breaking down tasks into smaller problems until I found my rhythm. Given the inherent limitations of tools and platforms in application development, my advisor encouraged me to first aim for the optimal solution A. If that proved unfeasible within limited time, I was to attempt an alternative solution B. I would strive to achieve the optimal solution, and if it was not immediately possible, I would present evidence, seek remedies, or adopt new approaches to resolve the issues. This process allowed both my advisor and me to stay informed about the dissertation's progress and direction, and to understand its limitations, which was vital for advancing the thesis. My second advisor provided detailed guidance on daylight aspects, which enhanced the rigor of my research. Additionally, the group meetings inspired me to focus more on the experimental and scientific part within my thesis. This comprehensive feedback was instrumental in shaping the final work.

Academic, Societal and Ethical Aspects

This thesis presents a comprehensive and detailed workflow that integrates GH simulation, BIM, WebGL GIS environment, and Rhino Compute to achieve room-level control and interaction with the BIM model. This approach addresses the fragmentation of the workflow and the inaccuracies that previously existed at the BIM-GIS integration. The research also offers a variety of options for solving encountered challenges. More importantly, this workflow is not confined to daylight simulation or room-level BIM models. Instead, it establishes a cloud-based framework applicable to any simulation (structural, acoustic, thermal comfort, energy, CFD, etc.) at any level of BIM model (per room, per floor, or any specific category or a single component) and facilitates integration with urban models.

This thesis also conducted a feasibility study on the new ABDM insolation metrics as an alternative to traditional CBDM insolation metrics, addressing a gap in academia. For the first time, it develops the SBI and View Lumen scripts based on physical definitions using GH and draws preliminary conclusions to validate the relationship between SBI, DA, sDA, and UDI. Several moderating variables affecting the relationship between these metrics are also proposed, paving the way for further research on daylight metrics. Furthermore, the thesis offers the option of ABDM calculation in the application, demonstrating the potential of ABDM to reduce simulation time. This offers conceptual frameworks and practical evidence for future daylighting studies at the urban scale, particularly in contexts where there is limited information about the interior layout of the rooms.

Indoor comfort, especially daylight comfort is very close to our daily life, our health, efficiency and mental state. However, due to the incompatibility between BIM and Rhino modeling software, as well as city modeling and GIS platform, the processes of data preparation, integration, result sharing, and iterative design acceleration became complex. Architecture modeling software operate independently, following distinct modeling principles. Furthermore, they are primarily designed for the architectural scale, which introduces challenges when integrating them with city and environmental models. Complex GH scripts and extensive simulations can pose challenges when it comes to seamlessly sharing workflows among teams. This complexity necessitated that designers and decision-makers learn various software programs and repeatedly input and adjust data manually in the early stage of designing. This workflow simplifies these steps by providing a user-friendly all-in-one application, and further hinders collaboration between architects and urban designers, as well as communication with governments and policymakers. The envisioned solution involves a user-friendly interface, operating on a room-by-room basis with a simple point-and-click system. This approach empowers users to swiftly make adjustments to building elements and surroundings. And could be supported by a server capable of efficiently computing and displaying simulation results. Reduce barriers for designers, making it possible to quickly visualize the impact of changes in outdoor factors on indoor lighting in completed buildings, so that quick measures can be taken to improve it, and the impact on existing buildings can be avoided during outdoor planning. This will contribute to maintaining and improving daylighting in public spaces.

Project Transferability

Although this research uses only the BK building as a BIM case study, the proposed workflow is designed for general application to various BIM models and urban environments. As previously mentioned, the workflow is not confined to daylight simulations but can be applied to different types of simulations and of BIM models of varying LODs. The requirements for the BIM model are discussed in Section 6.2. With several manual modifications, users can develop similar applications tailored to specific areas, BIM models, and a variety of simulations.

Personal growth

I have always been deeply interested in computational design, and I believe my thesis topic presented a challenging yet invaluable opportunity for me to engage in digital tool development and synthesize my acquired knowledge. The learning curve during my thesis was steep. My undergraduate background and experience in building technology enabled me to familiarize myself with the GH workflow and Python, and I had some experience with 2D interactive map. However, I had no prior experience with Rhino Compute technology, 3D GIS platforms, Three.js, or front-end design. Consequently, choosing a topic intersecting with geomatics presented a significant challenge for me. I am very exciting and satisfying that in the end I successfully implemented a lot of interactive functions using JavaScript, and that the workflow effectively engaged with various data processing formats. I believe that the integration of BIM, GIS, and simulation holds significant potential and will greatly benefit engineers and designers. Additionally, I faced some health challenges throughout the thesis, but I am grateful for overcoming these difficulties and for the extensive learning experience I gained.